Strain Sensing Technology to Enable Next-Generation Industry and Smart Machines for the Factories of the Future: A Review

Yazan Hamed, *Member, IEEE*, Garret O'Donnell, Natalia Lishchenko, and Irina Munina, *Member, IEEE*

***Abstract*—In the era of digitalization, there is a huge focus on capturing data from manufacturing processes and systems. Since the promotion of Industry 4.0, the industrial marketplace has been crowded with solution providers who excel in capturing and aggregating data on the cloud and presenting it on dashboards. From machine states to production targets, this type of data has become more readily available from tools, controllers, switches, and factory bus systems. As the industry pushes deeper into the machine for information and aspires to have smart machines that can feel and react to experiences during the manufacturing process, more sophisticated technology is necessary. Strain sensor technology is a logical measurement principle to address this challenge for many industrial sectors. For researchers and industrialists to progress toward the smart machine agenda, there must be a firm grasp of the "technology-solution fit," i.e., what strain technology could provide the most appropriate solution. This article presents a review of the state of the art in strain sensors that are foreseen as frontrunners to enable next-generation smart components and intelligent tools. The review focuses on industrial strain sensing technologies that are at a mature place on the technology readiness levels (TRLs) and present themselves as highly practical solutions for smart components and digitized machines, considering sensitivity, powered or passive, wired or wireless, and robustness. Through this review, researchers and industrialists will have a suite of solutions to move on with their innovative designs of smart machines based on embedded strain sensor technology.**

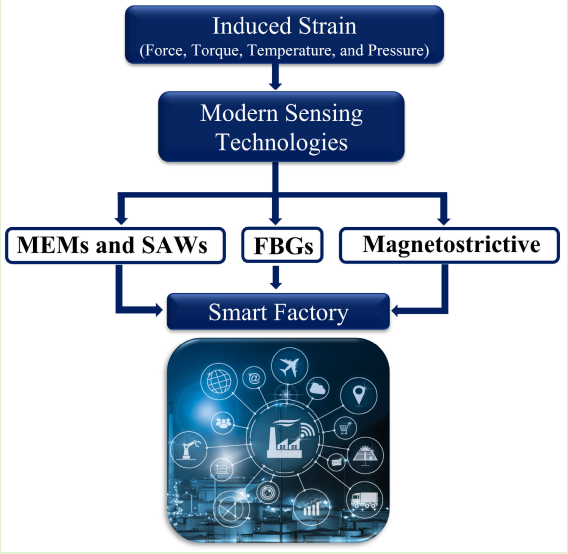

***Index Terms*— Fiber Bragg gratings (FBGs), future factories, industrial strain sensors, magnetostrictive (MR), smart manufacturing, strain sensing, surface acoustic wave (SAW) sensors.**

I. Introduction

STRAIN measurement is a geometric definition of body deformation, representing the relative displacement between the original and loaded states of an element. In other words, the normal strain (ε) caused by a uniaxially stressed rod can be defined as the elongation of the body per unit length, while shear strain (γ) occurs when stress is exerted parallel to the object surface as

$$\varepsilon = \frac{\Delta L}{L} \tag{1}$$

$$\gamma = \frac{\Delta L}{h} \tag{2}$$

where ε is the normal strain, γ is the shear strain, L is the object length, and h is its height.

In addition to mechanical strain modes, which encompass different loading scenarios (i.e., tension, bending, and compression), thermal stresses initiated within a solid material are caused by particles' vibrations that weaken the intermolecular forces leading to expansion or contraction of the substance at different temperatures. This induced thermal strain relies strongly on material properties and can be simplified into a linear expression as

$$\tau = a_T(\Delta T) \tag{3}$$

Manuscript received 6 August 2023; revised 29 August 2023 and 4 September 2023; accepted 5 September 2023. Date of publication 12 September 2023; date of current version 31 October 2023. The associate editor coordinating the review of this article and approving it for publication was Dr. Chun Zhao. *(Corresponding author: Yazan Hamed.)*

Yazan Hamed is with the School of Mechanical and Manufacturing Engineering, Trinity College Dublin, Dublin, D02 PN40 Ireland (e-mail: hamedya@tcd.ie).

Garret O'Donnell was with the National University of Ireland (NUI Dublin), Dublin, D02 V583 Ireland. He is now with the School of Mechanical and Manufacturing Engineering, Trinity College Dublin, Dublin, D02 PN40 Ireland (e-mail: odonnege@tcd.ie).

Natalia Lishchenko was with the National Technical University "Kharkiv Polytechnic Institute," 61000 Kharkiv, Ukraine. She is now with the School of Mechanical and Manufacturing Engineering, Trinity College Dublin, Dublin, D02 PN40 Ireland (e-mail: lishchen@tcd.ie).

Irina Munina was with the Saint Petersburg Electrotechnical University "LETI," 197022 Saint Petersburg, Russia. She is now with the School of Mechanical and Manufacturing Engineering, Trinity College Dublin, Dublin, D02 PN40 Ireland (e-mail: muninai@tcd.ie).

Digital Object Identifier 10.1109/JSEN.2023.3313013

where τ is the thermal strain, a_T is the material thermal expansion coefficient, and ΔT is the change of applied temperature.

Such a general definition of strain types (i.e., mechanical and thermal strains) covers a wide variety of subjects that are integral to most physical engineering systems. Measuring strain values has been fundamentally important for all branches of engineering and has been investigated for centuries. Studies on the strength of materials have had a close relationship with the evolution of strain sensing. Relying on Galileo's seminal work on elastic bodies, pioneers like Hooke, Euler, Navier, Cauchy, and Poisson formulated the concept of elasticity, establishing a bridge between numerical modeling and real-world engineering applications. A comprehensive review of their work can be found in [1] and [2].

Contemporary strain sensing technologies are highly industrialized, highly integrated, and data-rich solutions that can play a crucial role in maintaining product quality and enhancing safety in industrial settings. With the opportunities of increased yield, reduced size, and simplified installation, these techniques can be customized and incorporated with a sophisticated design to monitor induced strains in harsh surroundings while minimizing the need for external components and complex integration processes. Therefore, strain sensing mechanisms adopted in these technologies are typically based on inorganic alloys of semiconductors, metals, glass, or piezoelectric materials to acquire mechanical stability, high sensitivity, and reliability in such demanding industrial environments.

Besides microelectromechanical systems (MEMSs) that leverage different principles to convert mechanical deformation into measurable electrical signals (i.e., resistance, capacitance, and electric charge), modern industrial strain sensors combine the power of advanced electronics with novel approaches for harvesting strain values as variations in magnetic field intensity [3], acoustic emissions [4], and time-of-flight of ultrasonic waves [5]. While the range of these revolutionary solutions is so extensive, this review article concentrates on recent advances in magnetostrictive (MR) and surface acoustic wave (SAW) sensors for strain sensing. More importantly, fiber optic industrial strain sensors still hold a dominant position in the industrial market. In addition to the fiber Bragg grating (FBG) technology, which is discussed in this article, both extrinsic and intrinsic Fabry–Perot interferometric sensors stand as a cornerstone in the realm of modern industrial sensing as they can capture interference patterns of light waves between a pair of reflective surfaces to decode strain-induced changes with extraordinary accuracy [6], [7]. In addition, microbend sensors that experience light intensity variations under bending effects and polarimetric sensors that collect strain-induced birefringence as changes in the polarization state of the traveling light have been successfully implemented in a variety of manufacturing applications [8], [9]. By delving into the energy conversion laws and the interaction between light photons and material molecules, fiber optic sensors based on Raman and Rayleigh scattering techniques have been explored to provide spatially resolved strain data and dual functionality of strain and temperature monitoring [10], [11].

Thanks to their high reliability, industrial strain sensors have shown promising results across different applications such as industrial process monitoring [12], ultrahigh-temperature gauging [13], structural health monitoring (SHM) [14], orthopedic implant tracking [15], and structure failure detection [16]. Up until now, however, over 50% of all strain sensing applications still use the traditional strain gauge, despite the emergence of numerous promising solutions on the market. The advantages of metal foil strain gauges, which include inexpensive circuit design and effortless installation procedures, made these devices able to compete with more advanced technologies, such as MRs, SAWs, and FBGs, which suffer from fragility, exorbitant processing energy, and calibration complexity. Concerning resolution and temporal responsiveness, current strain sensing devices perform remarkably well. These innovations, however, depend on a physical medium for signal transmission, a source of energy, and a costly apparatus for gathering strain data. Due to these drawbacks, commercial strain sensing solutions cannot be confidently used to capture sensory data in complex and dynamic applications, such as minimally invasive interventions, robotic arms, and rotating shafts, nor in extreme conditions, such as thermal treatment vessels, transportation vehicles, and manufacturing processes. Therefore, many efforts are still needed to build a robust sensor design that can extract valuable strain data from complicated processes in harsh environments.

Of course, several attempts have been made to create embedded sensing technologies that incorporate passive, remote, and miniaturized strain sensing elements with improved performance and higher durability [17], [18], [19]. Nonetheless, most efforts exerted by researchers and scientists were aimed at the enhancement of wearable and stretchable strain sensors by imposing novel microstructures, thin films, and nanowire (NW)-based sensing elements to attain higher sensitivity and a wider application range [20], [21], [22]. The currently available literature on modern industrial strain sensors is very limited, and various technologies have not been systematically addressed yet. This review article concentrates on recent advances in industrial strain sensors, which can reflect very delicate shifts in the surrounding phenomena and survive in severe conditions, unlike conventional piezoresistive [23], capacitive [24], and piezoelectric [25] strain sensors. In order to provide insight into the behavior of mechanical systems or processes that generate an associated machinery reaction, industrial strain sensors can be operated passively and/or wirelessly to capture real-time strains in hard-to-reach locations and under extreme pressure, temperature, or electromagnetic (EM) interference [26], [27]. In addition to the multimodal sensing capabilities of different measurands [28], industrial strain sensors possess a set of unique properties that can overcome the traditional devices' limitations of narrow measurement range, inconsistency, and insufficient sensitivity, allowing for extended functionality and wider applicability.

As shown in Fig. 1, MEMS-based and traditional strain measurement techniques usually capture surface deformations under applied strains as variations in resistance, capacitance, or voltage, typically as a linear relationship. Nevertheless,

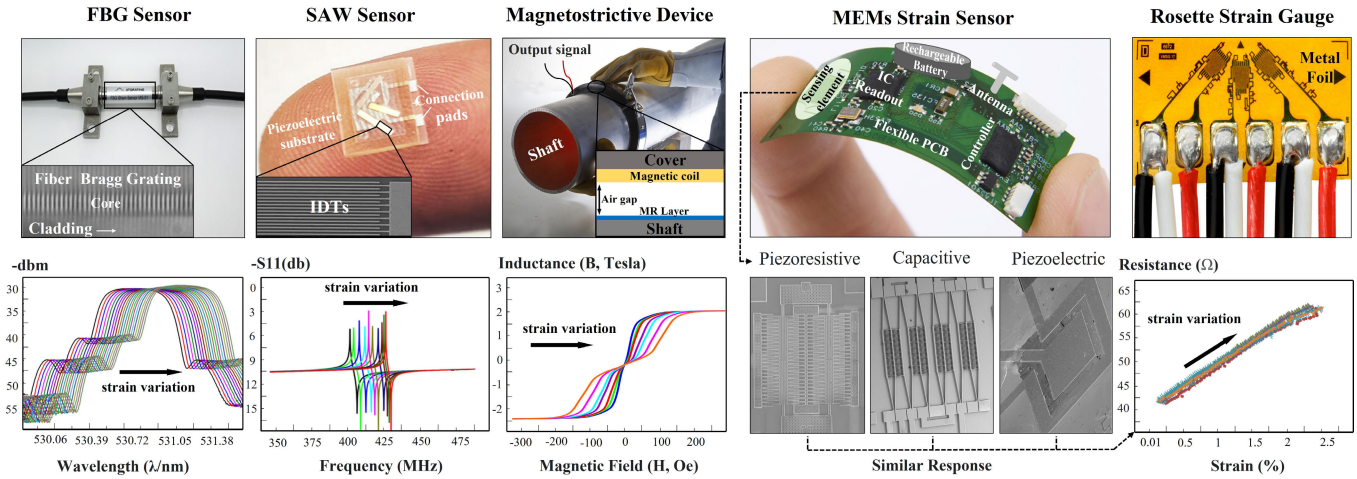

Fig. 1. Response to externally induced mechanical and thermal strains of industrial sensors (i.e., FBGs [17], SAWs [20], and MRs) compared to conventional and MEMS-based measurement techniques (i.e., piezoresistive [23], capacitive [24], and piezoelectric [25] sensors).

innovative industrial strain sensing technologies (i.e., FBGs, SAWs, and MRs) can translate delicate shifts in resonant frequency, optical refraction index, and magnetic field intensity as microstrains for ultrasensitive, remote, and robust measuring systems. Aside from force and torque monitoring, strain sensors can also be integrated with a sophisticated design of diaphragm or cantilever assembly to provide a unique solution for pressure, liquid level, and flow rate monitoring. In addition, strain sensing principles can be used as the basis for temperature tracking where the thermal expansion/contraction of a material participates in the resultant induced strain. This is fundamentally true and practically viable for bulky devices, such as piezoelectric sensors and SAWs. However, in technologies where thermomagnetic and thermo-optic effects are unavoidable, system complexity outweighs the desired outcomes. The burdens of temperature compensation for absolute strain measurement are still a critical issue to be addressed across several technologies in both experimental and industrial applications. This article focuses on strain measurement that can be interpreted as force, torque, pressure, or temperature and considers some selected cases of other measurands and multisensing prototypes where particular innovations show high potential for simultaneous and hybrid monitoring.

In addition to signal decoupling and temperature compensation requirements, industrial strain sensing technologies suffer from other serious drawbacks that prevent them from being completely commercialized. For example, FBGs require wiring infrastructure and a sophisticated interrogation system with high processing power, along with a physical light source. Some recent attempts to use advanced machine learning (ML) algorithms and novel multiplexing techniques have succeeded in reducing processing time with lower noise levels [29], [30], [31]. However, system complexity and real-time "big" data processing are still major obstacles ahead. SAW sensors, in contrast, are very fragile and go through an exhausting sequence of fabrication processes, starting from cutting the quartz substrate at the desired direction to the photolithography of the interdigital transducers (IDTs) and then wafer dicing [32], [33]. Moreover, the SAWs' resonance frequency can be easily altered by residual stresses associated with mounting and packaging procedures. In addition to that, MR strain sensors, which are suitable for various industrial applications, need to be synthesized via magnetron sputtering of thin-film elements and rely strongly on the material properties, sputtering parameters, ambient temperature, and the applied magnetic field conditions [34], [35].

Optimistically, the current rapid development in sensing technologies at device and system levels, accompanied by a huge leap in data science, has opened new avenues for both ordinary and industrial strain sensing applications. Researchers have been working on the development of industrial sensing technologies, scoring excellent results with the implementation of advanced data processing algorithms for reduced computational power [36], [37], [38]. Moreover, many successful attempts at novel materials and fabrication techniques to enhance sensing performance and repeatability were reported [39], [40], [41]. Once this step is accomplished, industrial sensors can play a key role in connecting numerous processes in a single facility, allowing for real-time monitoring of tools and equipment at different production stages. Also, the integration of local data processing systems and the Internet of Things (IoT) platform can convert these sensors into standalone "smart" devices that can apply multiple in situ algorithms to the harvested data and activate an output actuator [42]. Researchers and industrialists, who are endeavoring to capture the benefits of the thriving manufacturing market and who wish to build solid long-term profitability, have focused on establishing agile, compact, and lightweight devices that can be instrumented for complex systems and operate in extreme environments. Innovative solutions, with reliable sensors and embedded electronics, are vital for many automated systems that can feel, adapt, and learn (i.e., intelligent robots). However, again, up until now, issues such as machine noise [43], signal degradation [44],

and dynamic response [45] have not been fully discussed.

Almost everyone who is involved in the industrial sector is intrigued by the concept of Industry 4.0, which incorporates a variety of innovations. Future production models must make use of expanding sensing technologies, big data, cloud-based manufacturing, artificial intelligence (AI), intelligent robots, ultrafast actuators, and automated control systems in order to adjust to the supply and demand requirements of future factories [46], [47]. In this context, sensors can aid in improving product quality while lowering manufacturing expenses and pushing toward commercialization. In other words, these sensors can form the building blocks of an interconnected and sophisticated network that promotes adaptive manufacturing and self-optimization to avoid production bottlenecks [48]. In addition, sensors can record and analyze data to participate in decision-making strategies and predictive maintenance plans [49]. In terms of commercial use, a customer can use a variety of sensors to securely monitor input stimuli from the surrounding environment and convert a set of traditional industrial units into a smart facility. Thus, the winding path toward smart manufacturing and the Industry 4.0 paradigm is still drawing investors' attention, leading to a constant evolution of sensing technologies driven by fierce market competition among rival protocols [50], [51].

In recent years, reviews on strain sensing mechanisms have mainly focused on investigating traditional techniques, such as resistive, capacitive, and piezoelectric sensors from different perspectives. As illustrated in Table I, the key advantages and disadvantages of traditional strain sensing technologies and MEMS-based sensing devices were summarized, pointing out comprehensively reviewed topics in the engineering and healthcare fields. MEMS-based strain sensors are unique solutions that integrate various sensing technologies with electronic components for in situ signal processing. Topics such as materials, fabrication techniques, device optimization, and work principles have been reviewed thoroughly for different strain transmission mechanisms. Very recently, surveys on graphene- [100] and carbon-based [101] strain sensors were also conducted, showing the great potential of such prototypes in medical and civil engineering applications. However, this work aims to shed some light on industrial strain sensors, which can survive where no other conventional sensor can. Many researchers have reported detailed reviews of FBG sensors, discussing the underlying physical principles, fabrication approaches, device implementation, and interrogation techniques [102], [103], [104], [105], [106]. For complete applications, however, Sahota et al. [107] have recently published a comprehensive review of FBGs' fundamentals and recent significant advances in temperature, pressure, and strain sensing applications.

FBG strain sensors have been widely employed in various fields compared to other technologies (i.e., SAWs and magnetostrictive devices) because of their distributed measurement capability and the availability of efficient interrogation equipment. In civil and structural engineering applications, several reviews of FBG-based strain sensing solutions were reported in SHM [108], [109], [110], [111], [112], [113], [114], [115], [116], geotechnical health monitoring [117], [118], [119], and damage detection and failure monitoring of wind turbines [120], [121], [122]. In addition, reviews on FBG-based force sensing systems [123], [124] and FBG strain sensors in biomedical applications [125], [126], [127] have already been conducted. On the other hand, advanced technologies, such as SAWs and magnetostrictive elements, have not been sufficiently investigated yet. The available survey studies on SAW strain sensors are very limited and only discuss topics such as theory, material, and fabrication processes [128], [129], [130]. Similarly, reviews on MR devices have particularly concentrated on material properties, structures, and manufacturing technologies [3], [131], [132], [133].

In this article, a systematic literature review of promising strain sensing technologies, including FBG sensors, SAW sensors, and MR, is conducted, focusing on potential advances in strain sensing that enable smart machines and intelligent processes. Despite major fabrication, calibration, and installation drawbacks, as well as system complexity, these young strain sensing innovations offer a variety of unique benefits, such as passive operation, wireless sensing, reliable performance, and accurate measurements. This allowed some of these cutting-edge techniques to be transferred from the research lab to the market with readily commercialized patents [134], [135], [136].

Based on the literature of the previous ten years, the working principles, sensing mechanisms, and innovative solutions of these technologies are summarized with their respective features and potential to enable smart, yet cost-effective machines for future factories. Finally, the key features of FBGs, SAWs, and MR sensing technologies are demonstrated with an outlook on current challenges and future research directions.

II. Smart Components and Future Factories

New "smart" products are hitting the market and substantially distinguishing themselves from earlier versions thanks to attributes like intelligence, connectivity, and autonomy. The development capabilities of smart products and components must include features around intelligence, connectedness, service integration, and data-driven models [137], [138]. In this context, industrial strain sensors can merge intelligent features with unique physical and functional mechatronics to create smart components and digitized tools. These sensors play a pivotal role in shaping the landscape of smart manufacturing and the factories of the future as they can provide accurate and real-time insights into the mechanical behavior of different industrial processes. Industrial strain sensors can be aptly described as data-rich systems or components that provide a wealth of critical information. Such a stream of actionable data is necessarily needed not only for automation techniques but also for data-driven decision-making and predictive maintenance strategies. In future factories, these devices can allow for real-time monitoring, which supports quality control efforts and aids in optimizing resource utilization. Furthermore, these sensors can be seamlessly integrated with the IoT ecosystem forming closed-loop feedback mechanisms for minimum waste and consumption [139], [140].

TABLE I
COMPARISON OF TRADITIONAL AND MEMS-BASED STRAIN SENSING TECHNOLOGIES

Strain Sensing Technology		Pros.	Cons.	Reviewed topics
Traditional strain sensors	Piezoresistive sensors	• Simplicity and low-cost. • Relatively high stiffness. • High stability and minimal maintenance. • Integrability to MEMS and various structures. • Installation and interrogation simplicity.	• Limited measurement range and low sensitivity. • Power consumption requirements. • Failure under elevated temperatures and severe conditions. • Electromagnetic interference and thermal noise sensitivity. • Poor long-term durability and sources of non-linearity.	**Design and fabrication:** • Theory, material characterization, and device implementation [52], [53], [54], [55], [56], [57]. • 3D printed flexible strain sensors [58], [59]. • Nanomaterials based flexible sensors [60], [61], [62], [63]. • Conductive polymers for enhanced wearable sensors [64], [65], [66]. **Devices and applications:** • Stretchable and wearable strain sensors [67], [68], [69], [70], [71]. • Wearable devices and tactile sensing for biomonitoring and healthcare [72], [73], [74], [75], [76]. • Force/torque sensors for intelligent robots [77], [78], [79]. • Strain sensors for Structural Health Monitoring (SHM) [80], [81], [82]. • Flexible pressure sensors [83]. • Nanometer resolution positioning [84].
	Capacitive sensors	• Relatively low-cost and excellent linearity. • High resolution and bandwidth. • Robustness and durability. • Low noise and large dynamic range. • Good linearity and reliable signal. • Extended range via encoder-style electrode array. • Potential in nano-positioning applications.	• Sensitivity to both humidity and temperature. • Serious hysteresis. • Additional interrogation units. • Demodulation circuits for measuring capacitance. • Tilting and bowing effects. • Vulnerability to signal drifting due to mounting forces, and variations overtime. • Limited temperature range based on material Curie temperature.	
	Piezoelectric sensors	• Consistency and high sensitivity. • High resolution and minimal installation space. • Robustness and less signal conditioning. • Immunity to electromagnetic interference (EMI). • Detection of high frequency signals. • Dynamic performance capability. • Simultaneous multi-strain detection.	• Complex fabrication techniques. • Relatively higher material costs. • Sensor packaging and mounting complications. • Temperature compensation and signal decoupling requirements. • Long-term instability and signal drifting due to adhesive aging. • Additional interrogation and processing hardware.	
MEMS-based strain sensors		• Combing traditional strain sensing mechanisms with electronic components for chip-based signal processing. • Mass production capability of customized designs and structures. • Wireless and/or passive operation depending on the implemented sensing element. • Compatible to a variety of standard integration systems. • Extended functionality and wider applications range.	• Suffer from the common disadvantages of the traditional sensing element used (i.e., resistive, capacitive, inductive, or piezoelectric). • Increased system complexity and footprint. • Undesirable for low voltage and low power systems. • Temperature compensation and electronics damage under severe conditions.	**Design and fabrication:** • Theory, types of grating, material characterization, and device implementation [85], [86], [87], [88], [89], [90], [91], [92]. **Devices and applications:** • Micro-force sensors and MEMS-based robotics [93], [94], [95]. • MEMS pressure sensors [96], [97], [98]. • MEMS piezoresistive flowmeters [99].

Future factories are inspired by the concept of "smart manufacturing," which extends beyond enabling key innovations, such as the IoT, remote monitoring, big data, cloud services, and embedded systems to the implementation of more advanced technologies that can be utilized to optimize the industrial process, boost productivity, and lower emissions. One of the main goals of smart manufacturing is to approach the zero emissions agenda while increasing factory profitability and minimizing faults [141]. In addition, to keep up with abrupt changes in consumers' demands, the manufacturing flow must be capable of modifying product features and production output seamlessly. To address these challenges, the smart factory should be sufficiently productive, scalable, and accessible to both suppliers and clients. A traditional factory, which employs separate and standalone systems, suffers from weak synergy between real and virtual systems and poorer system reusability. On the other hand, a smart factory with a multilevel structure represents a transition from traditional automation control to a coupled and adaptable system of continuous data flow through strongly interlinked operations that can learn and adjust to altering requirements [142].

To enable production optimization, proactive maintenance strategies, inventory control, and operations' digitalization, future factories must integrate data from physical, functional, and intellectual capital while adopting the concept of Industry 4.0. Understanding the various technologies, particularly

sensors, is essential in any effort to comprehend the efficient use of the IoT in the manufacturing sector [48]. The connection between industrial strain sensors and smart manufacturing lies in their ability to provide real-time, accurate, and actionable data that drive informed decision-making and process improvements. It is possible to collect information, evaluate it, and develop an action that learns from events by merging process characteristics with interconnected devices and cloud-based platforms. Zuehlke [143] identified today's world of technology and smart factories' challenges of extreme complexity in planning and operations. Despite the long and winding road from the vision to the reality of a smart factory, the researcher discussed systematic approaches toward the factory of things made up of intelligent components communicating through cognitive networks.

Analyzing sensory data from industrial processes is vital to create an intelligent technology that monitors and adjusts production parameters. A trustworthy sensing technique, which is the physical building block of any adoptive smart factory, is also very important. From conventional resistive, capacitive, and piezoelectric sensors to nanotechnology-based and industrial sensing technologies, strain measurement has drawn huge attention as it can be interpreted to reflect physical phenomena, such as temperature, force, torque, pressure, flow, and position. Various strain sensing techniques have shown enormous potential in the promotion of intelligent robots and smart systems that provide data-rich solutions at the interface between the physical and digital worlds. For instance, traditional strain sensors such as piezoresistive elements have been successfully deployed in wearable electronics, soft machines, and tactile sensing systems to be instrumented to different parts of robots. These technologies have played an important role in robot environment recognition, surface morphology acquisition, and surrounding item detection [144], [145].

From pick-and-drop mechanisms to soft robotic grippers, modern strain sensors were fabricated, equipped, and calibrated for applications involving motion monitoring and positioning accuracy [146], [147]. This tight relationship between strain sensing and intelligent manufacturing is not only built upon the value of strain data for automation commands but also on the need for novel solutions that are more sensitive and invulnerable to severe environments. Recently, FBG strain sensors have been successfully implemented in continuum robots as flexible elements for curvature, torsion, and force sensing [148], [149]. Thanks to FBGs' flexibility and distributed sensing capability, such a technology can play a crucial role in developing highly stretchable strain sensors for tactile sensing and delicate robotic motion monitoring [150]. Moreover, instead of the bulky SAW sensors, IDTs have been successfully synthesized on top of ZnO flexible substrates to be conformable with various soft robotic applications [151], [152]. MR strain sensors, on the other hand, have been utilized to enhance ambient environment awareness for modern robots as force and stiffness detection techniques to improve tactile perception and robot-assisted functions [153], [154].

In addition to robotics, industrial strain sensors play a significant role in converting traditional manufacturing units into smart facilities and allow for the simultaneous monitoring of various tools and processes. Nevertheless, passive and wireless sensing issues are other considerations in complex manufacturing processes where fast-rotating parts, extreme loads, and harsh environmental conditions need to be faced. Apart from flexible strain sensors, this review article focuses on the challenge of getting rich data connected to the manufacturing process with industrial strain sensor technologies that can be integrated into rigid components, considering local power supply and signal transmission needs. Therefore, within this article, the mindset is not to "attach" a strain sensor but rather to enhance the product or component by integrating the sensor efficiently to gain the maximum impact, therefore "sensors-in" instead of "sensors-on" [155].

III. State-of-the-Art Strain Sensing Technologies

Numerous successful prototypes were developed to capture strain data in a wide variety of industrial applications. From microfabrication techniques to robotics, and from ultrasensitive procedures to heavy-duty machines, precise deformation monitoring via industrial strain sensors is crucially needed to convert classical processes into smart tools and intelligent data-driven systems. In Sections III-A–III-C, cutting-edge industrial strain sensing technologies with promising practical and commercial capabilities are discussed, focusing on applications of force, torque, pressure, and temperature monitoring that are directly associated with mechanically and thermally induced strains within the sensing element. Performance evaluation parameters, such as sensitivity, detection range, and stability, are also summarized for each sensing technology.

A. Fiber Bragg Gratings' Strain Sensors

Through the deployment of more durable telecommunication lines to attain enhanced efficiency and steadily declining bandwidth costs, fiber-optic devices have become a distinct opportunity to meet Industry 4.0 requirements in different sectors. The advancement of fiber optic communication technology has been a key player in the development of fiber optic sensors [156]. Fiber-optic strain sensors provide higher sensitivity, lower attenuation, a wider bandwidth, and a versatile form factor compared to other modern sensing techniques [157]. The operational peculiarities of fiber optic strain sensors have been exploited to replace traditional sensors, particularly in SHM applications [158], [159]. Due to their dielectric property, FBGs can be employed in challenging conditions, such as elevated temperatures, inductive loads, or corrosive environments. In addition to enabling nonelectrical, passive, and distributed measurement, these sensors are immune to radio frequency (RF) and EM effects, and conformable with a wide variety of communication protocols.

FBGs belong to the interferometric sensors, which primarily function by sensing strain-induced phase changes along a single-mode optical fiber. There are five basic types of interferometric fiber-optic sensors: Mach–Zehnder, Michelson, Fabry–Perot, Bragg, and Sagnac [160]. Among these configurations, point sensors based on FBGs have acquired the largest

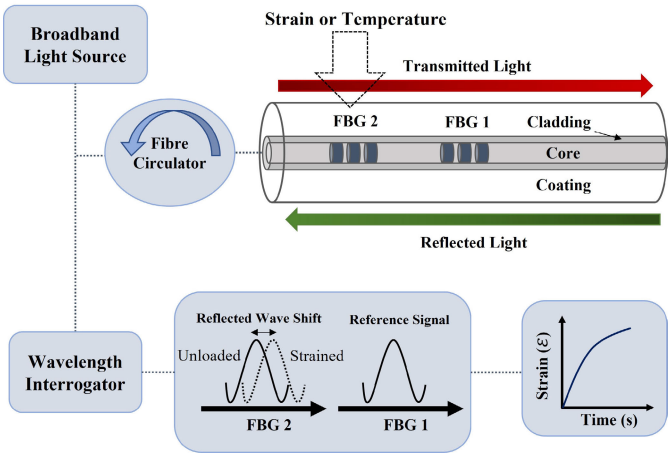

Fig. 2. Schematic of working principle and interrogation system of FBG sensor under applied load and/or temperature.

market share due to their capability of being integrated with commercially available and efficient data processing systems. The FBG sensor is based on a periodic variation in the refraction index of the core of a photosensitive fiber, where only light wavelengths matching the local periodicity can be mirrored [161]. Variations of this laser-induced reflection of central light signals can be interpreted to reveal strains from applied loads or temperature changes (see Fig. 2). Fiber optic strain sensors based on a single point are compact, reliable, and highly sensitive. FBGs can also be multiplexed and located at critical points along the fiber to form a quasi-distributed system. Typically, distributed sensing systems are based on Raman and Brillouin scattering phenomena that use the entire length of fiber-optical cable to measure strains over the whole span of the structure [162], [163].

With a strong commercial attitude, industrialists and researchers have been eager to extract the maximum capacity of FBG sensors by developing novel designs and more strain-sensitive structures. The literature is filled with studies on the enhancement of FBG strain sensitivity, particularly at device and material levels. For example, Wang et al. [164] improved fiber-optic strain sensitivity by using an etched and regenerated FBG (ER-FBG) applicable across a wide temperature range. This design showed excellent linearity and five times higher strain sensitivity (i.e., 4.5 pm/$\mu\varepsilon$) over a temperature range of 20 °C–800 °C. Li et al. [165] presented a robust structural design of an FBG strain sensor to mechanically amplify the collected strain values. This design of FBGs mounted onto a lever structure managed to achieve a strain sensitivity of 6.2 pm/$\mu\varepsilon$, which is 5.2 times higher than that of a bare FBG sensor. In their succeeding work [166], a maximum sensitivity of 7.72 pm/$\mu\varepsilon$ was reported with an efficient temperature compensation model. Recently, Peng et al. [167] developed a microstrain sensing technique for lithium-ion batteries. By employing a sophisticated assembly of lever mechanisms, flexure hinges, and serpentine springs, a strain sensitivity of 11.49 pm/$\mu\varepsilon$ was attained with low hysteresis within a range of $\pm$500 $\mu\varepsilon$. In addition to these interesting studies on amplifying strain sensitivity, more serious efforts were focused on real-life solutions to strain sensing in the engineering and medical fields. In Sections III-A.1 and III-A.2, the current advances in FBG strain sensors' applications are systematically reviewed and summarized, focusing solely on strain-based innovations for force, torque, pressure, level, and flow monitoring, as depicted in Table II.

1) Force and Torque Sensors: FBGs have been successfully implemented in cutting force sensing and multicomponent systems due to their broad spectrum, compact size, excellent durability, leanness, and flexibility. For instance, Bosetti and Bruschib [168] explored the capabilities of FBG strain sensors to improve the positioning accuracy of CNC machine tools by adopting a triangular mesh of struts integrated with FBGs for active error compensation during the machining process. Haslinger et al. [169] developed a precise robotic arm based on a miniaturized 6-DoF FBG force–torque sensor that is suitable for noninvasive surgical interventions and subtle manipulations. In another interesting work, He et al. [170] introduced an FBG-based submillimeter force sensor for microgrippers in retinal microsurgery applications. To obtain complete axial and transverse force decoupling, they established a sophisticated arrangement of four FBG sensing points, leading to reliable consistency and sensor repeatability of 1.3 pm/N. In another publication, Liu et al. [171] reported a prototype of a smart spindle based on the FBG strain detection principle to analyze and track cutting forces during the machining process. In addition, Guo et al. [172] managed to eliminate crosstalk effects and presented a three-axis force robotic fingertip relying on a single fiber of three pairs of FBGs. The proposed prototype offered a strain sensitivity of 32.567, 33.97, and 44.116 pm/N for forces F_X, F_Y, and F_Z, respectively. Kim and Lee [173] developed a precise 6-DoF FBG-based strain sensor for force and moment measurements to provide haptic feedback of applied loads at the tip of cutting tools used in minimally invasive robots. In this context and to allow real-time monitoring of position, torsional loads, and axial forces, Xu et al. [149] introduced a unique spirally coiled FBG strain sensor design to enhance sensing in continuum robots. In addition, Xu et al. [174] designed and tested multiplexed FBG strain sensors for 3-D force detection, allowing for monitoring microdeformations of the tested specimen. Xiong et al. [175] proposed a traditional Maltese-cross structure instrumented with distributed FBGs for 3-D force sensing. With careful load calibration and temperature compensation, they achieved an innovative design of robot plantar force monitoring using five FBG strain sensors of 3 nm size. Finally, Liu et al. [176] demonstrated a robust prototype of a novel dynamometer that is built upon FBG sensors to assess cutting forces and torsional loads simultaneously. The customized elastic body was positioned on a revolving spindle, and the dynamometer was instrumented with adhesively bonded FBGs. Very recently, Huang et al. [177] developed a real-time smart tool coupled with FBG strain sensors for long-range monitoring of multipoint cutting forces in the turning process. Moreover, Li et al. [178] revealed an intelligent monitoring scheme that relies on the coapplication of FBG sensors and a curvature-deformation algorithm in an attempt to translate load-induced deflections in heavy-duty industrial machinery.

TABLE II
SUMMARY OF RECENT APPLICATIONS OF FBG STRAIN SENSORS WITH THE REPORTED APPLICATION RANGE AND MAXIMUM SENSITIVITY

Strain Sensor	Application	Range	Max. Sensitivity	Ref.
FBG Force-Torque Sensors	Microfabrication and micromanipulation interventions	$F_{Axial, Lateral}$ = (0 – 1, 0 – 0.7) N M = 0 – 1.4 Nmm	$F_{Axial, Lateral}$ = (120, 2175) pm/N M = 115 pm/Nmm	[184]
	Haptic interface and minimally invasive interventions	$F_{X, Y, Z}$ = 0 – 10 N $M_{X, Y, Z}$ = 0 – 100 Nmm	$F_{X, Y, Z}$ = (50, 60, 1.875) pm/N $M_{X, Y, Z}$ = (2.17, 1.75, 1) pm/Nmm	[173]
	Industrial robotic arms and micro-manipulation fingers	$F_{X, Y, Z}$ = (± 10, ± 10, ± 25) N $M_{X, Y, Z}$ = ±156 Nmm	$F_{X, Y, Z}$ = (149.32, 152.22, 12.11) pm/N $M_{X, Y, Z}$ = (1.270, 1.376, 0.632) pm/Nmm	[185]
	Cutting forces measurements in metal manufacturing	$F_{X, Y}$ = 0 – 1,400, F_Z = 0 – 3,000 N M = 0 – 30,000 Nm	$F_{X, Y, Z}$ = (1.2815, 1.2964, 0.1788) pm/N M = 9.4333 pm/Nm	[176]
FBG Force Sensors	Robotic fingertip manipulation	$F_{X, Y, Z}$ = 0 – 25 N	$F_{X, Y, Z}$ = (32.567, 33.97, 44.116) pm/N	[172]
	Industrial robotic arms and micro-manipulation procedures	$F_{X, Y}$ = ± 50 N F_Z = 0 – 60 N	$F_{X, Y, Z}$ = (20.745, 23.366, 11.259) pm/N	[175]
	Cutting forces measurements in metal manufacturing	$F_{X, Y, Z}$ = 0 – 3,000 N	$F_{X, Y, Z}$ = (0.273, 0.039, 0.282) pm/N	[177]
	Heavy-duty processes and Structural Health Monitoring (SHM)	$F_{X, Y, Z}$ = 0 – 5,000 N	$F_{X, Y, Z}$ = (0.255, 0.256, .256) pm/N	[174]
FBG Torque Sensors	Miniaturized torque sensing in industrial robots and manufacturing tools	± 0.1 Nm	16,040 pm/Nm	[183]
	Online torque monitoring in rotary machines and industrial tools	0 – 3.4 Nm	7.684 pm/Nm	[182]
	Online torque monitoring in rotary machines and industrial tools	0 – 10 Nm	7.02 pm/Nm	[183]
	High-torque monitoring in rotating shafts and heavy-duty applications	± 550 Nm	3.6 pm/Nm	[187]
FBG Pressure Sensors	Low-pressure remote monitoring in industrial processes	0 – 10 kPa	329.56 pm/kPa	[195]
	Low-pressure remote monitoring in industrial processes	0 – 15 kPa	116 pm/kPa	[194]
	Leakage detection and pipelines corrosion monitoring	20 – 150 kPa	16.67 pm/kPa	[201]
	Liquid level, specific gravity, and medium pressure measurements	0 – 276 kPa	13.14 pm/kPa	[193]
	Static/dynamic pressure online monitoring in gas and liquid industries	0 – 500 kPa	3.21 pm/kPa	[191]
	High-pressure monitoring in oil and gas pipelines and exhaust abatement systems	0 – 1,000 kPa	5.227 pm/kPa	[199]
	High-pressure monitoring in oil and gas pipelines and exhaust abatement systems	0 – 2,000 kPa	0.2583 pm/kPa	[196]
	Ultimate pressure monitoring in oil, and chemical applications	0 – 100,000 kPa	0.0797 pm/kPa	[200]
FBG Level Sensors	Liquid-level monitoring in fuel storage and biochemical systems	0 – 25 mm	6,000 pm/mm	[209]
	Liquid-level monitoring in chemical industries	0 – 500 mm	2.74 pm/mm	[359]
	Liquid-level monitoring in chemical industries	0 – 750 mm	5.72 pm/mm	[360]
	Simultaneous level and specific gravity measurements in chemical industries	450 – 780 mm	1.419 pm/mm	[361]
	Simultaneous temperature and pressure online monitoring	0 – 1,000 mm	2.484 pm/mm	[210]
	Simultaneous temperature and pressure online monitoring	0 – 1,000 mm	2.3 pm/mm	[362]
	Simultaneous temperature and pressure online monitoring	0 – 1,000 mm	6.39 pm/mm	[363]
	Simultaneous temperature and pressure online monitoring	0 – 2,000 mm	2.53 pm/mm	[364]
	Liquid-level monitoring in extreme conditions and pressurized vessels	0 – 10,000 mm	0.185 pm/mm	[365]
	Liquid-level monitoring in extreme conditions and pressurized vessels	0 – 21,092 mm	0.072 pm/mm	[366]
FBG Flow Sensors	Cryogenic mass flowmeter	0 – 1 g/s	9 pm/(g/s)	[219]
	Cryogenic mass flowmeter	0 – 2 g/s	20 pm/(g/s)	[218]
	Cryogenic mass flowmeter	2 – 5 g/s	37 pm/(g/s)	[219]
	Cryogenic mass flowmeter	2 – 5 g/s	50 pm/(g/s)	[218]
	Velocity flow meter	0.27 – 2.47 m/s	3.3% (Repeatability error)	[220]
	Velocity flow meter	4.25 – 10.62 m/s	5.06% (Repeatability error)	[223]
	Volumetric flow meter	5 – 16 m^3/h	2.27% (Accuracy)	[221]
	Volumetric flow meter	0 – 18.5 m^3/h	1.5% (Precision)	[222]
	Volumetric flow meter	0 – 22.5 m^3/h	3.6% (Accuracy)	[367]

This suggested technique was precise and able to recreate the deformation in the gantry boring and milling machine base under various loads and unidentified physical factors. In a very recent study, Biazi-Neto et al. [179] created a strain rosette-based temperature-compensated FBG system to track stress–strain patterns of a robotic manipulation instrument. Inside a notch of two 3-D-printed claws, three FBGs were arranged in a deformable rosette pattern. To confirm the system's viability in real-time systems, grip trials with various items were carried out using the robotic arm.

In addition to force-induced strains, torque measurement aids in meeting the needs of modern engines and motors by enhancing mechanical performance with precise mechanical power and a tuned rotational speed for higher efficiency. Moreover, decoupling torque and force loads is critically essential in robotic applications for ultraprecise positioning [180] and for enhancing the rotate vector (RV) reducer, which forms the core component of most advanced robots [181]. FBG strain sensors have been successfully implemented in many torque applications in extreme environments with complex geometries. For instance, Wang et al. [182] managed to monitor the torque of a rotating shaft and its twisting angle using the wavelength demodulation technique and two FBG strain sensors inclined at ±45° onto the surface of the solid shaft. With a similar arrangement, Li et al. [183] introduced an innovative technique to examine and separate the coupled vibrations of bending and torsional strains exerted on a rotating shaft, scoring a torque sensitivity of 7.02 pm/Nm. For minimally invasive interventions, Taghipour et al. [184] introduced a triaxial force and torque sensor utilizing FBGs strain data, reporting excellent linearity and high resolution of force and torque measurements under both static and dynamic conditions. With proper temperature compensation, this design showed remarkable performance in measuring different forces and torques while eliminating temperature cross-sensitivity. In recent work, Xiong et al. [185] implemented FBG elements to demonstrate a 6-D force–torque sensor prototype that is integral to several robot parts to acquire in-depth strain data with low cross-coupling. This prototype of multilayer measurement design was fabricated to assist intelligent robots in achieving dexterous and reliable manipulation (see Fig. 3). Similarly, Lai et al. [186] reported a cylindrical hexaform structure supported by adjustable hinges and integrated with an FBG-based torque sensor to obtain high sensitivity and a small footprint. The authors proposed a suitable design for multifinger robots and minimally invasive surgical (MIS) instruments. Finally, Konstantaki et al. [187] relied on utilizing FBG technology to measure torque-induced strain in tubular shafts made of carbon fiber-reinforced polymer (CFRP). This work, which offered a strain sensitivity of 3.6 pm/Nm, demonstrated again the great potential of surface-mounted FBG strain sensors in detecting torsional loads across several manufacturing industries.

2) Pressure Sensors and Flowmeters: The challenge of securing online pressure and flow monitoring systems under severe conditions is still attracting many investments and imposing urgently needed developments. From microstructure solutions on hollow and solid fiber cores to high-elasticity polymer-based FBGs, many innovations were tested to acquire

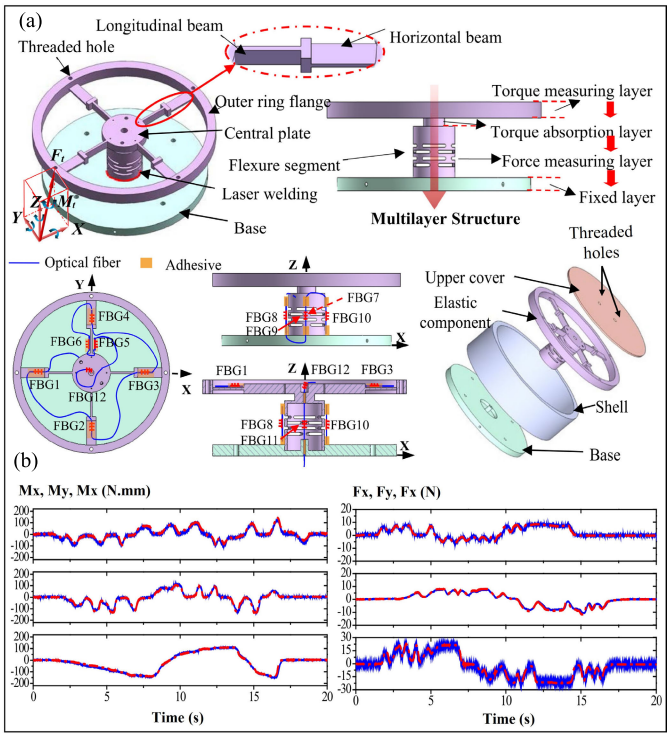

Fig. 3. 6-D force/torque FBG-based strain sensor: (a) sensor prototype of elastic structure design and FBG array layout and (b) temperature-compensated FBGs response in three axes for moment and force [185].

improved pressure sensitivity and low hysteresis [188]. Unfortunately, these advancements are usually accompanied by extremely high costs and more ramifications in the manufacturing and interrogation procedures. However, feasible designs involving traditional mechanical structures, such as springs, diaphragms, and cantilevers, have been investigated, showing greater device sensitivity. A raw FBG's inherent pressure sensitivity is only 3.04 pm/MPa [189], which is very limited for accurate pressure measurements in industrial applications. Therefore, strain-based FBG pressure sensing is typically conducted implicitly by harvesting induced loads at structural supports, such as cantilevers and thin-walled diaphragms. Several approaches have been proposed to enhance the pressure sensitivity of FBG strain sensors. For instance, Huang et al. [190] reported a temperature-compensated FBG pressure sensor with a sensitivity of 1.57 pm/KPa and a range of up to 1 MPa using a diaphragm with two adhesively bonded FBG elements. In their following work [191], they proposed a diaphragm-type FBG pressure sensor applicable to static and dynamic pressure oscillations in liquid and gaseous surroundings. They reported a pressure sensitivity of 3.21 pm/kPa in a range from 0 to 500 kPa. Rajan et al. [192] presented a polymer FBG pressure sensor integrated with a vinyl diaphragm. A sensitivity of 1.32 pm/Pa, which is over six times higher than other FBG pressure sensors, was achieved due to a dramatic reduction in the sensor's Young's modulus. Moreover, Pachava et al. [193] designed a high-sensitivity FBG pressure sensor based on a metal bellows structure made of stainless steel, reaching a pressure sensitivity of 13.14 pm/kPa and a resolution of 0.17 kPa. In another

interesting study, Allwood et al. [194] developed an extremely sensitive FBG-based pressure sensor by mounting FBGs to a rubber diaphragm, scoring a sensitivity of 0.116 nm/kPa across a range of 0–15 kPa. Later, Vorathin et al. [195] reported improved performance of a pressure sensor prototype by transferring strains from a natural rubber diaphragm to an ultrathin cantilever sheet instrumented with a multiplexed FBG network. With thermal cross-effect compensation, they managed to record a high-pressure sensitivity of 329.56 pm/kPa in a range between 0 and 10 kPa with excellent linearity. For high-pressure applications, Zhao et al. [196] presented a robust FBG pressure sensor using a diaphragm-cantilever structure for industrial pipeline pressure monitoring (see Fig. 4). Twin FBG strain sensors were attached to the cantilever and tested after temperature compensation, reaching a pressure sensitivity of 258.28 pm/MPa in the range of 0–2 MPa with good repeatability. Huang et al. [197] presented a novel multiparameter dynamical system using FBG sensors for real-time condition monitoring of complex industrial hydraulic piping systems in harsh environments. The excellent durability of this prototype, along with its temperature, pressure, and acceleration monitoring capabilities, makes it applicable to a wide range of mainstream processes in the gas and chemical industries. Moreover, Leal-Junior et al. [198] prototyped a single polymer diaphragm-based FBG sensor for simultaneous pressure and temperature tracking. The proposed system was built on the basis of the frequency difference between temperature and pressure variations, providing errors of less than 6% for both measurands. In a more recent study, Liu et al. [199] succeeded in improving the sensitivity of an FBG-based pressure sensor with a novel design of a diaphragm and hinge-lever structure. With complete temperature cross-sensitivity compensation, they reported a pressure sensitivity of 5.227 pm/kPa within a range of 0–1 MPa. Furthermore, Li et al. [200] developed an FBG sensing prototype integrated with a spring-diaphragm elastic structure (SDES) for measuring ultimate pressures. They reported an enhanced pressure sensitivity of 79.7 pm/MPa in a range of 0–100 MPa and a linearity of 99.98%. This design showed a strong potential for ultimate pressure detection across oil exploration and chemical monitoring applications.

For complete applications, strain-based FBG pressure sensors have been successfully implemented in real-life facilities for health and process monitoring. For example, Ren et al. [201] presented an indirect pipeline corrosion monitoring approach depending on detecting circumferential strains using FBGs. Wang et al. [202] designed a pipeline leakage detection system based on the negative pressure wave (NPW) and FBG pressure sensors. They built a system that can identify smaller leakage amounts with improved localization precision for condition-based maintenance and minimal false alarms. Lai et al. [186] and Konstantaki et al. [187] worked on developing a novel hoop strain FBG sensor to mimic the pipeline's internal pressure variations and wall thickness degradation. This prototype can enable simultaneous monitoring of processes in water, oil, and gas pipelines. Later, Wong et al. [205] established a real-time continuous monitoring system of pipe strength for static and dynamic leakage

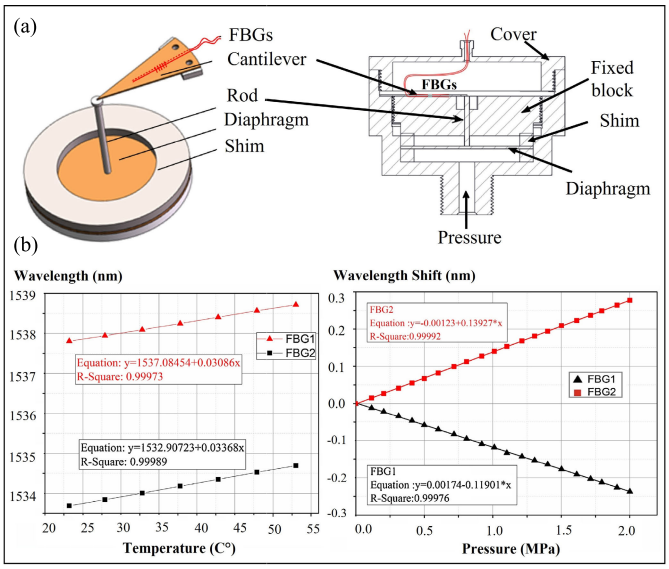

Fig. 4. Diaphragm-cantilever-based FBG pressure sensor: (a) schematic of the proposed sensor and (b) temperature and compensated FBGs' response under varying pressure [196].

detection using a submersible optical fiber pressure sensor. Despite submersible performance under water pressure of up to 600 kPa, the reported sensitivity and accuracy were relatively poor and should be enhanced by a different design to meet a wider range of applications. Finally, Wang et al. [206] presented a novel gas pipeline burst detection and localization approach relying on an array of FBG caliber-based sensors to capture NPW strains. By doing so, they reported stable localization accuracy and an average error of 1.1 m. In a more recent publication, Wang et al. [207] designed a real-time monitoring system of pressure and temperature variations in oil wells using carbon-coated bellow-packaged FBGs. This study opens the doors for dynamic monitoring of pressure variations in critical applications and under severe environmental conditions, such as in power plants, and exhaust abatement systems.

In terms of severe environments, Rosolem et al. [208] utilized electroless nickel plating to encapsulate an FBG array as a pressure sensor for thermoelectric power plant engine monitoring. The FBGs were attached to the engine injector nozzle and freely compressed by a combustion chamber pressure of nearly 20 MPa and a temperature above 300 °C. In a different field, liquid-level tracking based on the principles of FBG pressure sensors has attracted a lot of attention due to the sensors' robustness and reliability. A practical approach for tracking liquid levels by attaching an FBG element between the container wall and a floating body was accomplished earlier, as in [209]. Later, Ameen et al. [210] proposed a level and temperature dual FBG sensor using a graphene diaphragm to capture hydrostatic pressures. With a level detection sensitivity near 24.84 pm/cm and a temperature sensitivity of 13.31 pm/°C, the sensor offered reliable performance within an applicable range. However, sensor sensitivity declined significantly when more protection layers of graphene sheets were used for an extended temperature

range, limiting the sensor's practicality under extreme conditions. Recently, Almeida et al. [211] proposed an FBG level sensor using two FBGs and a cylindrical cover filled with silicone rubber to be compressed by an attached float. The sensor was tested with the FBG embedded at 5, 10, and 15 mm in the silicone rubber, and the obtained sensitivities were (155.7 ± 2.4), (80.7 ± 1.2), and (43.5 ± 2.5) pm/m, respectively. Very recently, Schenato et al. [212] presented a temperature-compensated FBG level sensor inspired by a 3-D-printed mechanical transducer and aluminum alloy case to monitor water level in open basins.

Once again, the design and implementation of a smart facility that involves pressure and flow monitoring rely strongly on intelligent online systems and smart tools to meet profitability, sustainability, and energy efficiency goals. Regarding real-time monitoring and device accuracy, FBG flow sensors, which are based on strain-induced effects, have shown great potential for competing with other commercialized smart flowmeters in the liquid and gas industries. Apart from vortex and thermal FBG flowmeters, researchers managed to develop a strain-based dual FBG flow sensor using a cantilever beam design for oil pumping monitoring [213]. In addition, other studies focused on engineering complex designs and deformable structures for nonintrusive airflow and pressure monitoring in gas pipelines [214], [215]. In an interesting publication, Schena et al. [216] presented an ultrasensitive FBG gas flowmeter based on macrobending strains that occur in the fiber tip itself, acting like a cantilever. Later, Zamarreño et al. [217] developed a flow and turbulence monitoring system based on FBG mesh for continuous strain detection across the piping network. Similarly, Thekkethil et al. [218] described a new approach for calculating cryogenic fluid mass flow rate by implementing FBG sensors to harvest drag force shifts. Their prototype was feasible for a wide range of liquid velocities and cryogenic temperatures, recording an overall sensitivity of 20 pm/(g/s) in a range of 0–2 g/s and 50 pm/(g/s) in a range of 2–5 g/s. In their succeeding work [219], they conducted experimental investigations on the FBG mass flow sensor to enable early fault diagnosis and more efficient cryogenic processes. In another novel design, Kirwan et al. [220] developed a flow measurement device that captures strains introduced by the momentum effect of fluid turbulence at the pipe elbow. They demonstrated a reliable sensing mechanism that can read flow rate solely with complete compensation against static pressure and temperature variations within a range of 0.27–2.47 m/s. Recently, Lv et al. [221] proposed an FBG sensor for dual monitoring of flow rate and temperature in different industrial applications. Two adhesively bonded FBG elements enclosed by a protective shell were assembled in a capillary steel cantilever to transfer flow-induced strains (see Fig. 5). With a judicious design of their target-type flowmeter, they achieved flow rate accuracy near 2.27% in the range of 5–16 m^3/h and temperature accuracy below ±1 °C in the range of 23 °C–83 °C. More interestingly, Zhao et al. [222] presented a unique solution for temperature, pressure, and flow rate measurement using FBG sensors. One element was fixed in the target for temperature compensation, while two FBGs were attached to the inner wall of a hollow

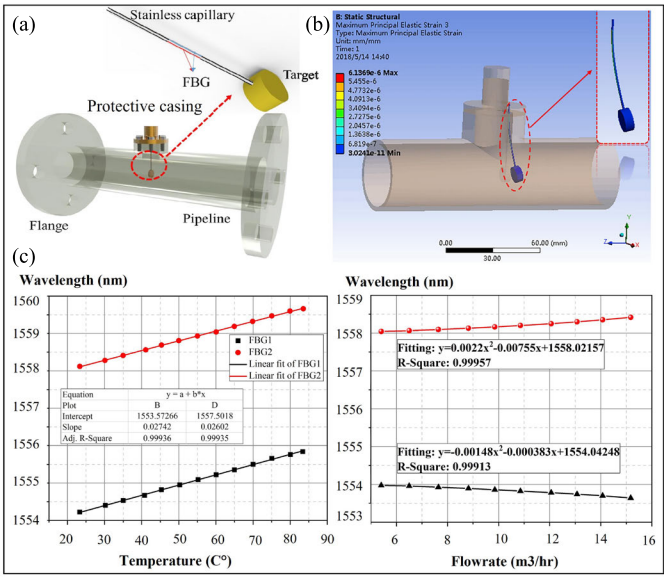

Fig. 5. Simultaneous temperature and flow rate FBG sensor: (a) schematic of the proposed sensor, (b) static structural FEA simulation, and (c) temperature and compensated FBGs response under varying flow rate [221].

cylindrical cantilever to detect flow rate. Also, another two FBGs were mounted to the outside of the thin-walled cylinder to measure pressure. Very recently, Li et al. [223] introduced a noninvasive online monitoring technique for distributed flow velocity measurements in industrial pipelines. By eliminating the crosstalk effect via differential FBG signals, excellent linearity in the velocity range of 4.25–10.62 m/s was achieved with a repeatability error of less than 5.06% full scale (FS). This study confirms again how FBG technology is capable of converting traditional processes inside old piping networks into intelligent systems for online remote monitoring and constructive feedback. These immune smart flowmeters, in some way or another, contribute to the ''big data" collected from the smart facility to enhance decision-making techniques and promote initiative-taking maintenance strategies.

Despite higher costs and exhausting processing systems, strain-based FBGs have shown promising results in a number of more exotic applications for online monitoring and smart processes. FBG sensors' immunity to extreme conditions of EM interference and high temperatures was adopted to build a high-stress monitoring system of prestressing tendons in nuclear concrete vessels [224]. FBG strain sensors were also implemented inside the plastic deformation process of cast parts for design optimization [225]. In addition to soil strain analysis [226] and gear pitting fault diagnosis [227], [228], FBG sensors were also adopted for in situ monitoring of material fatigue and structural health [229].

As discussed earlier, FBG strain sensors can offer a set of feasible solutions to convert traditional machines into digitized manufacturing units. In industrial applications, a smart factory, which employs predictive maintenance and resource optimization schemes in addition to failure prevention techniques, relies strongly on sensory data collected from sensors within the facility. FBG strain sensors can transfer valuable

information about process performance and machine status in the form of force, torque, temperature, pressure, or flow rate. More importantly, this technology has drawn a lot of interest due to its distributed sensing capability, which allows simultaneous monitoring of various components and locations in the automated facility.

B. Surface Acoustic Wave Strain Sensors

The first generation of MEMSs was introduced early to the market in the 1970s as pressure sensors, gyroscopes, and accelerometers [24]. Later, MEMS-based devices were used in RF components, microfluidic applications, and biomedical instruments due to their robustness and adoptability [230], [231]. With their distinctive ability to perform a set of specific functionalities, MEMSs were widely implemented to create customized sensors and actuators. A variety of MEMS structures are accessible or can be easily manufactured, depending on the required tasks and customer interests. Thanks to the current rapid development in microfabrication and micromachining techniques, MEMS can now be fabricated more efficiently, offering miniaturized and durable solutions. These systems, which combine the features of mechanical and electrical components, have the advantages of compactness, lightweight, superb performance, simplicity in mass production, and competitive prices [232], [233]. Contrary to bulky fiber-optic strain sensors, MEMS devices can be operated wirelessly and instrumented in difficult locations, such as temperature and load sensors. This solution of integrating selected sensing mechanisms with wireless interrogation was successfully applied in various applications from process monitoring to robotic manipulations [234].

Regarding smart tools and intelligent systems, MEMS strain devices have shown peerless performance as sensors and actuators in many industrial applications [235]. For example, Zhao et al. [236] established a triaxial force sensor based on a MEMS strain resonator that is instrumented to a CNC lathe cutting tool. With an online monitoring system, the authors reported sensitivities of 0.32, 0.32, and 0.05 mV/N in the triaxial directions, respectively. Recently, Qin et al. [237] designed a smart milling tool by employing a new design of a piezoresistive MEMS sensor that converts delicate deformations into electrical signals to reveal applied loads. They reported a prototype with a sufficient frequency range for practical high-speed applications and enhanced torque sensitivity of 2.85×10^{-2} mV/N in the axial direction and 2.90 mV/Nm in the lateral direction. Moreover, Zhang et al. [238] presented a sawtooth capacitive MEMS strain sensor with a 0–1000-$\mu\varepsilon$ range and a 34-kHz/$\mu\varepsilon$ strain sensitivity to track rotor bearing health in industrial rotary machines. This prototype offered rigid performance under high temperatures and great centrifugal forces in addition to wireless signal transmission through a readout coil. Recent successful attempts at creating wireless and passive communication with MEMS-based strain sensors have been reported in different applications [239], [240], [241], [242], [243]. However, these devices' architectural complexity, footprint, and power consumption requirements are still major drawbacks of this evolving technology. Fortunately, SAW sensors can overcome these limitations and survive in extreme conditions of high levels of radiation, temperature, and EM interference, unlike conventional MEMS devices.

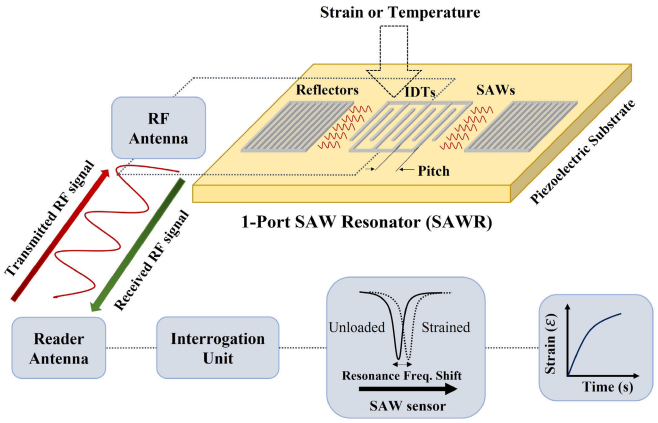

Fig. 6. Schematic of working principle and interrogation system of one-port SAWR strain sensor under applied load and/or temperature.

The SAW was first explained by Rayleigh [244], who described the propagation modes of an acoustic wave in a piezoelectric material. Later, a convenient method for generating SAWs was proposed by White and Voltmer [245] using deposited IDTs. SAW devices have been in commercial use for more than 60 years in the telecommunications industry as bandpass filters in the RF and intermediate frequency (IF) sections of the transceiver electronics. SAWs as sensors, however, were mainly utilized for chemical vapor and gas detection applications [246] and biosensing technologies [247] as a result of the huge leap in wireless interrogation systems and data acquisition (DAQ) hardware in recent years. In terms of strain sensing applications, SAW devices have attracted a lot of attention because of their low energy requirement, wafer-scale manufacturing, responsiveness, reliability, and wireless/passive integration. These inimitable characteristics made SAWs suitable for harsh environments faced in the aerospace industry [247], the water industry [248], the automotive industry [249], and SHM [250]. There are multiple architectural configurations of SAW sensors that are utilized for strain measurement. Delay-line (DL), two-port SAW resonators (SAWRs), and single-port SAWRs are common designs that vary in the IDTs and reflective gratings (RGs) configuration, as well as sensing layer area. In the DL structure, the region between the two IDTs is covered with specifically sensitive material for extended functionality. This allows for isolating stress or temperature readings while tracking other external effects such as humidity and magnetic fields [251]. Single-port devices, or, alternatively, SAWRs, are commonly used for strain monitoring due to their minimal footprint, fast response, and fabrication simplicity. As depicted in Fig. 6, when strain is applied, any SAW configuration exhibits frequency, velocity, and/or amplitude shifts in the reflected signal due to pitch and substrate geometric deterioration. The reflected RF waves are collected via a reader antenna and interrogated to derive strain measurements associated with induced loads or thermal strains [252], [253].

Unlike FBGs, which reflect thermal loads through a combination of thermal strains and thermo-optic effects, SAW strain sensors exclusively experience thermal strains as deformations initiated within the device substrate and IDTs. This unique property inspired many researchers to isolate temperature for more efficient cross-sensitivity compensation and to create dual monitoring systems in heavy-duty applications. High-quality single quartz, lithium niobate ($LiNbO_3$), and lithium tantalate ($LiTaO_3$) crystals are three frequently used piezoelectric substrates for SAW sensors. The substrate can be finished at different cuts (i.e., ST-cut, At-cut, and YX-cut) with a customized plane/angle to manipulate key parameters of the final product like resonance frequency, sensitivity, and measurement range. Among the most popular cuts, ST-cut quartz has the least sensitivity toward temperature, with zero temperature coefficient of frequency (TCF) at room temperature [254]. This advantage was seized to produce innovative absolute-strain measurement techniques without temperature drift burdens. YX-cut quartz, on the other hand, has much higher temperature sensitivity and excellent stability and responsiveness. Hence, this substrate design can be employed in various wireless temperature sensing applications under severe conditions. Along with current improvements in SAW piezoelectric materials and device optimization, Sections III-B.1–III-B.3 present a survey of recent applications of SAW strain sensors in process monitoring and smart tools focusing on force, torque, pressure, and temperature monitoring, as summarized in Table III.

1) Force and Torque Sensors: Following Varadan's seminal work [255], SAW sensors were widely investigated for building strain measurement systems through batteryless and passive operation. Nowadays, many smart tools and intelligent processes have become achievable through the combination of SAW strain sensing and advanced control algorithms in robotics and metal-cutting applications. This technology can aid in building online smart tools due to its excellent features in monitoring complex cutting forces, tool position, and process temperature. For example, Stoney et al. [256] proposed a packaged SAW strain resonator based on AT-cut quartz instrumented to a CNC tool holder for online process monitoring. They reported strain sensitivity around 500 Hz/$\mu\varepsilon$ with FS hysteresis in SAW response below 1.1% of FS output (FSO). In their subsequent study [257], a differential SAW sensor arrangement was designed to explore two-axis oblique cutting force data. Moreover, Wang et al. [258] presented a novel smart cutting tool based on dual SAW strain sensors to capture the cutting and feed forces of a tool shank (see Fig. 7). They reported load sensitivities of 152 and 185 Hz/N and hysteresis of 7.3% and 4.7% for horizontal and vertical SAWs, respectively. Later, the same research group [259] developed a smart fly-cutting tool for ultraprecise, high-speed, and hybrid material machining. The tool head was instrumented with an SAW sensor and wireless antenna for remote operation with a spindle speed of up to 20 000 rpm. Similarly, Cheng et al. [260] proposed a smart tool design based on two SAW sensors fixed to both sides of a cutting tool shank. With proper temperature compensation, they attained excellent SAW readings at spindle speeds up to 900 rpm and 1-mm cut depth. In recent research, Lin et al. [261] created an ScAlN-/AlN-based SAWR, providing an excellent quality factor for delicate strain measurements. The linear approximation of resonance frequency shifts against measured strain had a maximum slope of 46.2 kHz/N. They recorded a maximum force sensitivity of 103.2 ppm/N for parallel resonance frequency, paving the way toward precise smart tools in the manufacturing, medical, and semiconductor industries. In a very interesting publication, Tan et al. [262] presented a standalone strain sensing technique for passive and wireless monitoring. This approach combined the advantages of a wireless SAW sensor and a self-powered triboelectric nanogenerator (TENG). The authors reported good model linearity and a maximum sensitivity of 2.63 V/N in a range of 0–2.5 N, making this design suitable for wireless microforce monitoring in robotics and microfabrication.

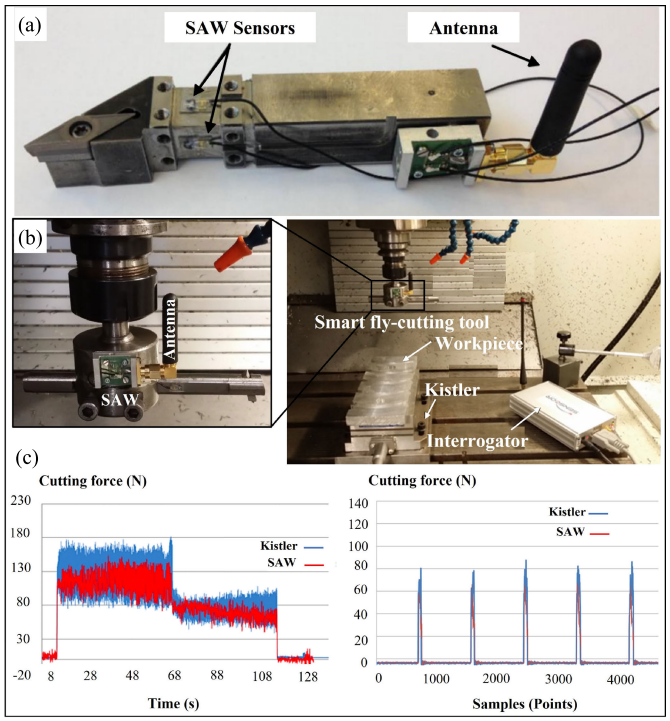

Fig. 7. SAW-based smart cutting tool: (a) illustration of the proposed sensor and antenna instrumented to milling tool shank, (b) SAW installation on fly-cutting tool head and interrogation instruments, and (c) SAW response to cutting force compared to the Kistler dynamometer for milling tool and fly-cutting tool on multilayer hybrid material [258], [259].

In terms of remote intelligent systems, Kalinin et al. [263] designed an SAW-based torque sensor and RF coupler to be attached to high-speed shafts inside wind turbines' gearboxes. Within a temperature range of 20 °C–80 °C, the accuracy of torque measurement after calibration was greater than 1% across the full range. This monitoring technology, which allows for online wind energy tracking and early warning of shaft failure, was also developed for marine applications in their succeeding work [264]. They presented a sophisticated SAW sensor design for recording torsional loads applied to marine propeller shafts to optimize mechanical power transferred from main engines and track shaft oscillations for predictive maintenance. Ji et al. [265] developed a wireless demodulation system for passive SAW torque monitoring by

TABLE III
SUMMARY OF RECENT APPLICATIONS OF SAW STRAIN SENSORS WITH THE REPORTED APPLICATION RANGE AND MAXIMUM SENSITIVITY

Strain Sensor	Application	Range	Max. Sensitivity	Ref.
SAW Force Sensors	Ultrasensitive force detection in robotics and microfabrication	0 – 3 N	32.183 kHz/N	[262]
	Ultrasensitive force detection in robotics and microfabrication	1 – 5 N	46.2 kHz/N	[261]
	Cutting forces monitoring in smart tools in the manufacturing industry	0 – 100 N	0.185 kHz/N	[258]
SAW Torque Sensors	Online torque monitoring in industrial tools and rotating shafts	0 – 100 Nm	7.78 kHz/Nm	[266]
	Online torque monitoring in industrial tools and rotating shafts	± 100 Nm	1.951 kHz/Nm	[269]
	High vibrations and torsional loads monitoring in heavy-duty machines	0 – 500 Nm	1.3570 kHz/Nm	[368]
	High vibrations and torsional loads monitoring in heavy-duty machines	± 750 Nm	0.171 kHz/Nm	[263]
	High-torque monitoring in rotary machines (e.g., motors, pumps, and engines)	0 – 800 Nm	2.03 kHz/Nm	[265]
	Ultimate torque monitoring in boring drilling works	0 – 4,000 Nm	0.1443 kHz/Nm	[369]
SAW Pressure Sensors	Low-pressure monitoring in medical applications.	0 – 40 kPa	14.25 kHz/kPa	[370]
	Temperature-humidity-pressure (THP) online multi-sensing	0 – 42 kPa	0.9 kHz/kPa	[275]
	Online pressure monitoring in industrial piping networks	0 – 300 kPa	0.137 kHz/kPa	[279]
	Online pressure monitoring in industrial piping networks	100 – 400 kPa	3.3 kHz/kPa	[271]
	Online pressure monitoring in industrial piping networks	0 – 480 kPa	0.258 kHz/kPa	[371]
	High-pressure monitoring in pressurized vessels and extreme conditions	0 – 1,723.69 kPa	0.01075 kHz/kPa	[273]
	High-pressure monitoring in pressurized vessels and extreme conditions	0 – 2,000 kPa	0.0605 kHz/kPa	[276]
	Real-time downhole pressure monitoring in gas and oil exploration	0 – 9,700 kPa	0.083 kHz/kPa	[274]
	Ultimate pressure monitoring in oil and chemical industries	0 – 103,420 kPa	0.00214 kHz/kPa	[272]
SAW Temperature Sensors	Flexible SAW temperature sensor for complex structures	20 – 75 °C	8.7 kHz/°C	[287]
	Real-time pressure-temperature dual monitoring in many industrial processes	20 – 120 °C	466 kHz/°C	[283]
	Real-time pressure-temperature dual monitoring in many industrial processes	20 – 120 °C	93.4 kHz/°C	[290]
	Wireless anti-irradiation temperature sensing in harsh environment	22 – 200 °C	15.79 kHz/°C	[297]
	Temperature monitoring in industrial and aerospace applications	25 – 250 °C	125.4 kHz/°C	[302]
	Low-temperature monitoring in microwave power circuits	-268 – 150 °C.	300 kHz/°C	[282]
	High-temperature monitoring in thermal treatment processes and powerplants	20 – 500 °C.	34.73 kHz/°C	[286]
	High-temperature monitoring in thermal treatment processes and powerplants	20 – 600 °C	7.46 kHz/°C	[291]
	Ultrahigh-temperature monitoring in severe environments	900 –1300 °C	4.38 kHz/°C	[296]

using signal amplification and processing algorithms. They scored excellent linearity and a remarkably high sensitivity of 2.03 kHz/Nm within a range of 0–800 Nm. Moreover, Fan et al. [266] achieved enhanced performance of the SAW torque sensor by implementing a customized response detection method based on the bandwidth of the SAWR and energy-entropy response. The authors reported a repeatability error of 0.23% and a linearity of 99.34%. Nonetheless, Silva et al. [267] established a real-time SAW-based monitoring system calibrated via a thermal chamber and universal testing machine for simultaneous torque and temperature measurements in a rotating shaft. Finally, Scheiner et al. [268] presented miniaturized six-port SAW strain resonators of different delay lines working in the 2.45-GHz ISM band for contactless torque measurement within the ±20-Nm range. In a more recent study, Han et al. [269] built a robust torque monitoring system using SAW strain sensors integrated with compressive sensing (CS) and support vector machine (SVM) interpolation algorithms for signal prediction. The prototype was based on a pair of 45°-inclined SAWs and tested under the ±100-Nm range, reaching a sensitivity of 1.951 kHz/Nm (see Fig. 8). This study highlights a set of new opportunities, such

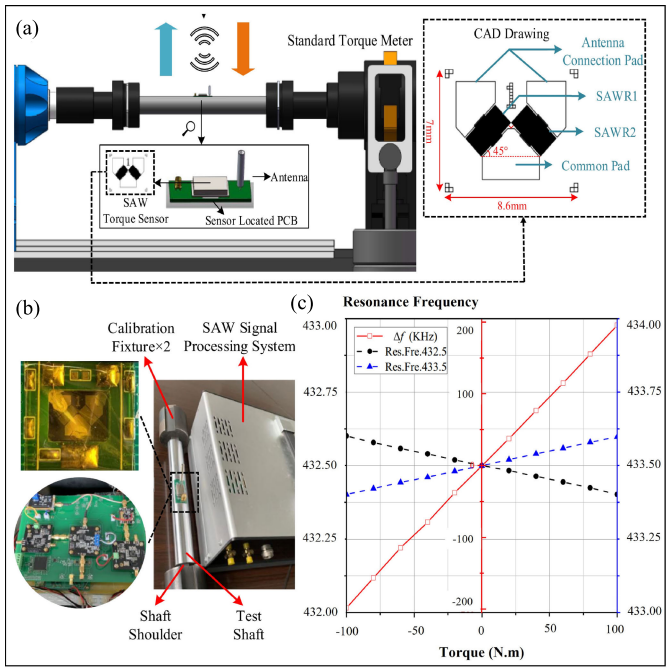

Fig. 8. SAW sensor-based torque monitoring system: (a) schematic of the proposed sensor prototype and torque calibration setup, (b) twin of inclined SAWs instrumented to a rigid rotating shaft, and (c) SAW calibration results showing sensor response to various torques [269].

as lower hardware expenses, reduced data volume, and higher interference immunity for noninvasive measurement of torque and axial load in high-speed rotating shafts. This experiment illustrated SAW's capabilities of turning rotating machinery, such as pumps, motors, and engines into smart systems that can learn and adapt to meet load requirements in various fields, such as the water and food industries.

2) Pressure Sensors: With its exceptional potential, the SAW strain sensor design was expanded to provide real-time temperature-compensated pressure sensing that is powerful in many fields, especially in the aerospace, automotive, and oil drilling industries. Similar to FBGs, SAW strain sensors are integrated with mechanical structures, such as cantilevers and diaphragms to intensify the collected strains and attain higher sensitivity. SAW pressure sensing fundamentally relies on the resonance frequency shift associated with the applied strain on a piezoelectric substrate. Earlier, Binder et al. [270] developed a pressure/temperature sensor with unique identification for condition monitoring applications in the baking industry. They reported a phase shift-measured pressure sensitivity of 0.037 rad/kPa and a temperature drift of 0.013 rad/°C. Rodríguez-Madrid et al. [271] established a one-port SAWR operating in a high-frequency range of 10–14 GHz for pressure monitoring. Using an optimized 300-nm AIN diaphragm deposited on free-standing nanocrystalline diamond (NCD), they reported precise SAW performance and a pressure sensitivity of 3.3 kHz/kPa. Moreover, Della Lucia et al. [272] established a two-port SAW device of 2.14-Hz/kPa sensitivity to replace the traditional bulk acoustic wave (BAW) pressure sensors often utilized in the oil and gas industries (see Fig. 9). The pressure sensor was tested and calibrated in a pressure range from 0 to 103.42 MPa and at temperatures as high as 150 °C. Wang et al. [273] proposed AlN-based SAWRs with different diaphragm shapes to examine various sensitivities. They recorded a maximum pressure sensitivity of 10.75 Hz/kPa across a wide application range. Moreover, Quintero et al. [274] proposed a real-time pressure monitoring system for downhole applications. By using a metal diaphragm structure, a pressure sensitivity of 0.083 kHz/kPa was reported, along with packaging considerations for harsh environments. Finally, Zhang et al. [275] developed an SAW temperature-humidity-pressure (THP) sensing prototype based on $LiNbO_3$ for environmental monitoring. The THP sensor, which consisted of three SAWRs, had an element for temperature compensation, a resonator coated with graphene oxide for humidity measurement, and a third resonator instrumented to a deformable cantilever beam for pressure sensing. The presented THP sensor was tested, showing strong reproducibility and consistency in an ambient environment with a temperature range of 25 °C–200 °C, a pressure range of 0–42 kPa, and a humidity range of 10%–90% relative humidity (RH). Furthermore, Memon et al. [276] reported a highly sensitive SAW pressure sensor using an AlN/Mo/SOI multilayer structure of a 50-μm-thick silicon diaphragm. They presented a specific configuration to improve pressure sensitivity, taking into consideration SAW propagation direction and induced strain orientation. They recorded high sensitivity near 228.46 ppm/MPa in a pressure range of up to 2 MPa. In terms of complete applications, Xie et al. [277] developed an embedded SAW pressure sensor filled with silicone oil for monitoring civil engineering structures in a range of 0–500 kPa. Tang et al. [248] developed an SAW-based water pressure sensor for passive and wireless monitoring by optimizing interrogation signal pulsewidth and frequency. In their succeeding work [278], they enhanced the proposed prototype by employing temperature-compensated SAWs of a bidirectional reflective DL (RDL) resonator, attaining good linearity in a range of up to 28-m water-pressure head. Recently, Xue et al. [279] demonstrated a viable SAW pressure sensing system based on langasite (LGS) to survive in extreme environments. For temperatures of up to 1000 °C, they scored a pressure sensitivity of 137 Hz/kPa. This work explored SAW sensors' readiness to track high-temperature and high-pressure processes in industrial applications, such as pumping stations and power plants, which allows for upgrading such traditional systems into digitized facilities.

3) Temperature Sensors: As a fundamentally physical quantity, temperature is the most universal parameter encountered in countless industries, from traditional processes involving turbines, generators, pressure vessels, and heat exchangers to modern technologies in the metallurgy, aviation, and aerospace sectors. Online temperature monitoring can play a pivotal role in capturing rich data to support smart manufacturing and adoptive control techniques. Optimizing injection heat requirements and tracking thermal shocks can add valuable features to any facility, enabling energy reduction plans and predictive maintenance strategies. This is essential under the Industry 4.0 paradigm for future factories and smart manufacturing processes. However, the challenge of developing a

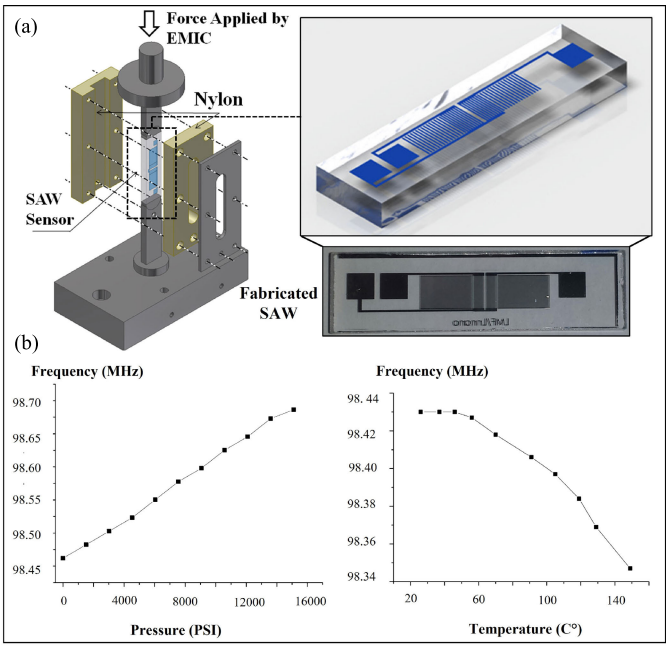

Fig. 9. Simultaneous temperature and pressure SAW sensor: (a) schematic of the proposed sensor structure and manufactured prototype, and (b) SAW sensor response with respect to pressure and temperature [272].

stable and robust sensing technique that can function under extreme conditions has not been completely met yet.

Despite many breakthroughs in temperature sensing mechanisms to improve sensitivity and application range, issues such as wireless communication, self-powered systems, and real-time monitoring are still unsolved. Among different technologies, SAW strain sensors are based on detecting only thermal-induced strains to provide precise temperature monitoring. Tracking temperature by measuring SAW substrate deformation is vital for isolating other thermo-optic and thermomagnetic effects. Therefore, SAW strain sensors are immune to harsh ambient conditions and can return a stable response across a wide temperature range compared to FBGs and MRs. In addition to a selectively fabricated substrate for customized range and sensitivity, SAWs can also be attached to complex structures with a few millimeters of footprint. The detection of thermal strain using SAW piezoelectric substrate is a unique way of building "smart" and online temperature monitoring systems based on in-depth analysis of tool thermal conditions and process dynamics to guarantee safety, higher efficiency, and lower operational and maintenance costs.

Many researchers were influenced by SAWs' unique capabilities to develop passive and wireless temperature monitoring systems using new designs and rigid structures. For example, Kang et al. [280] proposed an SAW-RFID-enabled temperature sensor with a large coding capacity and high temperature accuracy suitable for industrial applications. Moreover, Aubert et al. [281] reported a design of a DL SAW sensor based on an AlN/sapphire structure and iridium IDTs. They achieved a quasi-linear sensitivity of −71 ppm/°C between 20 °C and 1050 °C under vacuum conditions. Müller et al. [282] developed a GaN/Si-based single SAWR for temperature monitoring operating in the GHz frequency range. By tuning the SAW structure via nanolithographic techniques, they reported a temperature sensitivity of 300 kHz/°C from –268 °C to +150 °C. Later, the same research group [283] extended their work to create a GaN membrane-supported SAW pressure sensor with embedded temperature sensing capability. In another interesting publication, Shi et al. [284] built a self-powered wireless temperature sensor by integrating an SAW sensor with a thermoelectric generator. This innovative solution offered remote and passive operation with a reasonable transmission distance, suitable for critical manufacturing processes. Similarly, Zhu et al. [285] presented a self-powered SAW temperature sensor integrated with a buck–boost converter to extract power from a piezoelectric energy harvester (PEH). Nevertheless, Li et al. [286] fabricated an AlN-based SAWR for temperature sensing applications, scoring a maximum sensitivity of 821 ppm/°C and stable performance in the range between room temperature and 500 °C. More interestingly, Tao et al. [287] developed a flexible SAW sensing prototype to detect small temperature changes on nonplanar and curved surfaces. By building different layered SAW structures based on ZnO/Al foils, they reported a maximum temperature sensitivity of 8.7 kHz/°C from room temperature up to 75 °C. This prototype is a good candidate for numerous electrical and mechanical systems where using bulky devices is cumbersome. Fu et al. [288] proposed a robust temperature monitoring technique using binary phase shift keying (BPSK) codes of eight chips implemented with a DL SAW sensor on a Y-Z $LiNbO_3$ substrate. In a more recent study, Bruckner and Bardong [289] established a distributed temperature monitoring network based on the parallel readout of four independent SAW sensors in the 2.45-GHz ISM band for industrial applications. Within a similar operation band, Lamanna et al. [290] proposed an AlN-based multiple-mode SAW temperature sensor fabricated from a piezoelectric substrate. They acquired a temperature sensitivity of 93.4 kHz/°C for the Rayleigh wave mode in a range of 20 °C–120 °C. Recently, Li et al. [291] introduced an innovative LGS-based SAW temperature sensor, offering good linearity in a wide range from 20 °C up to 600 °C. In their next work [292], they proposed a three-resonator-based SAW strain sensor with excellent linearity to be operated between 20 °C and 250 °C. In a recent study, however, Yan et al. [293] fabricated and tested an LGS-based SAW strain sensor under strains of up to 500 $\mu\varepsilon$ and a temperature range of 18 °C–700 °C, reaching ultimate sensitivity of nearly 20 Hz/$\mu\varepsilon$. In addition, Streque et al. [294] managed to fabricate a high-Q SAWR using an AlN/sapphire structure for wireless monitoring of temperatures up to 400 °C. Gao et al. [295] presented a high-sensitivity temperature measurement technique by processing SAW data via adaptive least mean square (LMS) algorithm. They reported excellent accuracy of ±0.2 °C within a range of −30 °C to 100 °C. Very recently, Zhou et al. [296] suggested a new design of a multilayer SAW sensor for ultrahigh-temperature environments. In the low-temperature range (100 °C–400 °C), a sensitivity of 0.72 kHz/°C was observed, increasing first to 2.01 kHz/°C for the mid-temperature range (400 °C–900 °C) and then to 4.38 kHz/°C for the high-temperature range

(900 °C–1300 °C). In a more recent study, Zhou et al. [297] developed an anti-irradiation SAW temperature sensor using 128° YX $LiNbO_3$ single crystal, recording a maximum frequency shift of 0.38% under γ-ray irradiation.

These advancements in SAW temperature sensing at material and device levels have unlocked new opportunities for completely remote monitoring applications under severe conditions. Using this technology, researchers worked on upgrading conventional industrial machines and complex processes in metallurgical and ceramic manufacturing with online temperature monitoring systems [298], [299]. Moreover, applications in high-voltage powerline monitoring and fault detection systems were achieved using wireless SAW temperature sensing [300]. Besides the digitalization of classical industrial processes, Furniss et al. [301] presented a wireless monitoring system using an SAW strain sensor to be operated under cryogenic conditions in aerospace and marine applications. Later, Hu et al. [302] developed a wireless fault detection system for aerospace vehicles based on an L-band SAWR deposited by electron-beam lithography on a 128° Y-X $LiNbO_3$ substrate. They reported a strain sensitivity of −831 Hz/$\mu\varepsilon$ and a temperature sensitivity of 125.4 kHz/°C in a range of 25 °C–250 °C. Moreover, Kim et al. [303] integrated one- and two-port SAW sensors with magnetic antennas for underground soil temperature testing recording a sensitivity of 0.3 MHz/°C for the single-port SAW and 0.96 MHz/°C for the double-port SAW from 30 °C to 100 °C. Recently, Tomaz et al. [304] presented a microscale analysis of an SAW temperature sensor embedded in additively manufactured parts to produce wireless and passive smart devices. In another study, Leff et al. [305] developed a dual temperature and dynamic strain sensing prototype based on SAW technology for temperatures up to 400 °C. This innovative design highlighted SAW sensors' distinct capabilities for simultaneous measurement of cyclic fatigue loads and thermal shocks in industrial machines to enable noise-reduction techniques and condition-based maintenance.

C. Magnetostrictive (MR) Strain Sensors

In 1842, James P. Joule was the first to discover the magnetostriction effect by investigating the ferromagnetic properties of nickel specimens to explain the magnetization response in accordance with the material's susceptibility and permeability parameters [306]. When an external magnetic field is applied, magnetostrictive elements experience shape deformations due to the alignment of magnetic domains. Therefore, magnetostrictive materials can convert magnetic energy into mechanical energy through the so-called Joule effect. Vice versa, when MR materials are subjected to mechanical strains, the direction and magnitude of the measured magnetic field are affected by the inverse magnetostrictive effect (i.e., the Villari effect) [307]. Due to the bidirectional nature of this energy exchange, magnetostrictive materials can be employed for both actuation and sensing. As illustrated in Fig. 10, the working principle of an MR strain sensor is typically based on the Villari effect and involves the use of a magnetostrictive material that exhibits sufficient magnetomechanical coupling coefficients. The sensor typically consists of a cylinder or a rod of magnetostrictive component, surrounded by a coil of wire connected to a signal amplifier and processing unit to detect changes in the magnetic field as electrical signals. The magnetostrictive element is also coated with a strain-sensitive thin layer of metal or polymer to ensure amplifying detected deformations when subjected to mechanical loads. Permanent magnets can be used to initiate a constant magnetic flux and avoid the influence of unipolar MR characteristics. Alternatively, a sensing chip based on the Hall effect can be implemented for noncontact torque measurement to interpret magnetic inductance variations as output voltage [308], [309].

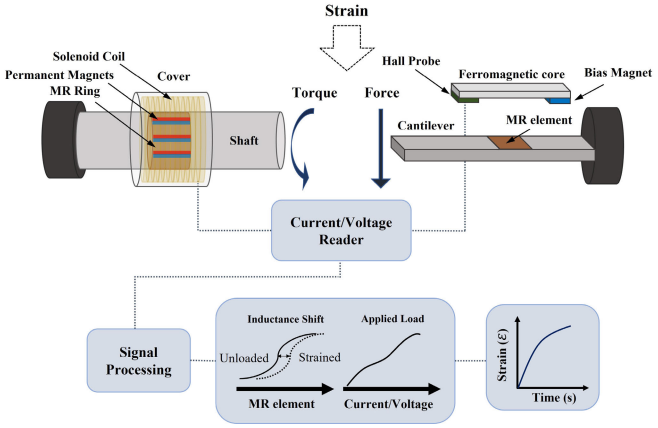

Fig. 10. Schematic of working principle and interrogation system of magnetostrictive strain sensing techniques based on direct pickup coil (left) and Hall effect sensor (right).

In recent years, magnetostrictive materials have been widely implemented as energy harvesters to capture strain-induced vibrations and convert them into usable electrical power for storage [310], [311], [312]. High energy density, low hysteresis, high Curie temperature, and fast response time have made MR devices viable solutions to actuation, sensing, and energy harvesting techniques in SHM, robotics, and aerospace engineering. In terms of strain sensing, these materials can undergo a large elongation range and provide high sensitivity to compete with traditional strain sensing methods. Moreover, MR strain sensors can be a feasible option in difficult locations and real-time monitoring systems due to their passive and wireless interrogation compatibility [313]. However, this passive noncontact technology is vulnerable to magnetic field interference and suffers from complex signal drift at elevated temperatures. This particular disadvantage prevented magnetostrictive strain sensors from being employed in harsh environments across many industrial processes.

Many researchers were fascinated by MR strain sensors' features to create smart composites and intelligent systems in SHM [314], [315], biomedical applications [316], [317], and robotics [153], [318]. On the other hand, abundant studies have concentrated on developing novel composites with improved magnetostriction coupling and higher sensitivity by doping cobalt ferrite ($CoFe_2O_4$) MR material with metal elements (e.g., Cu, Zr, Tb, and Mn) for tuned lattice configuration [319], [320], [321], [322], [323]. More interestingly, other researchers worked on examining new designs and device structures to enhance system accuracy and

applicability. For example, Pepakayala et al. [324] described a resonant wireless strain sensor fabricated from 28-μm-thick foil of Metglas 2826 MB ($Fe_{40}Ni_{38}Mo_4B_{18}$) with differential elements for temperature compensation. This prototype of tracking strain as a resonant frequency shift was designed to offer tunable sensitivity and adjustable dynamic range to meet the requirements of a wide variety of monitoring applications. In addition, Bhame and Joy [325] worked on enhancing strain sensitivity in MR spinel ferrite ($CoFe_2O_4$) by implementing Zn nanopowder. They reported a 30% increase in sensitivity with moderate magnetostriction at room temperature. In a very recent study, Anantharamaiah et al. [326] succeeded in enabling $CoFe_2O_4$ alloy for MR strain sensing applications at lower magnetic fields. By employing the autocombustion method to synthesize Zn-substituted samples, the researchers achieved three times higher sensitivity and a reliable magnetostrictive response.

For robotics and industrial applications, magnetostrictive strain sensors can be employed to develop smart tools and online stress/torque monitoring systems to improve machining precision and process accuracy with minimal interventions. This technology can be achieved passively and wirelessly to examine processes at difficult locations and moving parts to support maintenance and rehabilitation schemes. Sections III-C.1 and III-C.2 provide a review of recent advances in MR strain sensing, focusing on strain sensing mechanisms of force, torque, and pressure, as summarized in Table IV. This survey focuses on innovative solutions that can enable "smart" components and intelligent machines for future factories and digital manufacturing.

1) Force and Torque Sensors: Magnetostrictive force sensors are based on the inverse magnetostriction effect (i.e., the Villari effect), so, when subjected to a mechanical force, their permeability varies, leading to a shift in the magnetic field density that can be translated to the quantity of applied loads. Different investigations of MR force sensors were reported to improve accuracy and enable localized load detection. For example, Ghodsi et al. [327] presented a numerical and experimental analysis of a giant magnetostrictive (GM) force sensor utilizing Terfenol-D and scoring a maximum sensitivity of 0.51 mV/N in a range between 0 and 1000 N. Moreover, Yoffe et al. [328] employed an epoxy-based composite material filled with Terfenol-D particles to create an online stress monitoring approach. This prototype of a thin-layer compressive load sensor was tested, showing considerable viability in real-life applications. Al-Hajjeh et al. [329] proposed an electrically isolated strain sensor based on the Villari effect to analyze different orientations of stress and magnetic susceptibility axes. They proposed an innovative sensing approach that offers wireless and nondestructive monitoring of mechanical stress for smart components and intelligent industrial processes. Moreover, Karafi and Ehteshami [330] developed a composite sensor using a tubular MR rod to monitor torque and axial loads simultaneously. They reported a force sensitivity of 0.012 mV/N under loads of up to 10 kN and a torque sensitivity of 1.18 mV/Nm in a range of up to 20 Nm. Unfortunately, the contactless approach was not achieved due to the hybrid sensor design, and a

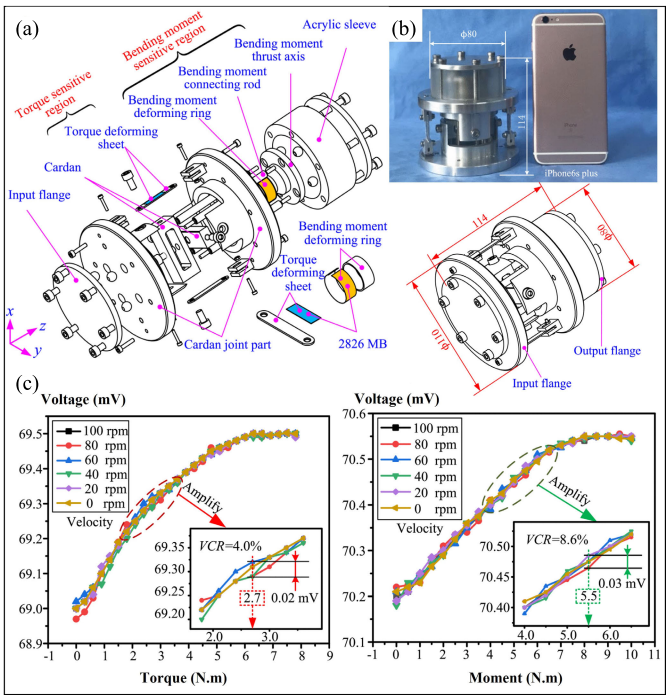

Fig. 11. Torque and moment wireless magnetostrictive strain sensor: (a) schematic of the proposed sensor, (b) fabricated prototype, and (c) sensor response to torque and moment loads under different motor speeds [339].

14.8% FSO nonlinearity error was observed. For feasible tactile systems, Wan et al. [331] developed a cantilever-like tactile sensor based on the inverse-magnetostrictive effect, the flexure mode, and the Jiles–Atherton model for a maximum load of 6 N. More interestingly, Li et al. [332] proposed a novel magnetostrictive tactile sensor for detecting the force and stiffness of manipulated objects. They reported a good prototype of rapid response and force sensitivity of 114 mV/N in a range of 0–5 N, suitable for various robotic applications. In a recent study, Weng et al. [333] developed an MR tactile sensor demonstrating a measurement range of 0–3 N and an average sensitivity of 126 mV/N. The sensing system was built upon permanent magnets, Fe–Ga wires, and Hall sensors to detect static and dynamic forces. In another field, Liang et al. [334] prototyped a new force sensor design using the magnetostrictive DL technique to monitor localized residual stresses on steel surfaces. With uncertainty less than 2%, they reported a nonhysteretic response and an automated measurement approach suitable for several industrial applications, such as additive manufacturing, cold and hot rolling processes, and steel production. Recently, Shu et al. [335] presented an MR impact force sensor based on an Fe–Ga tapered cantilever, reporting nonlinearity errors within 5.8%. They recorded 3.5–34.1 times higher sensitivity compared to the conventional rod configuration. This customized sensor design can provide nondestructive monitoring of static and dynamic loads for an insight-based analysis of machine noise and vibrations. In a very recent study, Ren et al. [336] presented a moment and axial force sensing technique using a self-decoupled, passive, and wireless magnetostrictive sensor. By mounting differential MR components into the mechanical structure of a joint ball bearing, they managed to record the moment and thrust loads

TABLE IV
SUMMARY OF RECENT APPLICATIONS OF MAGNETOSTRICTIVE STRAIN SENSORS WITH THE REPORTED APPLICATION RANGE AND MAXIMUM SENSITIVITY

Strain Sensor	Application	Range	Max. Sensitivity	Ref.
MR Force-Torque Sensors	Online dual monitoring for smart tools and manufacturing processes	F = 0 – 3,432.33 N M = 0 – 20 Nm	F = 0.0749 mV/N M = 2.24 mV/Nm	[343]
	Online dual monitoring for smart tools and manufacturing processes	F = 0 – 10,000 N M = 0 – 20 Nm	F = 0.012 mV/N M = 1.18 mV/Nm	[330]
MR Force Sensors	Tactile sensing in robotic manipulations	0 – 3 N	23.86 mV/N	[154]
	Tactile sensing in robotic manipulations	0 – 3 N	126 mV/N	[333]
	Tactile sensing in robotic manipulations	0 – 5 N	114 mV/N	[332]
	Non-destructive load monitoring in industrial processes and SHM	0 – 1,000 N	0.51 mV/N	[327]
	Non-destructive load monitoring in industrial processes and SHM	0 – 1,000 N	0.40 mV/N	[372]
MR Torque Sensors	Online torque measurement in robotic arms and machine spindles	± 4 Nm	45 mV/Nm	[346]
	Wireless torque monitoring in rotary machines and industrial motors' shafts	0 – 16 Nm	2.87 mV/Nm	[352]
	Wireless torque monitoring in rotary machines and industrial motors' shafts	0 – 16.947 Nm	88.51 mV/Nm	[345]
	Contactless torque monitoring in solid shafts and heavy-duty equipment	9.71 – 93.35 Nm	17.7 mV/Nm	[348]
	Contactless torque monitoring in solid shafts and heavy-duty equipment	± 100 Nm	3.8 mV/Nm	[352]
MR Pressure Sensors	Contactless pressure monitoring in industrial and automotive applications	0 – 300 kPa	0.079 %/kPa	[357]

independently as output voltage. In their following study [337], the prototype was instrumented to a machine tool spindle for cutting load measurement. By applying MR materials to the force- and torque-sensitive regions, excellent decoupling was achieved. Earlier, Tan et al. [338] demonstrated a 2-D MR stress sensor for long-term detection of mechanical loads within moving objects in robots and industrial machines. The proposed sensing method achieved an effective measurement range of 0–40 N for the tension force and 0–4 Nm for the applied moment. Very recently, the same group [339] developed a bending moment and torque measurement approach for industrial applications. By integrating magnetostrictive material with a cardan-type structure of flexible ring and thin sheet assembly (see Fig. 11), the authors managed to establish a self-decoupled and self-powered system to detect dynamic loads during machining and metal-cutting processes. At the system level, Apicella et al. [340] presented a novel mapping technique with a completely passive force sensor based on the inverse magnetostriction effect to increase the sensing accuracy in applications such as robotics, SHM, and metal-cutting processes. Moreover, Talebian [341] investigated the linearity and bias in the magnetic field under different ranges using a force sensor model based on Terfenol-D as a GM material. Shi et al. [342] developed a high-linearity and large-range force detection method using a system of Hall element and GM material. In a range of up to 1000 N, they scored a load sensitivity of 0.337 mV/N with a bias current of 1.2 A and a preload of 120 N. Very recently, Mirzamohamadi et al. [343] utilized Galfenol to fabricate an MR force–torque sensor for contactless monitoring in industrial tools and manufacturing applications. With carful calibration, they reported maximum sensitivity of 0.0749 and 2.24 mV/Nm for axial and torsional loads, respectively.

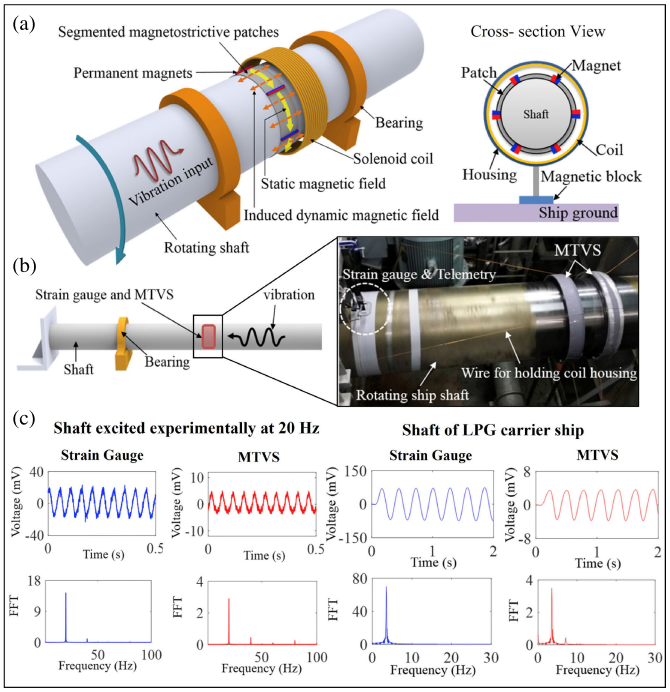

Fig. 12. Magnetostrictive torsional vibration sensor (MTVS): (a) schematic of the proposed sensor design and installation, (b) schematic description of setup work principle and final sensing system, and (c) MTV versus strain gauge calibration and dynamic testing results on propeller shaft of an 84 000-m^3 LPG carrier [347].

Magnetostrictive strain sensors have also shown magnificent results in torsional vibration detection and torque monitoring systems. Earlier, Rao et al. [344] worked on enhancing the MR performance of Co–Mn alloy synthesized via conventional ceramic technique. The authors proposed a new prototype to develop an applicable shaft-torque monitoring

method for automotive and industrial applications involving heavy-duty motors and engines. Raghunath et al. [345] prototyped a noncontact torque measurement sensor utilizing Galfenol strips and the Hall effect, acquiring a torque sensitivity of 88.51 mV/Nm in a range of 0–16.95 Nm. This contactless technology can be a good candidate for many tools and components that require preventive actions against machine malfunctions and excessive loads. Moreover, Muro et al. [346] designed a robust torque sensor made of a $Fe_{49}Co_{49}V_2$ magnetostrictive ring and instrumented to a rigid shaft. By employing differential detection and signal conditioning techniques, they attained a maximum sensitivity of 45 mV/Nm and a range of ±4 Nm with controlled temperature shifts. In very interesting research, Lee et al. [347] established a passive, real-time, and intelligent health monitoring system using MR elements to catch the torsional vibrations of a rotating shaft. The magnetostrictive ribbons were integrated with compact magnets and encapsulated by a solenoid coil to record strains as electrical voltage (see Fig. 12). This prototype was investigated in a real-life propulsion shaft of a carrier ship and compared against traditional stain gauges. This work offered a viable technique to support condition-based maintenance and early fault detection systems by tracking component vibrations. Later, Huang et al. [348] reported an online torque monitoring approach relying on advanced ML models to harvest magnetization vector deflection angle and different torsional loads. The authors recorded a maximum torque sensitivity of 17.7 mV/Nm and a nonlinearity error of 0.77% FS in a range from 9.71 to 93.35 Nm. This design can be vital in creating fault-diagnosis intelligent systems and analyzing the mechanical power of classical drive shafts to reveal transmission efficiency and operating conditions. Recently, Hein et al. [349] achieved a successful magnetostrictive torque measurement approach applicable to several applications in rotary machines. Using Galfenol and rotating cylinder electrode (RCE) deposition, the sensing element was fabricated circumferentially, leading to a 260% increase in susceptibility and a 150% increase in torque response. In a later study, Beirle and Seemann [350] managed to build a remote torque sensor fabricated from $Fe_{32}Co_{46}Hf_{11}N_{12}$ and $Fe_{40}Co_{37}Zr_{11}N_{12}$ thin films, reaching sensitivity near 10 MHz/Nm in a range of 0–100 Nm. In another attempt, Xu et al. [351] equipped a solid rotating shaft with a magnetostrictive ring and eight permanent magnets for torque measurement and twist angle detection. With an error of less than 1%, this configuration was appropriate for both static and dynamic conditions. Very recently, Niu et al. [352] presented a noncontact torque sensing method that depends on $Fe_{30}Co_{70}$ MR material, achieving a sensitivity of 2.87 mV/Nm and a range of 0–16 Nm. This study confirms again the magnetostrictive strain sensors' unique capabilities for building remote torque monitoring systems for high-speed and heavy-duty industrial parts in numerous applications.

2) Pressure Sensors: Despite relatively good temperature stability and a high Curie temperature, magnetostrictive strain sensors are prone to significant signal drifts and material degradation in harsh environments. Besides thermal-induced strains, these devices experience complicated thermomagnetic

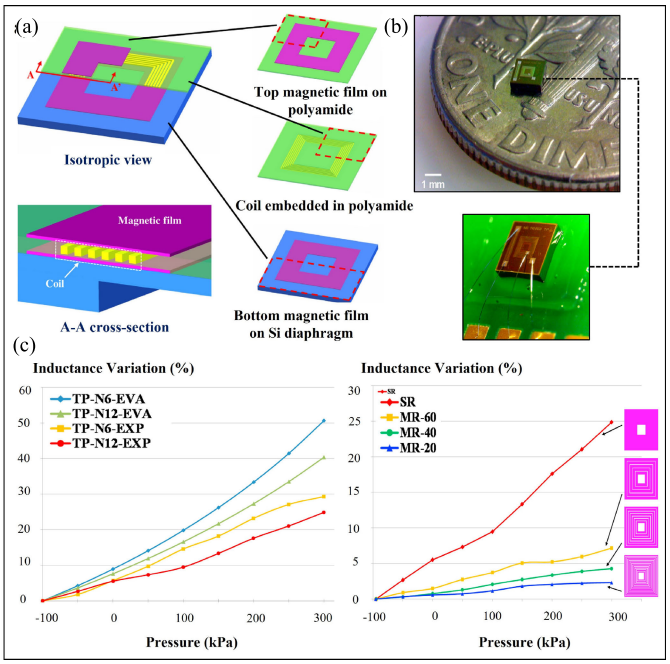

Fig. 13. Magnetostrictive type inductive sensing pressure sensor: (a) schematic of the proposed sensor design, and fabrication procedure, (b) fabricated magnetostrictive pressure sensor, and (c) sensor response to pressure loads and the results of different coil designs of the proposed prototype [357].

effects and changes in their temperature-driven parameters. While wireless long-term near-field thermometry is a fascinating topic, the thermal behavior of magnetostrictive alloys has not been explored yet. On the other hand, some researchers were inspired by the MR strain sensing techniques to construct wireless pressure monitoring systems suitable for various microscale industrial applications, such as microfluidics, humanoid robotics, and minimally invasive procedures. For instance, Aragón et al. [353] developed an MR microwires-based ring to track changes in fluid pressure flowing through a flexible pipeline for wireless localized monitoring. The researchers achieved an inexpensive and robust approach suitable for controlling hydraulic circuits in low-pressure industrial and biomedical applications. Later, Löffler et al. [354] created a batteryless miniaturized pressure sensor by integrating a magnetostrictive microcantilever with a magnetized membrane to harvest delicate pressure-induced strains. In a later study, Park et al. [355] introduced an MR pressure sensor that relies on the magnetomechanical transduction of NWs' array of $Fe_{80}Ga_{20}$ material. NWs' deflections under applied mechanical strains were interpreted as pressure measurements. This study again focused on low-pressure monitoring necessary for advanced technologies in microfluidics and microfabrication.

In terms of high-pressure applications, Chang et al. [356] described a pressure sensor design that contains a planar coil and magnetostrictive material to collect pressure loads. In their next study [357], they built a wireless MR inductive pressure sensor with enhanced sensitivity based on the inverse-magnetostrictive principle (see Fig. 13). Their prototype was fabricated and tested with different designs of coil turns and magnetic films using a setup of pressurized

TABLE V
COMPARISON BETWEEN MODERN INDUSTRIAL STRAIN SENSING TECHNOLOGIES

Technology	Pros	Cons	Featured Applications
FBG sensors	• Excellent durability and ultrahigh sensitivity. • Wide measurement range (broad spectrum). • Single-point and distributed sensing. • Immunity to high-temperatures and electromagnetic interference. • Simultaneous loads and temperature measurement. • Compactness and nonelectrical operation. • Intrinsically safe and nonreactive.	• Bulkiness and wiring and installation requirements. • Physical light source and complex processing system. • Fragility and relatively higher footprint. • Temperature compensation and signal decoupling requirements. • Higher installation and interrogation costs.	• Cutting force sensing and online process monitoring systems. • Manufacturing robots and robotic assisted minimally invasive applications. • Pipeline corrosion monitoring and leakage detection systems. • Liquid-level sensing techniques and smart flowmeters.
SAW sensors	• Good reliability and high sensitivity. • High response and wide dynamic range. • Immunity to high levels of radiation and electromagnetic interference. • Dual loads and temperature monitoring. • In-situ thermal cross-effect compensation. • Passive and wireless interrogation. • Applicability to complex geometries and minimal footprint. • Wafer-scale manufacturing and affordable processing system.	• Sensitive to fabrication quality and crystal selection. • Adhesive aging and signal drifting. • Mounting and packaging requirements. • Unstandardized calibration procedures and complex dynamic behaviour. • Limited distributed sensing based on wireless interrogation range. • Measurements decoupling and temperature compensation requirements. • Relatively high interrogation costs.	• Manufacturing process monitoring in the metal cutting processes (e.g., milling and turning). • Torsional vibrations and torque measurement systems in the automotive and rotary machines. • Smart tools and remote load-temperature monitoring in health monitoring systems. • Wireless pressure/temperature online monitoring in harsh environments. • Ultrahigh temperature tracking in the thermal treatment vessels and combustion engines. • Simultaneous multi-sensing of loads, chemicals, and magnetic field intensity.
MR devices	• Fast response and feasible installation. • Wireless interrogation compatibility. • Low hysteresis and temperature stability. • Simple acquisition hardware. • Passive and non-contact performance. • Non-destructive monitoring in difficult location and complicated structures. • Minimal depreciation and longer lifespan.	• Sensitivity to magnetic interference. • Complex thermomagnetic behavior. • Relatively higher material costs. • Magnetic field saturation and temperature drift effects. • Relatively lower sensitivity. • Limited temperature applicability (below Curie Temperature).	• Thrust and torsional loads monitoring in the automotive and industrial systems. • Torque and speed remote monitoring systems for heavy-duty rotating machines. • Micro-scale pressure monitoring in robotics and minimal intervention procedures. • Non-destructive high-pressure monitoring in industrial processes.

nitrogen gas. They recorded a maximum pressure sensitivity of 0.079 %/kPa under pressures of up to 300 kPa and a gauge factor that is 12 times greater than that of traditional piezoelectric pressure transducers. Very recently, Liu et al. [358] proposed a resonant pressure sensor based on the magnetostriction effect induced in magnetostrictive/piezoelectric material. An assembly of a Terfenol-D bar and PZT-5 elements was designed and tested, reaching a pressure sensitivity of 11.63 Hz/kPa in a range of 0–360 kPa. Despite insufficient literature, these studies have shown promising results of wireless pressure sensing across industrial and automotive applications where conventional sensing methods cannot be used.

IV. CONCLUSION AND OUTLOOK

The development of smart tools and intelligent systems has had a substantial impact on the future of global manufacturing. The concept of a ‘’smart” future factory adopted in the Industry 4.0 paradigm connects both physical and cyber innovations to enhance the productivity, reliability, and operability of manufacturing units in the era of the IoT. Sensors, which are the physical building blocks of robotics and automated systems, have offered a great opportunity to intellectualize classical machines and equip industrial processes with real-time monitoring and ultraprecise tooling. In this review article, modern industrial strain sensors, including FBG sensors, SAW sensors, and magnetostrictive sensors (MRs), are reviewed, focusing on innovative solutions for capturing mechanical and thermal strain data. As illustrated in Table V, the key advantages and major limitations of industrial strain sensors are summarized, showing featured applications in a wide range of industries.

While FBGs have been extensively reviewed compared to other technologies, many efforts are still needed to address several difficulties at the device and system levels. With a blatant tradeoff between the maximum attainable sensitivity and the application range, future work must focus on developing genuine structures and engineering FBG cores to amplify collected strains and expand the elongation range. In addition to temperature compensation and crosstalk issues, the virtue of FBGs’ distributed sensing is typically tackled by wiring infrastructure and costly processing hardware. Therefore, more innovative designs for viable differential sensing and localized signal decoupling are necessary for robustness and accuracy. Researchers should also work on reducing strain data processing burdens for more efficient FBG multiplexing and multimodal sensing. By seizing the current “hype” about data science and AI, advanced models of sophisticated ML algorithms can be coded to optimize computational power and time requirements. Regarding complete applications, FBGs were widely employed in numerous fields as force, torque, pressure, liquid-level, and flow sensors. From robotic manipulations and minimally invasive procedures to industrial process monitoring and “smart” flowmeters, FBG strain sensors offer ultrahigh sensitivity and a wide range of simultaneous online measurements. Unfortunately, device bulkiness and the need for a physical broadband light source are still major drawbacks

preventing FBGs from being equipped with rotating components and tight spaces.

On the other hand, SAWs have a set of unique properties compared to other industrial strain sensing mechanisms. Besides their few-millimeter footprint, SAW strain sensors can be operated wirelessly and passively in difficult locations and on rotating shafts. SAWs also offer excellent immunity to the most severe environments of destructive irradiations and ultrahigh temperatures. However, this technology is poorly addressed in the literature, especially in the mechanical strain sensing field. Unlike FBGs, more serious investigations are needed to explore this younger technology. Enhancing materials' piezoelectricity, strain amplification structures, dynamic performance analysis, and high-quality microfabrication are some challenges to be met at the device level. More importantly, standardized calibration procedures and innovative solutions to minimize temperature drift, cross-sensitivity, and adhesive aging effects are still essential for SAWs' commercialization. Researchers need to acquire a full understanding of device hysteresis and residual stresses associated with mounting and packaging procedures. From a broader perspective, SAWs have shown promising potential in process monitoring and fault-diagnosis systems; however, issues such as reliable wireless communication and sufficient interrogation range are still unsolved.

Magnetostrictive (MR) strain sensors are great solutions for batteryless and contactless measurement systems suitable for nondestructive monitoring. In different automotive and industrial applications, MRs have been successfully implemented as force and torque sensors for monitoring shaft torsional loads and motor mechanical power. Features such as responsiveness, low hysteresis, durability, and simple interrogation circuits have made them able to compete with other sensing technologies, especially when high installation and interrogation costs need to be avoided. Among their various properties, MRs' high energy density was the most attractive reason for researchers to work on developing reliable energy harvesters and actuators. Similar to SAWs, however, MR strain sensors are not addressed adequately and require additional studies. While some publications dealt with proposing novel composites and chemically enabled MR alloys, more investigations are needed to create cost-effective models and maximize magnetostriction coupling coefficients. In-depth studies on magnetron sputtering and metal doping techniques, as well as nanomaterial-based MR components, are still important for achieving higher sensitivity and more efficient MR devices. Other interesting topics such as thermomagnetic effects, temperature compensation, signal interference, and magnetic field saturation have not been fairly explored yet. Hence, breakthroughs in MR material and device improvements can lead to a giant leap in wireless and passive measurement techniques, allowing for the harvesting of valuable data in medical and industrial applications.

Several prototypes were reported showing promising results for FBGs, SAWs, and MRs in numerous applications. However, for all these sensing technologies, consistent strain sensitivity, device miniaturization, multimodal sensing, standardized calibration, wider applicability, and cost-effective high-volume fabrication are still major barriers ahead. To accelerate the development of self-learning and sustainable industrial systems, a sophisticated design based on one or a combination of these modern techniques can upgrade a variety of conventional processes into an automated facility. Many studies have also shown the exceptional potential of industrial strain sensors in improving detection accuracy, reducing hysteresis, and establishing efficient compensation and decoupling techniques for robotics and manufacturing tools. Moreover, these strain sensing mechanisms can play a significant role in future factories by providing an online monitoring system to optimize available resources and support condition-based maintenance. Nevertheless, from nanotechnology to AI, the winding path to "smart" manufacturing must first be paved with innovative solutions to many challenges at both device and system levels.

REFERENCES

[1] S. Timoshenko, *History of Strength of Materials: With a Brief Account of the History of Theory of Elasticity and Theory of Structures*. Chelmsford, MA, UA: Courier Corporation, 1983.

[2] R. B. Hetnarski and J. Ignaczak, "Mathematical theory of elasticity," *J. Thermal Stresses*, vol. 29, no. 5, pp. 505–506, May 2006, doi: 10.1080/01495730500495751.

[3] M. A. Khan, J. Sun, B. Li, A. Przybysz, and J. Kosel, "Magnetic sensors—A review and recent technologies," *Eng. Res. Exp.*, vol. 3, no. 2, Jun. 2021, Art. no. 022005, doi: 10.1088/2631-8695/ac0838.

[4] S. Gholizadeh, Z. Leman, and B. T. H. T. Baharudin, "A review of the application of acoustic emission technique in engineering," *Struct. Eng. Mech.*, vol. 54, no. 6, pp. 1075–1095, Jun. 2015, doi: 10.12989/sem.2015.54.6.1075.

[5] G. Wild and S. Hinckley, "Acousto-ultrasonic optical fiber sensors: Overview and state-of-the-art," *IEEE Sensors J.*, vol. 8, no. 7, pp. 1184–1193, Jul. 2008, doi: 10.1109/JSEN.2008.926894.

[6] B. H. Lee et al., "Interferometric fiber optic sensors," *Sensors*, vol. 12, no. 3, pp. 2467–2486, Feb. 2012, doi: 10.3390/s120302467.

[7] Y.-J. Rao, "Recent progress in fiber-optic extrinsic Fabry–Perot interferometric sensors," *Opt. Fiber Technol.*, vol. 12, no. 3, pp. 227–237, Jul. 2006, doi: 10.1016/j.yofte.2006.03.004.

[8] J. W. Berthold, "Historical review of microbend fiber-optic sensors," *J. Lightw. Technol.*, vol. 13, no. 7, pp. 1193–1199, Jul. 1995, doi: 10.1109/50.400697.

[9] B.-O. Guan, L. Jin, Y. Zhang, and H.-Y. Tam, "Polarimetric heterodyning fiber grating laser sensors," *J. Lightw. Technol.*, vol. 30, no. 8, pp. 1097–1112, Apr. 2012, doi: 10.1109/JLT.2011.2171916.

[10] A. Masoudi and T. P. Newson, "Contributed review: Distributed optical fibre dynamic strain sensing," *Rev. Sci. Instrum.*, vol. 87, no. 1, Jan. 2016, Art. no. 011501, doi: 10.1063/1.4939482.

[11] A. Ukil, H. Braendle, and P. Krippner, "Distributed temperature sensing: Review of technology and applications," *IEEE Sensors J.*, vol. 12, no. 5, pp. 885–892, May 2012, doi: 10.1109/JSEN.2011.2162060.

[12] O. Almubaied, H. K. Chai, M. R. Islam, K.-S. Lim, and C. G. Tan, "Monitoring corrosion process of reinforced concrete structure using FBG strain sensor," *IEEE Trans. Instrum. Meas.*, vol. 66, no. 8, pp. 2148–2155, Aug. 2017, doi: 10.1109/TIM.2017.2676218.

[13] L. Shu, B. Peng, Z. Yang, R. Wang, S. Deng, and X. Liu, "High-temperature SAW wireless strain sensor with langasite," *Sensors*, vol. 15, no. 11, pp. 28531–28542, Nov. 2015, doi: 10.3390/s151128531.

[14] A. Sofi, J. Jane Regita, B. Rane, and H. H. Lau, "Structural health monitoring using wireless smart sensor network—An overview," *Mech. Syst. Signal Process.*, vol. 163, Jan. 2022, Art. no. 108113, doi: 10.1016/j.ymssp.2021.108113.

[15] C. O'Connor and A. Kiourti, "Wireless sensors for smart orthopedic implants," *J. Bio-Tribo-Corrosion*, vol. 3, no. 2, p. 20, Mar. 2017, doi: 10.1007/s40735-017-0078-z.

[16] M. Ramakrishnan, G. Rajan, Y. Semenova, and G. Farrell, "Overview of fiber optic sensor technologies for strain/temperature sensing applications in composite materials," *Sensors*, vol. 16, no. 1, p. 99, Jan. 2016, doi: 10.3390/s16010099.

[17] C. W. Smelser, D. Grobnic, and Stephen. J. Mihailov, "High-reflectivity thermally stable ultrafast induced fiber Bragg gratings in H_2-loaded SMF-28 fiber," *IEEE Photon. Technol. Lett.*, vol. 21, no. 11, pp. 682–684, Jun. 2009, doi: 10.1109/LPT.2009.2016352.

[18] H. Park, H. Lee, S. Choi, and Y. Kim, "A practical monitoring system for the structural safety of mega-trusses using wireless vibrating wire strain gauges," *Sensors*, vol. 13, no. 12, pp. 17346–17361, Dec. 2013, doi: 10.3390/s131217346.

[19] X. Liao, Z. Zhang, Z. Kang, F. Gao, Q. Liao, and Y. Zhang, "Ultrasensitive and stretchable resistive strain sensors designed for wearable electronics," *Mater. Horizons*, vol. 4, no. 3, pp. 502–510, 2017, doi: 10.1039/C7MH00071E.

[20] L. E. Fissi, A. Jaouad, D. Vandormael, and L. A. Francis, "Fabrication of new interdigital transducers for surface acoustic wave device," *Phys. Proc.*, vol. 70, pp. 936–940, Jan. 2015, doi: 10.1016/j.phpro.2015.08.194.

[21] X. Liao, Z. Zhang, Q. Liang, Q. Liao, and Y. Zhang, "Flexible, cuttable, and self-waterproof bending strain sensors using microcracked gold Nanofilms@Paper substrate," *ACS Appl. Mater. Interfaces*, vol. 9, no. 4, pp. 4151–4158, Feb. 2017, doi: 10.1021/acsami.6b12991.

[22] X. Liao, W. Wang, L. Wang, K. Tang, and Y. Zheng, "Controllably enhancing stretchability of highly sensitive fiber-based strain sensors for intelligent monitoring," *ACS Appl. Mater. Interfaces*, vol. 11, no. 2, pp. 2431–2440, Jan. 2019, doi: 10.1021/acsami.8b20245.

[23] R. G. Azevedo et al., "A SiC MEMS resonant strain sensor for harsh environment applications," *IEEE Sensors J.*, vol. 7, no. 4, pp. 568–576, Apr. 2007, doi: 10.1109/JSEN.2007.891997.

[24] N. Chaimanonart and D. J. Young, "Remote RF powering system for wireless MEMS strain sensors," *IEEE Sensors J.*, vol. 6, no. 2, pp. 484–489, Apr. 2006, doi: 10.1109/JSEN.2006.870158.

[25] A. Kumar, M. Prasad, V. Janyani, and R. P. Yadav, "Design, fabrication and reliability study of piezoelectric ZnO based structure for development of MEMS acoustic sensor," *Microsyst. Technol.*, vol. 25, no. 12, pp. 4517–4528, Dec. 2019, doi: 10.1007/s00542-019-04524-x.

[26] H. Ohno, H. Naruse, M. Kihara, and A. Shimada, "Industrial applications of the BOTDR optical fiber strain sensor," *Opt. Fiber Technol.*, vol. 7, no. 1, pp. 45–64, Jan. 2001, doi: 10.1006/ofte.2000.0344.

[27] V. Tsouti, V. Mitrakos, P. Broutas, and S. Chatzandroulis, "Modeling and development of a flexible carbon black-based capacitive strain sensor," *IEEE Sensors J.*, vol. 16, no. 9, pp. 3059–3067, May 2016, doi: 10.1109/JSEN.2016.2524508.

[28] X. Liao et al., "A highly stretchable ZnO@Fiber-based multifunctional nanosensor for strain/temperature/UV detection," *Adv. Funct. Mater.*, vol. 26, no. 18, pp. 3074–3081, May 2016, doi: 10.1002/adfm.201505223.

[29] D. Tosi, "Review and analysis of peak tracking techniques for fiber Bragg grating sensors," *Sensors*, vol. 17, no. 10, p. 2368, Oct. 2017, doi: 10.3390/s17102368.

[30] O. Xu et al., "A multi-peak detection algorithm for fiber Bragg grating sensing systems," *Opt. Fiber Technol.*, vol. 58, Sep. 2020, Art. no. 102311, doi: 10.1016/j.yofte.2020.102311.

[31] S. Sarkar, D. Inupakutika, M. Banerjee, M. Tarhani, and M. Shadaram, "Machine learning methods for discriminating strain and temperature effects on FBG-based sensors," *IEEE Photon. Technol. Lett.*, vol. 33, no. 16, pp. 876–879, Aug. 15, 2021, doi: 10.1109/LPT.2021.3055216.

[32] J. Devkota, P. Ohodnicki, and D. Greve, "SAW sensors for chemical vapors and gases," *Sensors*, vol. 17, no. 4, p. 801, Apr. 2017, doi: 10.3390/s17040801.

[33] C. Y. Bing, A. A. Mohanan, T. Saha, R. N. Ramanan, R. Parthiban, and N. Ramakrishnan, "Microfabrication of surface acoustic wave device using UV LED photolithography technique," *Microelectronic Eng.*, vol. 122, pp. 9–12, Jun. 2014, doi: 10.1016/j.mee.2014.03.011.

[34] A. Tavassolizadeh et al., "Tunnel magnetoresistance sensors with magnetostrictive electrodes: Strain sensors," *Sensors*, vol. 16, no. 11, p. 1902, Nov. 2016, doi: 10.3390/s16111902.

[35] C. Gao, Z. Zeng, S. Peng, and C. Shuai, "Magnetostrictive alloys: Promising materials for biomedical applications," *Bioactive Mater.*, vol. 8, pp. 177–195, Feb. 2022, doi: 10.1016/j.bioactmat.2021.06.025.

[36] U. Yaqoob and M. I. Younis, "Chemical gas sensors: Recent developments, challenges, and the potential of machine learning—A review," *Sensors*, vol. 21, no. 8, p. 2877, Apr. 2021, doi: 10.3390/s21082877.

[37] M. W. Hoffmann et al., "Integration of novel sensors and machine learning for predictive maintenance in medium voltage switchgear to enable the energy and mobility revolutions," *Sensors*, vol. 20, no. 7, p. 2099, Apr. 2020, doi: 10.3390/s20072099.

[38] E. Blasch et al., "Machine learning/artificial intelligence for sensor data fusion-opportunities and challenges," *IEEE Aerosp. Electron. Syst. Mag.*, vol. 36, no. 7, pp. 80–93, Jul. 2021, doi: 10.1109/MAES.2020.3049030.

[39] R. Elhajjar, C.-T. Law, and A. Pegoretti, "Magnetostrictive polymer composites: Recent advances in materials, structures and properties," *Prog. Mater. Sci.*, vol. 97, pp. 204–229, Aug. 2018, doi: 10.1016/j.pmatsci.2018.02.005.

[40] M. E. Morales-Rodríguez, P. C. Joshi, J. R. Humphries, P. L. Fuhr, and T. J. Mcintyre, "Fabrication of low cost surface acoustic wave sensors using direct printing by aerosol inkjet," *IEEE Access*, vol. 6, pp. 20907–20915, 2018, doi: 10.1109/ACCESS.2018.2824118.

[41] R. Behanan et al., "Thin films and techniques for SAW sensor operation above 1000 °C," in *Proc. IEEE Int. Ultrason. Symp. (IUS)*, Jul. 2013, pp. 1013–1016, doi: 10.1109/ULTSYM.2013.0260.

[42] M. Javaid, A. Haleem, R. P. Singh, S. Rab, and R. Suman, "Significance of sensors for Industry 4.0: Roles, capabilities, and applications," *Sensors Int.*, vol. 2, Jan. 2021, Art. no. 100110, doi: 10.1016/j.sintl.2021.100110.

[43] M. Fakam, M. Hecquet, V. Lanfranchi, and A. Randria, "Design and magnetic noise reduction of the surface permanent magnet synchronous machine using complex air-gap permeance," *IEEE Trans. Magn.*, vol. 51, no. 4, pp. 1–9, Apr. 2015, doi: 10.1109/TMAG.2014.2360315.

[44] W. Zhang, W. Chen, Y. Shu, J. Wu, and X. Lei, "Degradation of sensing properties of fiber Bragg grating strain sensors in fatigue process of bonding layers," *Opt. Eng.*, vol. 53, no. 4, Apr. 2014, Art. no. 046102, doi: 10.1117/1.OE.53.4.046102.

[45] A. Maskay, D. M. Hummels, and M. P. da Cunha, "SAWR dynamic strain sensor detection mechanism for high-temperature harsh-environment wireless applications," *Measurement*, vol. 126, pp. 318–321, Oct. 2018, doi: 10.1016/j.measurement.2018.05.073.

[46] L. S. Dalenogare, G. B. Benitez, N. F. Ayala, and A. G. Frank, "The expected contribution of Industry 4.0 technologies for industrial performance," *Int. J. Prod. Econ.*, vol. 204, pp. 383–394, Oct. 2018, doi: 10.1016/j.ijpe.2018.08.019.

[47] A. Schütze, N. Helwig, and T. Schneider, "Sensors 4.0—Smart sensors and measurement technology enable Industry 4.0," *J. Sensors Sensor Syst.*, vol. 7, no. 1, pp. 359–371, May 2018, doi: 10.5194/jsss-7-359-2018.

[48] M. Majid et al., "Applications of wireless sensor networks and Internet of Things frameworks in the industry revolution 4.0: A systematic literature review," *Sensors*, vol. 22, no. 6, p. 2087, Mar. 2022, doi: 10.3390/s22062087.

[49] D. Catenazzo, B. OrFlynn, and M. Walsh, "On the use of wireless sensor networks in preventative maintenance for Industry 4.0," in *Proc. 12th Int. Conf. Sens. Technol. (ICST)*, Dec. 2018, pp. 256–262, doi: 10.1109/ICSensT.2018.8603669.

[50] T. Kalsoom, N. Ramzan, S. Ahmed, and M. Ur-Rehman, "Advances in sensor technologies in the era of smart factory and Industry 4.0," *Sensors*, vol. 20, no. 23, p. 6783, Nov. 2020, doi: 10.3390/s20236783.

[51] A. Varshney et al., "Challenges in sensors technology for industry 4.0 for futuristic metrological applications," *MAPAN*, vol. 36, no. 2, pp. 215–226, Jun. 2021, doi: 10.1007/s12647-021-00453-1.

[52] D. D. L. Chung, "A critical review of piezoresistivity and its application in electrical-resistance-based strain sensing," *J. Mater. Sci.*, vol. 55, no. 32, pp. 15367–15396, Nov. 2020, doi: 10.1007/s10853-020-05099-z.

[53] H. Souri et al., "Wearable and stretchable strain sensors: Materials, sensing mechanisms, and applications," *Adv. Intell. Syst.*, vol. 2, no. 8, Aug. 2020, Art. no. 2000039, doi: 10.1002/aisy.202000039.

[54] N. Afsarimanesh, A. Nag, S. Sarkar, G. S. Sabet, T. Han, and S. C. Mukhopadhyay, "A review on fabrication, characterization and implementation of wearable strain sensors," *Sens. Actuators A, Phys.*, vol. 315, Nov. 2020, Art. no. 112355, doi: 10.1016/j.sna.2020.112355.

[55] K. Singh, S. Sharma, S. Shriwastava, P. Singla, M. Gupta, and C. C. Tripathi, "Significance of nano-materials, designs consideration and fabrication techniques on performances of strain sensors—A review," *Mater. Sci. Semicond. Process.*, vol. 123, Mar. 2021, Art. no. 105581, doi: 10.1016/j.mssp.2020.105581.

[56] X. Liu et al., "Recent progress on smart fiber and textile based wearable strain sensors: Materials, fabrications and applications," *Adv. Fiber Mater.*, vol. 4, no. 3, pp. 361–389, Jun. 2022, doi: 10.1007/s42765-021-00126-3.

[57] A. S. Fiorillo, C. D. Critello, and S. A. Pullano, "Theory, technology and applications of piezoresistive sensors: A review," *Sens. Actuators A, Phys.*, vol. 281, pp. 156–175, Oct. 2018, doi: 10.1016/j.sna.2018.07.006.

[58] H. Liu et al., "3D printed flexible strain sensors: From printing to devices and signals," *Adv. Mater.*, vol. 33, no. 8, Feb. 2021, Art. no. 2004782, doi: 10.1002/adma.202004782.

[59] C. Tawk and G. Alici, "A review of 3D-printable soft pneumatic actuators and sensors: Research challenges and opportunities," *Adv. Intell. Syst.*, vol. 3, no. 6, Jun. 2021, Art. no. 2000223, doi: 10.1002/aisy.202000223.

[60] W. A. D. M. Jayathilaka et al., "Significance of nanomaterials in wearables: A review on wearable actuators and sensors," *Adv. Mater.*, vol. 31, no. 7, Feb. 2019, Art. no. 1805921, doi: 10.1002/adma.201805921.

[61] T. Yan, Z. Wang, and Z.-J. Pan, "Flexible strain sensors fabricated using carbon-based nanomaterials: A review," *Current Opinion Solid State Mater. Sci.*, vol. 22, no. 6, pp. 213–228, Dec. 2018, doi: 10.1016/j.cossms.2018.11.001.

[62] M. J. Yee et al., "Carbon nanomaterials based films for strain sensing application—A review," *Nano-Struct. Nano-Objects*, vol. 18, Apr. 2019, Art. no. 100312, doi: 10.1016/j.nanoso.2019.100312.

[63] W. Obitayo and T. Liu, "A review: Carbon nanotube-based piezoresistive strain sensors," *J. Sensors*, vol. 2012, Feb. 2012, Art. no. e652438, doi: 10.1155/2012/652438.

[64] Z. Wang, Y. Cong, and J. Fu, "Stretchable and tough conductive hydrogels for flexible pressure and strain sensors," *J. Mater. Chem. B*, vol. 8, no. 16, pp. 3437–3459, 2020, doi: 10.1039/C9TB02570G.

[65] H. Liu et al., "Electrically conductive polymer composites for smart flexible strain sensors: A critical review," *J. Mater. Chem. C*, vol. 6, no. 45, pp. 12121–12141, Nov. 2018, doi: 10.1039/C8TC04079F.

[66] G. Li et al., "Development of conductive hydrogels for fabricating flexible strain sensors," *Small*, vol. 18, Feb. 2022, Art. no. 2101518, doi: 10.1002/smll.202101518.

[67] M. Amjadi, K.-U. Kyung, I. Park, and M. Sitti, "Stretchable, skin-mountable, and wearable strain sensors and their potential applications: A review," *Adv. Funct. Mater.*, vol. 26, no. 11, pp. 1678–1698, Mar. 2016, doi: 10.1002/adfm.201504755.

[68] J. Chen et al., "Polydimethylsiloxane (PDMS)-based flexible resistive strain sensors for wearable applications," *Appl. Sci.*, vol. 8, no. 3, p. 345, Feb. 2018, doi: 10.3390/app8030345.

[69] L. Duan, D. R. D'hooge, and L. Cardon, "Recent progress on flexible and stretchable piezoresistive strain sensors: From design to application," *Prog. Mater. Sci.*, vol. 114, Oct. 2020, Art. no. 100617, doi: 10.1016/j.pmatsci.2019.100617.

[70] Y. Wu, Y. Ma, H. Zheng, and S. Ramakrishna, "Piezoelectric materials for flexible and wearable electronics: A review," *Mater. Des.*, vol. 211, Dec. 2021, Art. no. 110164, doi: 10.1016/j.matdes.2021.110164.

[71] A. Qiu, P. Li, Z. Yang, Y. Yao, I. Lee, and J. Ma, "A path beyond metal and silicon: Polymer/nanomaterial composites for stretchable strain sensors," *Adv. Funct. Mater.*, vol. 29, no. 17, Apr. 2019, Art. no. 2101518, doi: 10.1002/adfm.201806306.

[72] M. Cheng et al., "A review of flexible force sensors for human health monitoring," *J. Adv. Res.*, vol. 26, pp. 53–68, Nov. 2020, doi: 10.1016/j.jare.2020.07.001.

[73] Y. Lu, M. C. Biswas, Z. Guo, J.-W. Jeon, and E. K. Wujcik, "Recent developments in bio-monitoring via advanced polymer nanocomposite-based wearable strain sensors," *Biosensors Bioelectron.*, vol. 123, pp. 167–177, Jan. 2019, doi: 10.1016/j.bios.2018.08.037.

[74] S. Yao, P. Swetha, and Y. Zhu, "Nanomaterial-enabled wearable sensors for healthcare," *Adv. Healthcare Mater.*, vol. 7, no. 1, Jan. 2018, Art. no. 1700889, doi: 10.1002/adhm.201700889.

[75] X. Wang, Z. Liu, and T. Zhang, "Flexible sensing electronics for wearable/attachable health monitoring," *Small*, vol. 13, no. 25, Jul. 2017, Art. no. 1602790, doi: 10.1002/smll.201602790.

[76] S. Stassi, V. Cauda, G. Canavese, and C. Pirri, "Flexible tactile sensing based on piezoresistive composites: A review," *Sensors*, vol. 14, no. 3, pp. 5296–5332, Mar. 2014, doi: 10.3390/s140305296.

[77] M. Y. Cao, S. Laws, and F. R. Y. Baena, "Six-axis force/torque sensors for robotics applications: A review," *IEEE Sensors J.*, vol. 21, no. 24, pp. 27238–27251, Dec. 2021, doi: 10.1109/JSEN.2021.3123638.

[78] H. Wang, M. Totaro, and L. Beccai, "Toward perceptive soft robots: Progress and challenges," *Adv. Sci.*, vol. 5, no. 9, Sep. 2018, Art. no. 1800541, doi: 10.1002/advs.201800541.

[79] Y. Zhao, Y. Liu, Y. Li, and Q. Hao, "Development and application of resistance strain force sensors," *Sensors*, vol. 20, no. 20, p. 5826, Oct. 2020, doi: 10.3390/s20205826.

[80] P. Jiao, K.-J.-I. Egbe, Y. Xie, A. M. Nazar, and A. H. Alavi, "Piezoelectric sensing techniques in structural health monitoring: A state-of-the-art review," *Sensors*, vol. 20, no. 13, p. 3730, Jul. 2020, doi: 10.3390/s20133730.

[81] C. Tuloup, W. Harizi, Z. Aboura, Y. Meyer, K. Khellil, and R. Lachat, "On the use of in-situ piezoelectric sensors for the manufacturing and structural health monitoring of polymer-matrix composites: A literature review," *Compos. Struct.*, vol. 215, pp. 127–149, May 2019, doi: 10.1016/j.compstruct.2019.02.046.

[82] S. Das and P. Saha, "A review of some advanced sensors used for health diagnosis of civil engineering structures," *Measurement*, vol. 129, pp. 68–90, Dec. 2018, doi: 10.1016/j.measurement.2018.07.008.

[83] W. Chen and X. Yan, "Progress in achieving high-performance piezoresistive and capacitive flexible pressure sensors: A review," *J. Mater. Sci. Technol.*, vol. 43, pp. 175–188, Apr. 2020, doi: 10.1016/j.jmst.2019.11.010.

[84] A. J. Fleming, "A review of nanometer resolution position sensors: Operation and performance," *Sens. Actuators A, Phys.*, vol. 190, pp. 106–126, Feb. 2013, doi: 10.1016/j.sna.2012.10.016.

[85] H.-P. Phan, D. V. Dao, K. Nakamura, S. Dimitrijev, and N.-T. Nguyen, "The piezoresistive effect of SiC for MEMS sensors at high temperatures: A review," *J. Microelectromech. Syst.*, vol. 24, no. 6, pp. 1663–1677, Dec. 2015, doi: 10.1109/JMEMS.2015.2470132.

[86] Z. H. Khan, A. R. Kermany, A. Öchsner, and F. Iacopi, "Mechanical and electromechanical properties of graphene and their potential application in MEMS," *J. Phys. D, Appl. Phys.*, vol. 50, no. 5, Jan. 2017, Art. no. 053003, doi: 10.1088/1361-6463/50/5/053003.

[87] M. A. Fraga, H. Furlan, R. S. Pessoa, and M. Massi, "Wide bandgap semiconductor thin films for piezoelectric and piezoresistive MEMS sensors applied at high temperatures: An overview," *Microsyst. Technol.*, vol. 20, no. 1, pp. 9–21, Jan. 2014, doi: 10.1007/s00542-013-2029-z.

[88] J. Zhu et al., "Development trends and perspectives of future sensors and MEMS/NEMS," *Micromachines*, vol. 11, no. 1, p. 7, Dec. 2019, doi: 10.3390/mi11010007.

[89] G. L. Smith et al., "PZT-based piezoelectric MEMS technology," *J. Amer. Ceram. Soc.*, vol. 95, no. 6, pp. 1777–1792, Jun. 2012, doi: 10.1111/j.1551-2916.2012.05155.x.

[90] W.-M. Zhang, H. Yan, Z.-K. Peng, and G. Meng, "Electrostatic pull-in instability in MEMS/NEMS: A review," *Sens. Actuators A, Phys.*, vol. 214, pp. 187–218, Aug. 2014, doi: 10.1016/j.sna.2014.04.025.

[91] F. Khoshnoud and C. W. de Silva, "Recent advances in MEMS sensor technology-mechanical applications," *IEEE Instrum. Meas. Mag.*, vol. 15, no. 2, pp. 14–24, Apr. 2012, doi: 10.1109/MIM.2012.6174574.

[92] S. Takamatsu, S. Goto, M. Yamamoto, T. Yamashita, T. Kobayashi, and T. Itoh, "Plastic-scale-model assembly of ultrathin film MEMS piezoresistive strain sensor with conventional vacuum-suction chip mounter," *Sci. Rep.*, vol. 9, no. 1, p. 1893, Feb. 2019, doi: 10.1038/s41598-019-39364-2.

[93] I. S. Bayer, "MEMS-based tactile sensors: Materials, processes and applications in robotics," *Micromachines*, vol. 13, no. 12, p. 2051, Nov. 2022, doi: 10.3390/mi13122051.

[94] S. Yang and Q. Xu, "A review on actuation and sensing techniques for MEMS-based microgrippers," *J. Micro-Bio Robot.*, vol. 13, nos. 1–4, pp. 1–14, Oct. 2017, doi: 10.1007/s12213-017-0098-2.

[95] Y. Wei and Q. Xu, "An overview of micro-force sensing techniques," *Sens. Actuators A, Phys.*, vol. 234, pp. 359–374, Oct. 2015, doi: 10.1016/j.sna.2015.09.028.

[96] P. Song et al., "Recent progress of miniature MEMS pressure sensors," *Micromachines*, vol. 11, no. 1, p. 56, Jan. 2020, doi: 10.3390/mi11010056.

[97] R. B. Mishra, N. El-Atab, A. M. Hussain, and M. M. Hussain, "Recent progress on flexible capacitive pressure sensors: From design and materials to applications," *Adv. Mater. Technol.*, vol. 6, no. 4, Apr. 2021, Art. no. 2001023, doi: 10.1002/admt.202001023.

[98] Y. Javed, M. Mansoor, and I. A. Shah, "A review of principles of MEMS pressure sensing with its aerospace applications," *Sensor Rev.*, vol. 39, no. 5, pp. 652–664, Sep. 2019, doi: 10.1108/SR-06-2018-0135.

[99] F. Ejeian et al., "Design and applications of MEMS flow sensors: A review," *Sens. Actuators A, Phys.*, vol. 295, pp. 483–502, Aug. 2019, doi: 10.1016/j.sna.2019.06.020.

[100] A. Mehmood et al., "Graphene based nanomaterials for strain sensor application—A review," *J. Environ. Chem. Eng.*, vol. 8, no. 3, Jun. 2020, Art. no. 103743, doi: 10.1016/j.jece.2020.103743.

[101] O. Kanoun, A. Bouhamed, R. Ramalingame, J. R. Bautista-Quijano, D. Rajendran, and A. Al-Hamry, "Review on conductive polymer/CNTs nanocomposites based flexible and stretchable strain and pressure sensors," *Sensors*, vol. 21, no. 2, p. 341, Jan. 2021, doi: 10.3390/s21020341.

[102] S. J. Mihailov, "Fiber Bragg grating sensors for harsh environments," *Sensors*, vol. 12, no. 2, pp. 1898–1918, Feb. 2012, doi: 10.3390/s120201898.

[103] D. Tosi, "Review of chirped fiber Bragg grating (CFBG) fiber-optic sensors and their applications," *Sensors*, vol. 18, no. 7, p. 2147, Jul. 2018, doi: 10.3390/s18072147.

[104] J. Albert, L.-Y. Shao, and C. Caucheteur, "Tilted fiber Bragg grating sensors," *Laser Photon. Rev.*, vol. 7, no. 1, pp. 83–108, Jan. 2013, doi: 10.1002/lpor.201100039.

[105] I. Floris, J. M. Adam, P. A. Calderón, and S. Sales, "Fiber optic shape sensors: A comprehensive review," *Opt. Lasers Eng.*, vol. 139, Apr. 2021, Art. no. 106508, doi: 10.1016/j.optlaseng.2020.106508.

[106] C. Broadway, R. Min, A. G. Leal-Junior, C. Marques, and C. Caucheteur, "Toward commercial polymer fiber Bragg grating sensors: Review and applications," *J. Lightw. Technol.*, vol. 37, no. 11, pp. 2605–2615, Jun. 1, 2019, doi: 10.1109/JLT.2018.2885957.

[107] J. K. Sahota, N. Gupta, and D. Dhawan, "Fiber Bragg grating sensors for monitoring of physical parameters: A comprehensive review," *Opt. Eng.*, vol. 59, no. 6, Jun. 2020, Art. no. 060901, doi: 10.1117/1.OE.59.6.060901.

[108] A. Barrias, J. Casas, and S. Villalba, "A review of distributed optical fiber sensors for civil engineering applications," *Sensors*, vol. 16, no. 5, p. 748, May 2016, doi: 10.3390/s16050748.

[109] H. Murayama, D. Wada, and H. Igawa, "Structural health monitoring by using fiber-optic distributed strain sensors with high spatial resolution," *Photonic Sensors*, vol. 3, no. 4, pp. 355–376, Dec. 2013, doi: 10.1007/s13320-013-0140-5.

[110] X. W. Ye, Y. H. Su, and J. P. Han, "Structural health monitoring of civil infrastructure using optical fiber sensing technology: A comprehensive review," *Sci. World J.*, vol. 2014, Jul. 2014, Art. no. e652329, doi: 10.1155/2014/652329.

[111] C. Du, S. Dutta, P. Kurup, T. Yu, and X. Wang, "A review of railway infrastructure monitoring using fiber optic sensors," *Sens. Actuators A, Phys.*, vol. 303, Mar. 2020, Art. no. 111728, doi: 10.1016/j.sna.2019.111728.

[112] D. Kinet, P. Mégret, K. Goossen, L. Qiu, D. Heider, and C. Caucheteur, "Fiber Bragg grating sensors toward structural health monitoring in composite materials: Challenges and solutions," *Sensors*, vol. 14, no. 4, pp. 7394–7419, Apr. 2014, doi: 10.3390/s140407394.

[113] Y. Bao, Y. Huang, M. Hoehler, and G. Chen, "Review of fiber optic sensors for structural fire engineering," *Sensors*, vol. 19, no. 4, p. 877, Feb. 2019, doi: 10.3390/s19040877.

[114] G. Kouroussis, C. Caucheteur, D. Kinet, G. Alexandrou, O. Verlinden, and V. Moeyaert, "Review of trackside monitoring solutions: From strain gages to optical fibre sensors," *Sensors*, vol. 15, no. 8, pp. 20115–20139, Aug. 2015, doi: 10.3390/s150820115.

[115] A. Güemes, A. Fernandez-Lopez, A. R. Pozo, and J. Sierra-Pérez, "Structural health monitoring for advanced composite structures: A review," *J. Compos. Sci.*, vol. 4, no. 1, p. 13, Jan. 2020, doi: 10.3390/jcs4010013.

[116] M. F. Bado and J. R. Casas, "A review of recent distributed optical fiber sensors applications for civil engineering structural health monitoring," *Sensors*, vol. 21, no. 5, p. 1818, Mar. 2021, doi: 10.3390/s21051818.

[117] Y. Zheng, Z.-W. Zhu, W. Xiao, and Q.-X. Deng, "Review of fiber optic sensors in geotechnical health monitoring," *Opt. Fiber Technol.*, vol. 54, Jan. 2020, Art. no. 102127, doi: 10.1016/j.yofte.2019.102127.

[118] C.-Y. Hong, Y.-F. Zhang, M.-X. Zhang, L. M. G. Leung, and L.-Q. Liu, "Application of FBG sensors for geotechnical health monitoring, a review of sensor design, implementation methods and packaging techniques," *Sens. Actuators A, Phys.*, vol. 244, pp. 184–197, Jun. 2016, doi: 10.1016/j.sna.2016.04.033.

[119] H.-F. Pei, J. Teng, J.-H. Yin, and R. Chen, "A review of previous studies on the applications of optical fiber sensors in geotechnical health monitoring," *Measurement*, vol. 58, pp. 207–214, Dec. 2014, doi: 10.1016/j.measurement.2014.08.013.

[120] P. J. Schubel, R. J. Crossley, E. K. G. Boateng, and J. R. Hutchinson, "Review of structural health and cure monitoring techniques for large wind turbine blades," *Renew. Energy*, vol. 51, pp. 113–123, Mar. 2013, doi: 10.1016/j.renene.2012.08.072.

[121] D. Li, S.-C.-M. Ho, G. Song, L. Ren, and H. Li, "A review of damage detection methods for wind turbine blades," *Smart Mater. Struct.*, vol. 24, no. 3, Feb. 2015, Art. no. 033001, doi: 10.1088/0964-1726/24/3/033001.

[122] Y. Du, S. Zhou, X. Jing, Y. Peng, H. Wu, and N. Kwok, "Damage detection techniques for wind turbine blades: A review," *Mech. Syst. Signal Process.*, vol. 141, Jul. 2020, Art. no. 106445, doi: 10.1016/j.ymssp.2019.106445.

[123] Q. Liang et al., "Multi-component FBG-based force sensing systems by comparison with other sensing technologies: A review," *IEEE Sensors J.*, vol. 18, no. 18, pp. 7345–7357, Sep. 2018, doi: 10.1109/JSEN.2018.2861014.

[124] P. Roriz, L. Carvalho, O. Frazão, J. L. Santos, and J. A. Simões, "From conventional sensors to fibre optic sensors for strain and force measurements in biomechanics applications: A review," *J. Biomechanics*, vol. 47, no. 6, pp. 1251–1261, Apr. 2014, doi: 10.1016/j.jbiomech.2014.01.054.

[125] A. G. Leal-Junior, C. A. R. Diaz, L. M. Avellar, M. J. Pontes, C. Marques, and A. Frizera, "Polymer optical fiber sensors in healthcare applications: A comprehensive review," *Sensors*, vol. 19, no. 14, p. 3156, Jul. 2019, doi: 10.3390/s19143156.

[126] D. Lo Presti et al., "Fiber Bragg gratings for medical applications and future challenges: A review," *IEEE Access*, vol. 8, pp. 156863–156888, 2020, doi: 10.1109/ACCESS.2020.3019138.

[127] D. Tosi, E. Schena, C. Molardi, and S. Korganbayev, "Fiber optic sensors for sub-centimeter spatially resolved measurements: Review and biomedical applications," *Opt. Fiber Technol.*, vol. 43, pp. 6–19, Jul. 2018, doi: 10.1016/j.yofte.2018.03.007.

[128] D. Mandal and S. Banerjee, "Surface acoustic wave (SAW) sensors: Physics, materials, and applications," *Sensors*, vol. 22, no. 3, p. 820, Jan. 2022, doi: 10.3390/s22030820.

[129] B. Liu et al., "Surface acoustic wave devices for sensor applications," *J. Semiconductors*, vol. 37, no. 2, Feb. 2016, Art. no. 021001, doi: 10.1088/1674-4926/37/2/021001.

[130] K. Länge, "Bulk and surface acoustic wave sensor arrays for multianalyte detection: A review," *Sensors*, vol. 19, no. 24, p. 5382, Dec. 2019, doi: 10.3390/s19245382.

[131] Y. Y. Kim and Y. E. Kwon, "Review of magnetostrictive patch transducers and applications in ultrasonic nondestructive testing of waveguides," *Ultrasonics*, vol. 62, pp. 3–19, Sep. 2015, doi: 10.1016/j.ultras.2015.05.015.

[132] S. Bahl, H. Nagar, I. Singh, and S. Sehgal, "Smart materials types, properties and applications: A review," *Mater. Today, Proc.*, vol. 28, pp. 1302–1306, Jan. 2020, doi: 10.1016/j.matpr.2020.04.505.

[133] J. Oliveira, V. Correia, H. Castro, P. Martins, and S. Lanceros-Mendez, "Polymer-based smart materials by printing technologies: Improving application and integration," *Additive Manuf.*, vol. 21, pp. 269–283, May 2018, doi: 10.1016/j.addma.2018.03.012.

[134] V. A. Kalinin, R. D. Lohr, A. J. Leigh, and A. T. J. Stopps, "Saw sensor arrangements," Patent U.S. 9 885 622 B2, Feb. 6, 2018. [Online]. Available: https://patents.google.com/patent/US9885622B2/en

[135] J. Hao, J. H. Ng, and S. Takahasi, "Fiber Bragg grating sensor," Agency for Science Technology and Research Singapore, BAE Systems Enterprise Systems, Patent U.S. 7 702 190 B2, Apr. 20, 2010. [Online]. Available: https://patents.google.com/patent/US7702190B2/en

[136] Y. Shimizu, "Magnetostrictive torque sensor," Honda Motor Co, Patent U.S.7 752 923 B2, Jul. 13, 2010. [Online]. Available: https://patents.google.com/patent/US7752923B2/en?q=(Magnetostrictive+torque+sensor)&oq=Magnetostrictive+torque+sensor

[137] T. Tomiyama, E. Lutters, R. Stark, and M. Abramovici, "Development capabilities for smart products," *CIRP Ann.*, vol. 68, no. 2, pp. 727–750, 2019, doi: 10.1016/j.cirp.2019.05.010.

[138] J. Lenz, E. MacDonald, R. Harik, and T. Wuest, "Optimizing smart manufacturing systems by extending the smart products paradigm to the beginning of life," *J. Manuf. Syst.*, vol. 57, pp. 274–286, Oct. 2020, doi: 10.1016/j.jmsy.2020.10.001.

[139] Y. Cheng, Y. Zhang, P. Ji, W. Xu, Z. Zhou, and F. Tao, "Cyber-physical integration for moving digital factories forward towards smart manufacturing: A survey," *Int. J. Adv. Manuf. Technol.*, vol. 97, nos. 1–4, pp. 1209–1221, Jul. 2018, doi: 10.1007/s00170-018-2001-2.

[140] V. P. Matveenko, N. A. Kosheleva, I. N. Shardakov, and A. A. Voronkov, "Temperature and strain registration by fibre-optic strain sensor in the polymer composite materials manufacturing," *Int. J. Smart Nano Mater.*, vol. 9, no. 2, pp. 99–110, Apr. 2018, doi: 10.1080/19475411.2018.1450791.

[141] Y. Meng, Y. Yang, H. Chung, P.-H. Lee, and C. Shao, "Enhancing sustainability and energy efficiency in smart factories: A review," *Sustainability*, vol. 10, no. 12, p. 4779, Dec. 2018, doi: 10.3390/su10124779.

[142] A. Valente and E. Carpanzano, "Development of multi-level adaptive control and scheduling solutions for shop-floor automation in reconfigurable manufacturing systems," *CIRP Ann.*, vol. 60, no. 1, pp. 449–452, 2011, doi: 10.1016/j.cirp.2011.03.036.

[143] D. Zuehlke, "SmartFactory—Towards a factory-of-things," *Annu. Rev. Control*, vol. 34, no. 1, pp. 129–138, Apr. 2010, doi: 10.1016/j.arcontrol.2010.02.008.

[144] Z. Shen et al., "High-stretchability, ultralow-hysteresis conductingpolymer hydrogel strain sensors for soft machines," *Adv. Mater.*, vol. 34, no. 32, Aug. 2022, Art. no. 2203650, doi: 10.1002/adma.202203650.

[145] D. Zhang, S. Xu, X. Zhao, W. Qian, C. R. Bowen, and Y. Yang, "Wireless monitoring of small strains in intelligent robots via a Joule heating effect in stretchable graphene-polymer nanocomposites," *Adv. Funct. Mater.*, vol. 30, Mar. 2020, Art. no. 1910809, doi: 10.1002/adfm.201910809.

[146] C. Wei et al., "Conformal human-machine integration using highly bending-insensitive, unpixelated, and waterproof epidermal electronics toward metaverse," *Nano-Micro Lett.*, vol. 15, no. 1, pp. 1–17, Aug. 2023, doi: 10.1007/s40820-023-01176-5.

[147] W. Lin et al., "Programmable and ultrasensitive haptic interfaces enabling closed-loop human-machine interactions," *Adv. Funct. Mater.*, vol. 33, Aug. 2023, Art. no. 2305919, doi: 10.1002/adfm.202305919.

[148] S. C. Ryu and P. E. Dupont, "FBG-based shape sensing tubes for continuum robots," in *Proc. IEEE Int. Conf. Robot. Autom. (ICRA)*, May 2014, pp. 3531–3537, doi: 10.1109/ICRA.2014.6907368.

[149] R. Xu, A. Yurkewich, and R. V. Patel, "Curvature, torsion, and force sensing in continuum robots using helically wrapped FBG sensors," *IEEE Robot. Autom. Lett.*, vol. 1, no. 2, pp. 1052–1059, Jul. 2016, doi: 10.1109/LRA.2016.2530867.

[150] T. Li et al., "A skin-like and highly stretchable optical fiber sensor with the hybrid coding of wavelength-light intensity," *Adv. Intell. Syst.*, vol. 4, no. 4, Apr. 2022, Art. no. 2100193, doi: 10.1002/aisy.202100193.

[151] J. Chen et al., "Bendable transparent ZnO thin film surface acoustic wave strain sensors on ultra-thin flexible glass substrates," *J. Mater. Chem. C*, vol. 2, no. 43, pp. 9109–9114, 2014, doi: 10.1039/C4TC01307G.

[152] J. Chen et al., "Development of flexible ZnO thin film surface acoustic wave strain sensors on ultrathin glass substrates," *J. Micromech. Microeng.*, vol. 25, no. 11, Sep. 2015, Art. no. 115005, doi: 10.1088/0960-1317/25/11/115005.

[153] A. Hooshiar, A. Payami, J. Dargahi, and S. Najarian, "Magnetostriction-based force feedback for robot-assisted cardiovascular surgery using smart magnetorheological elastomers," *Mech. Syst. Signal Process.*, vol. 161, Dec. 2021, Art. no. 107918, doi: 10.1016/j.ymssp.2021.107918.

[154] S. Gao, L. Weng, Z. Deng, B. Wang, and W. Huang, "Biomimetic tactile sensor array based on magnetostrictive materials," *IEEE Sensors J.*, vol. 21, no. 12, pp. 13116–13124, Jun. 2021, doi: 10.1109/JSEN.2021.3068160.

[155] A. Caggiano, F. Napolitano, L. Nele, and R. Teti, "Study on thrust force and torque sensor signals in drilling of Al/CFRP stacks for aeronautical applications," *Proc. CIRP*, vol. 79, pp. 337–342, Jan. 2019, doi: 10.1016/j.procir.2019.02.079.

[156] C. Campanella, A. Cuccovillo, C. Campanella, A. Yurt, and V. Passaro, "Fibre Bragg grating based strain sensors: Review of technology and applications," *Sensors*, vol. 18, no. 9, p. 3115, Sep. 2018, doi: 10.3390/s18093115.

[157] T. Wu, G. Liu, S. Fu, and F. Xing, "Recent progress of fiber-optic sensors for the structural health monitoring of civil infrastructure," *Sensors*, vol. 20, no. 16, p. 4517, Aug. 2020, doi: 10.3390/s20164517.

[158] B. Torres, I. Payá-Zaforteza, P. A. Calderón, and J. M. Adam, "Analysis of the strain transfer in a new FBG sensor for structural health monitoring," *Eng. Struct.*, vol. 33, no. 2, pp. 539–548, Feb. 2011, doi: 10.1016/j.engstruct.2010.11.012.

[159] H. Guo, G. Xiao, N. Mrad, and J. Yao, "Fiber optic sensors for structural health monitoring of air platforms," *Sensors*, vol. 11, no. 4, pp. 3687–3705, Mar. 2011, doi: 10.3390/s110403687.

[160] R. M. Measures, "Fiber-optic-based smart structures," in *Encyclopedia of Physical Science and Technology*, R. A. Meyers, Ed., 3rd ed. New York, NY, USA: Academic Press, 2003, pp. 769–802, doi: 10.1016/B0-12-227410-5/00241-6.

[161] M. Malekzadeh, M. Gul, I.-B. Kwon, and N. Catbas, "An integrated approach for structural health monitoring using an in-house built fiber optic system and non-parametric data analysis," *Smart Struct. Syst.*, vol. 14, no. 5, pp. 917–942, Nov. 2014, doi: 10.12989/sss.2014.14.5.917.

[162] X. Bao and L. Chen, "Recent progress in distributed fiber optic sensors," *Sensors*, vol. 12, no. 7, pp. 8601–8639, Jun. 2012, doi: 10.3390/s120708601.

[163] T. Shiratsuchi and T. Imai, "Development of fiber Bragg grating strain sensor with temperature compensation for measurement of cryogenic structures," *Cryogenics*, vol. 113, Jan. 2021, Art. no. 103233, doi: 10.1016/j.cryogenics.2020.103233.

[164] Y. Wang, X. Qiao, H. Yang, D. Su, L. Li, and T. Guo, "Sensitivity-improved strain sensor over a large range of temperatures using an etched and regenerated fiber Bragg grating," *Sensors*, vol. 14, no. 10, pp. 18575–18582, Oct. 2014, doi: 10.3390/s141018575.

[165] R. Li, Y. Chen, Y. Tan, Z. Zhou, T. Li, and J. Mao, "Sensitivity enhancement of FBG-based strain sensor," *Sensors*, vol. 18, no. 5, p. 1607, May 2018, doi: 10.3390/s18051607.

[166] R. Li, Y. Tan, Y. Chen, L. Hong, and Z. Zhou, "Investigation of sensitivity enhancing and temperature compensation for fiber Bragg grating (FBG)-based strain sensor," *Opt. Fiber Technol.*, vol. 48, pp. 199–206, Mar. 2019, doi: 10.1016/j.yofte.2019.01.009.

[167] J. Peng, S. Jia, Y. Jin, S. Xu, and Z. Xu, "Design and investigation of a sensitivity-enhanced fiber Bragg grating sensor for micro-strain measurement," *Sens. Actuators A, Phys.*, vol. 285, pp. 437–447, Jan. 2019, doi: 10.1016/j.sna.2018.11.038.

[168] P. Bosetti and S. Bruschi, "Enhancing positioning accuracy of CNC machine tools by means of direct measurement of deformation," *Int. J. Adv. Manuf. Technol.*, vol. 58, nos. 5–8, pp. 651–662, Jan. 2012, doi: 10.1007/s00170-011-3411-6.

[169] R. Haslinger, P. Leyendecker, and U. Seibold, "A fiberoptic force-torque-sensor for minimally invasive robotic surgery," in *Proc. IEEE Int. Conf. Robot. Autom.*, May 2013, pp. 4390–4395, doi: 10.1109/ICRA.2013.6631199.

[170] X. He, J. Handa, P. Gehlbach, R. Taylor, and I. Iordachita, "A submillimetric 3-DOF force sensing instrument with integrated fiber Bragg grating for retinal microsurgery," *IEEE Trans. Biomed. Eng.*, vol. 61, no. 2, pp. 522–534, Feb. 2014, doi: 10.1109/TBME.2013.2283501.

[171] M. Liu, G. Chen, Z. Zhang, and J. Bing, "The research on spindle integrated measurement method of cutting force based on fiber Bragg grating," *Proc. SPIE*, vol. 10155, pp. 564–571, Oct. 2016, doi: 10.1117/12.2246912.

[172] Y. Guo, J. Kong, H. Liu, H. Xiong, G. Li, and L. Qin, "A three-axis force fingertip sensor based on fiber Bragg grating," *Sens. Actuators A, Phys.*, vol. 249, pp. 141–148, Oct. 2016, doi: 10.1016/j.sna.2016.08.020.

[173] C. Kim and C.-H. Lee, "Development of a 6-DoF FBG force-moment sensor for a haptic interface with minimally invasive robotic surgery," *J. Mech. Sci. Technol.*, vol. 30, no. 8, pp. 3705–3712, Aug. 2016, doi: 10.1007/s12206-016-0732-2.

[174] H.-C. Xu, S. Wang, and X.-G. Miao, "Research of three-dimensional force sensor based on multiplexed fiber Bragg grating strain sensors," *Opt. Eng.*, vol. 56, no. 4, Apr. 2017, Art. no. 047103, doi: 10.1117/1.OE.56.4.047103.

[175] L. Xiong, G. Jiang, Y. Guo, and H. Liu, "A three-dimensional fiber Bragg grating force sensor for robot," *IEEE Sensors J.*, vol. 18, no. 9, pp. 3632–3639, May 2018, doi: 10.1109/JSEN.2018.2812820.

[176] M. Liu, J. Bing, L. Xiao, K. Yun, and L. Wan, "Development and testing of an integrated rotating dynamometer based on fiber Bragg grating for four-component cutting force measurement," *Sensors*, vol. 18, no. 4, p. 1254, Apr. 2018, doi: 10.3390/s18041254.

[177] J. Huang, D. T. Pham, C. Ji, and Z. Zhou, "Smart cutting tool integrated with optical fiber sensors for cutting force measurement in turning," *IEEE Trans. Instrum. Meas.*, vol. 69, no. 4, pp. 1720–1727, Apr. 2020, doi: 10.1109/TIM.2019.2916240.

[178] T. Li, M. Liu, R. Li, Y. Liu, Y. Tan, and Z. Zhou, "FBG-based online monitoring for uncertain loading-induced deformation of heavy-duty gantry machine tool base," *Mech. Syst. Signal Process.*, vol. 144, Oct. 2020, Art. no. 106864, doi: 10.1016/j.ymssp.2020.106864.

[179] V. Biazi-Neto, C. A. F. Marques, A. Frizera-Neto, and A. G. Leal-Junior, "FBG-embedded robotic manipulator tool for structural integrity monitoring from critical strain-stress pair estimation," *IEEE Sensors J.*, vol. 22, no. 6, pp. 5695–5702, Mar. 2022, doi: 10.1109/JSEN.2022.3149459.

[180] J. Pan, L. Wang, W. Hou, and H. Lv, "Design and investigation of a high-sensitivity tilt sensor based on FBG," *Photonic Sensors*, vol. 13, Oct. 2022, Art. no. 230228, doi: 10.1007/s13320-022-0671-8.

[181] A. Rohan, I. Raouf, and H. S. Kim, "Rotate vector (RV) reducer fault detection and diagnosis system: Towards component level prognostics and health management (PHM)," *Sensors*, vol. 20, no. 23, p. 6845, Nov. 2020, doi: 10.3390/s20236845.

[182] Y. Wang, L. Liang, Y. Yuan, G. Xu, and F. Liu, "A two fiber Bragg gratings sensing system to monitor the torque of rotating shaft," *Sensors*, vol. 16, no. 1, p. 138, Jan. 2016, doi: 10.3390/s16010138.

[183] T. Li, C. Shi, Y. Tan, and Z. Zhou, "Fiber Bragg grating sensing-based online torque detection on coupled bending and torsional vibration of rotating shaft," *IEEE Sensors J.*, vol. 17, no. 7, pp. 1999–2007, Apr. 2017, doi: 10.1109/JSEN.2017.2669528.

[184] A. Taghipour, A. N. Cheema, X. Gu, and F. Janabi-Sharifi, "Temperature independent triaxial force and torque sensor for minimally invasive interventions," *IEEE/ASME Trans. Mechatronics*, vol. 25, no. 1, pp. 449–459, Feb. 2020, doi: 10.1109/TMECH.2019.2956148.

[185] L. Xiong, Y. Guo, G. Jiang, X. Zhou, L. Jiang, and H. Liu, "Six-dimensional force/torque sensor based on fiber Bragg gratings with low coupling," *IEEE Trans. Ind. Electron.*, vol. 68, no. 5, pp. 4079–4089, May 2021, doi: 10.1109/TIE.2020.2982107.

[186] D. Lai, Z. Tang, J. Zhao, S. Wang, and C. Shi, "Design and validation of a miniature fiber Bragg grating-enabled high-sensitivity torque sensor," *IEEE Sensors J.*, vol. 21, no. 18, pp. 20027–20035, Sep. 2021, doi: 10.1109/JSEN.2021.3095275.

[187] M. Konstantaki et al., "Monitoring of torque induced strain in composite shafts with embedded and surface-mounted optical fiber Bragg gratings," *Sensors*, vol. 21, no. 7, p. 2403, Mar. 2021, doi: 10.3390/s21072403.

[188] E. Vorathin, Z. M. Hafizi, N. Ismail, and M. Loman, "Review of high sensitivity fibre-optic pressure sensors for low pressure sensing," *Opt. Laser Technol.*, vol. 121, Jan. 2020, Art. no. 105841, doi: 10.1016/j.optlastec.2019.105841.

[189] M. G. Xu, L. Reekie, Y. T. Chow, and J. P. Dakin, "Optical in-fibre grating high pressure sensor," *Electron. Lett.*, vol. 29, no. 4, p. 398, 1993, doi: 10.1049/el:19930267.

[190] J. Huang, Z. Zhou, X. Wen, and D. Zhang, "A diaphragm-type fiber Bragg grating pressure sensor with temperature compensation," *Measurement*, vol. 46, no. 3, pp. 1041–1046, Apr. 2013, doi: 10.1016/j.measurement.2012.10.010.

[191] J. Huang, Z. Zhou, Y. Tan, M. Liu, and D. Zhang, "Design and experimental study of a fiber Bragg grating pressure sensor," in *Proc. Int. Conf. Innov. Design Manuf. (ICIDM)*, Aug. 2014, pp. 217–221, doi: 10.1109/IDAM.2014.6912697.

[192] G. Rajan, B. Liu, Y. Luo, E. Ambikairajah, and G.-D. Peng, "High sensitivity force and pressure measurements using etched singlemode polymer fiber Bragg gratings," *IEEE Sensors J.*, vol. 13, no. 5, pp. 1794–1800, May 2013, doi: 10.1109/JSEN.2013.2242883.

[193] V. R. Pachava, S. Kamineni, S. S. Madhuvarasu, K. Putha, and V. R. Mamidi, "FBG based high sensitive pressure sensor and its low-cost interrogation system with enhanced resolution," *Photonic Sensors*, vol. 5, no. 4, pp. 321–329, Dec. 2015, doi: 10.1007/s13320-015-0259-7.

[194] G. Allwood, G. Wild, A. Lubansky, and S. Hinckley, "A highly sensitive fiber Bragg grating diaphragm pressure transducer," *Opt. Fiber Technol.*, vol. 25, pp. 25–32, Oct. 2015, doi: 10.1016/j.yofte.2015.06.001.

[195] E. Vorathin, Z. M. Hafizi, A. M. Aizzuddin, and K. S. Lim, "A highly sensitive multiplexed FBG pressure transducer based on natural rubber diaphragm and ultrathin aluminium sheet," *Opt. Laser Technol.*, vol. 106, pp. 177–181, Oct. 2018, doi: 10.1016/j.optlastec.2018.04.003.

[196] Y. Zhao, H.-K. Zheng, R.-Q. Lv, and Y. Yang, "A practical FBG pressure sensor based on diaphragm-cantilever," *Sens. Actuators A, Phys.*, vol. 279, pp. 101–106, Aug. 2018, doi: 10.1016/j.sna.2018.06.004.

[197] J. Huang, D. T. Pham, C. Ji, Z. Wang, and Z. Zhou, "Multi-parameter dynamical measuring system using fibre Bragg grating sensors for industrial hydraulic piping," *Measurement*, vol. 134, pp. 226–235, Feb. 2019, doi: 10.1016/j.measurement.2018.10.069.

[198] A. G. Leal-Junior, C. A. R. Díaz, A. Frizera, C. Marques, M. R. N. Ribeiro, and M. J. Pontes, "Simultaneous measurement of pressure and temperature with a single FBG embedded in a polymer diaphragm," *Opt. Laser Technol.*, vol. 112, pp. 77–84, Apr. 2019, doi: 10.1016/j.optlastec.2018.11.013.

[199] X. Liu, L. Liang, K. Jiang, and G. Xu, "Sensitivity-enhanced fiber Bragg grating pressure sensor based on a diaphragm and hinge-lever structure," *IEEE Sensors J.*, vol. 21, no. 7, pp. 9155–9164, Apr. 2021, doi: 10.1109/JSEN.2020.3045992.

[200] X. Li et al., "An FBG pressure sensor based on spring-diaphragm elastic structure for ultimate pressure detection," *IEEE Sensors J.*, vol. 22, no. 3, pp. 2213–2220, Feb. 2022, doi: 10.1109/JSEN.2021.3136212.

[201] L. Ren, Z.-G. Jia, H.-N. Li, and G. Song, "Design and experimental study on FBG hoop-strain sensor in pipeline monitoring," *Opt. Fiber Technol.*, vol. 20, no. 1, pp. 15–23, Jan. 2014, doi: 10.1016/j.yofte.2013.11.004.

[202] J. Wang, L. Zhao, T. Liu, Z. Li, T. Sun, and K. T. V. Grattan, "Novel negative pressure wave-based pipeline leak detection system using fiber Bragg grating-based pressure sensors," *J. Lightw. Technol.*, vol. 35, no. 16, pp. 3366–3373, Aug. 15, 2017, doi: 10.1109/JLT.2016.2615468.

[203] T. Jiang, L. Ren, Z. Jia, D. Li, and H. Li, "Application of FBG based sensor in pipeline safety monitoring," *Appl. Sci.*, vol. 7, no. 6, p. 540, May 2017, doi: 10.3390/app7060540.

[204] Z.-G. Jia, L. Ren, H.-N. Li, S.-C. Ho, and G.-B. Song, "Experimental study of pipeline leak detection based on hoop strain measurement," *Struct. Control Health Monitor.*, vol. 22, no. 5, pp. 799–812, May 2015, doi: 10.1002/stc.1718.

[205] L. Wong et al., "Leak detection in water pipes using submersible optical optic-based pressure sensor," *Sensors*, vol. 18, no. 12, p. 4192, Nov. 2018, doi: 10.3390/s18124192.

[206] J. Wang, L. Ren, T. Jiang, Z. Jia, and G.-X. Wang, "A novel gas pipeline burst detection and localization method based on the FBG caliber-based sensor array," *Measurement*, vol. 151, Feb. 2020, Art. no. 107226, doi: 10.1016/j.measurement.2019.107226.

[207] Y.-Y. Wang, F.-X. Zhang, Q.-C. Zhao, and C.-R. Che, "Real-time monitoring of pressure and temperature of oil well using a carbon-coated and bellow-packaged optical fiber sensor," *Opt. Fiber Technol.*, vol. 67, Dec. 2021, Art. no. 102703, doi: 10.1016/j.yofte.2021.102703.

[208] J. B. Rosolem et al., "Electroless nickel-plating sealing in FBG pressure sensor for thermoelectric power plant engines applications," *J. Lightw. Technol.*, vol. 37, no. 18, pp. 4791–4798, Sep. 15, 2019, doi: 10.1109/JLT.2019.2920120.

[209] Y. Dai, "Highly sensitive liquid-level sensor based on weak uniform fiber Bragg grating with narrow-bandwidth," *Opt. Eng.*, vol. 51, no. 4, Mar. 2012, Art. no. 044401, doi: 10.1117/1.OE.51.4.044401.

[210] O. F. Ameen, M. H. Younus, M. S. Aziz, A. I. Azmi, R. K. R. Ibrahim, and S. K. Ghoshal, "Graphene diaphragm integrated FBG sensors for simultaneous measurement of water level and temperature," *Sens. Actuators A, Phys.*, vol. 252, pp. 225–232, Dec. 2016, doi: 10.1016/j.sna.2016.10.018.

[211] G. G. de Almeida, R. C. Barreto, K. F. Seidel, and R. C. Kamikawachi, "A fiber Bragg grating water level sensor based on the force of buoyancy," *IEEE Sensors J.*, vol. 20, no. 7, pp. 3608–3613, Apr. 2020, doi: 10.1109/JSEN.2019.2960089.

[212] L. Schenato, J. P. Aguilar-López, A. Galtarossa, A. Pasuto, T. Bogaard, and L. Palmieri, "A rugged FBG-based pressure sensor for water level monitoring in dikes," *IEEE Sensors J.*, vol. 21, no. 12, pp. 13263–13271, Jun. 2021, doi: 10.1109/JSEN.2021.3067516.

[213] W. Yao, W. Peng, X. Zhang, X. Zhou, and Y. Liu, "Self-compensating fiber optic flow sensor based on dual fiber Bragg gratings," *Proc. SPIE*, vol. 8418, pp. 427–432, Oct. 2012, doi: 10.1117/12.975926.

[214] L. Rodriguez-Cobo, M. A. Quintela, M. Lomer, A. Cobo, and J. M. Lopez-Higuera, "Pipe flow speed sensor based on fiber Bragg gratings," *Proc. SPIE*, vol. 8421, pp. 728–731, Oct. 2012, doi: 10.1117/12.970621.

[215] P. Salgado, M. L. Filograno, F. D. Senent, and P. Corredera, "Non-intrusive measurement of internal pressure and flow in pipelines using fiber Bragg grating," *Proc. SPIE*, vol. 8915, pp. 466–473, Oct. 2013, doi: 10.1117/12.2037401.

[216] E. Schena, P. Saccomandi, and S. Silvestri, "A high sensitivity fiber optic macro-bend based gas flow rate transducer for low flow rates: Theory, working principle, and static calibration," *Rev. Sci. Instrum.*, vol. 84, no. 2, Feb. 2013, Art. no. 024301, doi: 10.1063/1.4793227.

[217] C. R. Zamarreño et al., "Fluid turbulence monitoring by means of FBG mesh," in *Proc. IEEE SENSORS*, Nov. 2014, pp. 1150–1152, doi: 10.1109/ICSENS.2014.6985211.

[218] S. R. Thekkethil, V. N. Venkatesan, H. Neumann, and R. Ramalingam, "Design of cryogenic flow meter using fiber Bragg grating sensors," in *Proc. IEEE SENSORS*, Nov. 2015, pp. 1–4, doi: 10.1109/ICSENS.2015.7370453.

[219] S. R. Thekkethil, R. J. Thomas, H. Neumann, and R. Ramalingam, "Experimental investigation on mass flow rate measurements using fibre Bragg grating sensors," *IOP Conf. Ser., Mater. Sci. Eng.*, vol. 171, Feb. 2017, Art. no. 012136, doi: 10.1088/1757-899X/171/1/012136.

[220] P. P. Kirwan, D. Creighton, C. Costello, T. P. O'Brien, and K. W. Moloney, "Momentum change flow meter with pressure compensation using FBGs," *IEEE Sensors J.*, vol. 16, no. 19, pp. 7061–7064, Oct. 2016, doi: 10.1109/JSEN.2016.2594135.

[221] R.-Q. Lv, H.-K. Zheng, Y. Zhao, and Y.-F. Gu, "An optical fiber sensor for simultaneous measurement of flow rate and temperature in the pipeline," *Opt. Fiber Technol.*, vol. 45, pp. 313–318, Nov. 2018, doi: 10.1016/j.yofte.2018.08.003.

[222] Q. Zhao, H.-K. Zheng, R.-Q. Lv, Y.-F. Gu, Y. Zhao, and Y. Yang, "Novel integrated optical fiber sensor for temperature, pressure and flow measurement," *Sens. Actuators A, Phys.*, vol. 280, pp. 68–75, Sep. 2018, doi: 10.1016/j.sna.2018.07.034.

[223] C. Li, M.-Y. Liu, H. Song, X.-L. Yang, and Y.-H. Wu, "A non-invasive measurement method of pipeline flow rate based on dual FBG sensors," *IEEE Sensors J.*, vol. 22, no. 6, pp. 5669–5677, Mar. 2022, doi: 10.1109/JSEN.2022.3141733.

[224] M. Perry, Z. Yan, Z. Sun, L. Zhang, P. Niewczas, and M. Johnston, "High stress monitoring of prestressing tendons in nuclear concrete vessels using fibre-optic sensors," *Nucl. Eng. Des.*, vol. 268, pp. 35–40, Mar. 2014, doi: 10.1016/j.nucengdes.2013.12.038.

[225] F. Heilmeier et al., "In-situ strain measurements in the plastic deformation regime inside casted parts using fibre-optical strain sensors," *Prod. Eng.*, vol. 13, nos. 3–4, pp. 351–360, Jun. 2019, doi: 10.1007/s11740-019-00874-7.

[226] R. You, L. Ren, and G. Song, "A novel fiber Bragg grating (FBG) soil strain sensor," *Measurement*, vol. 139, pp. 85–91, Jun. 2019, doi: 10.1016/j.measurement.2019.03.007.

[227] S. Shi, L. Hong, Y. Qu, and Z. Zhou, "A novel diagnostic scheme for gear pitting fault using fiber Bragg grating based strain sensors," in *Proc. 11th Int. Conf. Prognostics Syst. Health Manag. (PHM- Jinan)*, Oct. 2020, pp. 385–390, doi: 10.1109/PHM-Jinan48558.2020.00075.

[228] J. Yu, L. Hong, and Y. Qu, "Fault diagnosis of gear pitting based on dynamic strain measurements from fiber Bragg grating sensors," in *Proc. Global Rel. Prognostics Health Manag. (PHM-Nanjing)*, Oct. 2021, pp. 1–6, doi: 10.1109/PHM-Nanjing52125.2021.9612893.

[229] J. Yu, C. Li, X. Qiu, and H. Chen, "A full-optical strain FBG sensor for in-situ monitoring of fatigue stages via tunable DFB laser demodulation," *Opt. Quantum Electron.*, vol. 53, no. 3, p. 156, Mar. 2021, doi: 10.1007/s11082-021-02800-7.

[230] T. Han, S. Kundu, A. Nag, and Y. Xu, "3D printed sensors for biomedical applications: A review," *Sensors*, vol. 19, no. 7, p. 1706, Apr. 2019, doi: 10.3390/s19071706.

[231] H. Saboonchi, D. Ozevin, and M. Kabir, "MEMS sensor fusion: Acoustic emission and strain," *Sens. Actuators A, Phys.*, vol. 247, pp. 566–578, Aug. 2016, doi: 10.1016/j.sna.2016.05.014.

[232] M. O. Kayed, A. A. Balbola, E. Lou, and W. A. Moussa, "Development of MEMS-based piezoresistive 3D stress/strain sensor using strain technology and smart temperature compensation," *J. Micromech. Microeng.*, vol. 31, no. 3, Feb. 2021, Art. no. 035010, doi: 10.1088/1361-6439/abdbd6.

[233] A. A. S. Mohammed, W. A. Moussa, and E. Lou, "Development and experimental evaluation of a novel piezoresistive MEMS strain sensor," *IEEE Sensors J.*, vol. 11, no. 10, pp. 2220–2232, Oct. 2011, doi: 10.1109/JSEN.2011.2113374.

[234] H. Zang, X. Zhang, B. Zhu, and S. Fatikow, "Recent advances in non-contact force sensors used for micro/nano manipulation," *Sens. Actuators A, Phys.*, vol. 296, pp. 155–177, Sep. 2019, doi: 10.1016/j.sna.2019.07.007.

[235] C. D. Do, A. Erbes, J. Yan, K. Soga, and A. A. Seshia, "Vacuum packaged low-power resonant MEMS strain sensor," *J. Microelectromech. Syst.*, vol. 25, no. 5, pp. 851–858, Oct. 2016, doi: 10.1109/JMEMS.2016.2587867.

[236] Y. Zhao, Y. Zhao, and X. Ge, "The development of a triaxial cutting force sensor based on a MEMS strain gauge," *Micromachines*, vol. 9, no. 1, p. 30, Jan. 2018, doi: 10.3390/mi9010030.

[237] Y. Qin, D. Wang, and Y. Yang, "Integrated cutting force measurement system based on MEMS sensor for monitoring milling process," *Microsyst. Technol.*, vol. 26, no. 6, pp. 2095–2104, Jun. 2020, doi: 10.1007/s00542-020-04768-y.

[238] C. Zhang, S.-Y. Zhang, and L.-F. Wang, "A sawtooth MEMS capacitive strain sensor for passive telemetry in bearings," *IEEE Sensors J.*, vol. 21, no. 20, pp. 22527–22535, Oct. 2021, doi: 10.1109/JSEN.2021.3107441.

[239] Q.-A. Huang, L. Dong, and L.-F. Wang, "LC passive wireless sensors toward a wireless sensing platform: Status, prospects, and challenges," *J. Microelectromech. Syst.*, vol. 25, no. 5, pp. 822–841, Oct. 2016, doi: 10.1109/JMEMS.2016.2602298.

[240] M. H. M. Kouhani, J. Wu, A. Tavakoli, A. J. Weber, and W. Li, "Wireless, passive strain sensor in a doughnut-shaped contact lens for continuous non-invasive self-monitoring of intraocular pressure," *Lab Chip*, vol. 20, no. 2, pp. 332–342, Jan. 2020, doi: 10.1039/C9LC00735K.

[241] M. Barzegar, S. Blanks, B.-A. Sainsbury, and W. Timms, "MEMS technology and applications in geotechnical monitoring: A review," *Meas. Sci. Technol.*, vol. 33, no. 5, May 2022, Art. no. 052001, doi: 10.1088/1361-6501/ac4f00.

[242] O. Lawal, A. Najafi, T. Hoang, S. A. V. Shajihan, K. Mechitov, and B. F. Spencer, "Development and validation of a framework for smart wireless strain and acceleration sensing," *Sensors*, vol. 22, no. 5, p. 1998, Mar. 2022, doi: 10.3390/s22051998.

[243] T. Torfs et al., "Low power wireless sensor network for building monitoring," *IEEE Sensors J.*, vol. 13, no. 3, pp. 909–915, Mar. 2013, doi: 10.1109/JSEN.2012.2218680.

[244] L. Rayleigh, "On waves propagated along the plane surface of an elastic solid," *Proc. London Math. Soc.*, vols. s1–17, no. 1, pp. 4–11, Nov. 1885, doi: 10.1112/plms/s1-17.1.4.

[245] R. M. White and F. W. Voltmer, "Direct piezoelectric coupling to surface elastic waves," *Appl. Phys. Lett.*, vol. 7, no. 12, pp. 314–316, Nov. 2004, doi: 10.1063/1.1754276.

[246] A. Mujahid and F. Dickert, "Surface acoustic wave (SAW) for chemical sensing applications of recognition layers," *Sensors*, vol. 17, no. 12, p. 2716, Nov. 2017, doi: 10.3390/s17122716.

[247] Y. Huang, P. K. Das, and V. R. Bhethanabotla, "Surface acoustic waves in biosensing applications," *Sens. Actuators Rep.*, vol. 3, Nov. 2021, Art. no. 100041, doi: 10.1016/j.snr.2021.100041.

[248] Z. Tang, W. Wu, and J. Gao, "Water pressure sensingbased on wireless passive SAW technology," *Proc. Eng.*, vol. 119, pp. 892–900, Jan. 2015, doi: 10.1016/j.proeng.2015.08.961.

[249] P. Mohankumar, J. Ajayan, R. Yasodharan, P. Devendran, and R. Sambasivam, "A review of micromachined sensors for automotive applications," *Measurement*, vol. 140, pp. 305–322, Jul. 2019, doi: 10.1016/j.measurement.2019.03.064.

[250] X. Li, Q. Tan, L. Qin, X. Yan, and X. Liang, "Novel surface acoustic wave temperature-strain sensor based on $LiNbO_3$ for structural health monitoring," *Micromachines*, vol. 13, no. 6, p. 912, Jun. 2022, doi: 10.3390/mi13060912.

[251] D. Barmpakos and G. Kaltsas, "A review on humidity, temperature and strain printed sensors—Current trends and future perspectives," *Sensors*, vol. 21, no. 3, p. 739, Jan. 2021, doi: 10.3390/s21030739.

[252] A. K. Namdeo and H. B. Nemade, "Simulation on effects of electrical loading due to interdigital transducers in surface acoustic wave resonator," *Proc. Eng.*, vol. 64, pp. 322–330, Jan. 2013, doi: 10.1016/j.proeng.2013.09.104.

[253] G. Zhang, "Nanostructure-enhanced surface acoustic waves biosensor and its computational modeling," *J. Sensors*, vol. 2009, pp. 1–11, Jan. 2009, doi: 10.1155/2009/215085.

[254] A. Pohl, "A review of wireless SAW sensors," *IEEE Trans. Ultrason., Ferroelectr., Freq. Control*, vol. 47, no. 2, pp. 317–332, Mar. 2000, doi: 10.1109/58.827416.

[255] V. V. Varadan, V. K. Varadan, X. Bao, S. Ramanathan, and D. Piscotty, "Wireless passive IDT strain microsensor," *Smart Mater. Struct.*, vol. 6, no. 6, pp. 745–751, Dec. 1997, doi: 10.1088/0964-1726/6/6/012.

[256] R. Stoney, B. Donohoe, D. Geraghty, and G. E. O'Donnell, "The development of surface acoustic wave sensors (SAWs) for process monitoring," *Proc. CIRP*, vol. 1, pp. 569–574, Jan. 2012, doi: 10.1016/j.procir.2012.05.001.

[257] R. Stoney, D. Geraghty, and G. E. O'Donnell, "Characterization of differentially measured strain using passive wireless surface acoustic wave (SAW) strain sensors," *IEEE Sensors J.*, vol. 14, no. 3, pp. 722–728, Mar. 2014, doi: 10.1109/JSEN.2013.2285722.

[258] C. Wang, K. Cheng, X. Chen, T. Minton, and R. Rakowski, "Design of an instrumented smart cutting tool and its implementation and application perspectives," *Smart Mater. Struct.*, vol. 23, no. 3, Feb. 2014, Art. no. 035019, doi: 10.1088/0964-1726/23/3/035019.

[259] C. Wang, K. Cheng, and R. Rakowski, "Development of smart tooling concepts applied to ultra-precision and high speed machining," *Presented at the ASME 2016 11th Int. Manuf. Sci. Eng. Conf., Amer. Soc. Mech. Eng. Digit. Collection*, Sep. 2016, doi: 10.1115/MSEC2016-8573.

[260] K. Cheng, Z.-C. Niu, R. C. Wang, R. Rakowski, and R. Bateman, "Smart cutting tools and smart machining: Development approaches, and their implementation and application perspectives," *Chin. J. Mech. Eng.*, vol. 30, no. 5, pp. 1162–1176, Sep. 2017, doi: 10.1007/s10033-017-0183-4.

[261] B. Lin et al., "A high Q value ScAlN/AlN-based SAW resonator for load sensing," *IEEE Trans. Electron Devices*, vol. 68, no. 10, pp. 5192–5197, Oct. 2021, doi: 10.1109/TED.2021.3107232.

[262] X. Tan et al., "A passive wireless triboelectric sensor via a surface acoustic wave resonator (SAWR)," *Nano Energy*, vol. 78, Dec. 2020, Art. no. 105307, doi: 10.1016/j.nanoen.2020.105307.

[263] V. Kalinin, A. Leigh, A. Stopps, and E. Artigao, "Resonant SAW torque sensor for wind turbines," in *Proc. Joint Eur. Freq. Time Forum Int. Freq. Control Symp. (EFTF/IFC)*, Jul. 2013, pp. 462–465, doi: 10.1109/EFTF-IFC.2013.6702093.

[264] V. Kalinin, A. Leigh, A. Stopps, and S. B. Hanssen, "SAW torque sensor for marine applications," in *Proc. Joint Conf. Eur. Freq. Time Forum IEEE Int. Freq. Control Symp. (EFTF/IFC)*, Jul. 2017, pp. 347–352, doi: 10.1109/FCS.2017.8088889.

[265] X. Ji, Y. Fan, H. Qi, J. Chen, T. Han, and P. Cai, "A wireless demodulation system for passive surface acoustic wave torque sensor," *Rev. Sci. Instrum.*, vol. 85, no. 12, Dec. 2014, Art. no. 125001, doi: 10.1063/1.4902180.

[266] Y. Fan, P. Kong, H. Qi, H. Liu, and X. Ji, "A surface acoustic wave response detection method for passive wireless torque sensor," *AIP Adv.*, vol. 8, no. 1, Jan. 2018, Art. no. 015321, doi: 10.1063/1.5003178.

[267] D. Silva, J. Mendes, A. Pereira, F. Gégot, and L. Alves, "Measuring torque and temperature in a rotating shaft using commercial SAW sensors," *Sensors*, vol. 17, no. 7, p. 1547, Jul. 2017, doi: 10.3390/s17071547.

[268] B. Scheiner, F. Probst, F. Michler, R. Weigel, A. Koelpin, and F. Lurz, "Miniaturized hybrid frequency reader for contactless measurement scenarios using resonant surface acoustic wave sensors," *Sensors*, vol. 21, no. 7, p. 2367, Mar. 2021, doi: 10.3390/s21072367.

[269] W. Han, X. Bu, M. Song, and X. Huang, "Research into a novel surface acoustic wave sensor signal-processing system based on compressive sensing and an observed-signal augmentation method based on secondary information prediction," *Meas. Sci. Technol.*, vol. 32, no. 7, May 2021, Art. no. 075902, doi: 10.1088/1361-6501/abe3ab.

[270] A. Binder, G. Bruckner, N. Schobernig, and D. Schmitt, "Wireless surface acoustic wave pressure and temperature sensor with unique identification based on $LiNbO_3$," *IEEE Sensors J.*, vol. 13, no. 5, pp. 1801–1805, May 2013, doi: 10.1109/JSEN.2013.2241052.

[271] J. G. Rodríguez-Madrid, G. F. Iriarte, O. A. Williams, and F. Calle, "High precision pressure sensors based on SAW devices in the GHz range," *Sens. Actuators A, Phys.*, vol. 189, pp. 364–369, Jan. 2013, doi: 10.1016/j.sna.2012.09.012.

[272] F. Della Lucia, P. Zambrozi, F. Frazatto, M. Piazzetta, and A. Gobbi, "Design, fabrication and characterization of SAW pressure sensors for offshore oil and gas exploration," *Sens. Actuators A, Phys.*, vol. 222, pp. 322–328, Feb. 2015, doi: 10.1016/j.sna.2014.12.011.

[273] T. Wang, X. Mu, A. B. Randles, Y. Gu, and C. Lee, "Diaphragm shape effect on the sensitivity of surface acoustic wave based pressure sensor for harsh environment," *Appl. Phys. Lett.*, vol. 107, no. 12, Sep. 2015, Art. no. 123501, doi: 10.1063/1.4931363.

[274] S. Quintero, S. Figueiredo, V. Takahashi, R. Llerena, and A. Braga, "Passive downhole pressure sensor based on surface acoustic wave technology," *Sensors*, vol. 17, no. 7, p. 1635, Jul. 2017, doi: 10.3390/s17071635.

[275] Y. Zhang, Q. Tan, L. Zhang, W. Zhang, and J. Xiong, "A novel SAW temperature-humidity-pressure (THP) sensor based on $LiNbO_3$ for environment monitoring," *J. Phys. D, Appl. Phys.*, vol. 53, no. 37, Jun. 2020, Art. no. 375401, doi: 10.1088/1361-6463/ab9138.

[276] M. M. Memon, S. Pan, J. Wan, T. Wang, and W. Zhang, "Highly sensitive thick diaphragm-based surface acoustic wave pressure sensor," *Sens. Actuators A, Phys.*, vol. 331, Nov. 2021, Art. no. 112935, doi: 10.1016/j.sna.2021.112935.

[277] L. Xie, T. Wang, J. Xing, and X. Zhu, "An embedded surface acoustic wave pressure sensor for monitoring civil engineering structures," *IEEE Sensors J.*, vol. 18, no. 13, pp. 5232–5237, Jul. 2018, doi: 10.1109/JSEN.2018.2833155.

[278] Z. Tang et al., "Improving water pressure measurement using temperature-compensated wireless passive SAW bidirectional RDL pressure sensor," *IEEE Trans. Instrum. Meas.*, vol. 71, pp. 1–11, 2022, doi: 10.1109/TIM.2021.3120146.

[279] T. Xue, F. Xu, Q. Tan, X. Yan, and X. Liang, "LGS-based SAW sensor that can measure pressure up to 1000 °C," *Sens. Actuators A, Phys.*, vol. 334, Feb. 2022, Art. no. 113315, doi: 10.1016/j.sna.2021.113315.

[280] A. Kang, C. Zhang, X. Ji, T. Han, R. Li, and X. Li, "SAW-RFID enabled temperature sensor," *Sens. Actuators A, Phys.*, vol. 201, pp. 105–113, Oct. 2013, doi: 10.1016/j.sna.2013.06.016.

[281] T. Aubert et al., "In situ high-temperature characterization of AlN-based surface acoustic wave devices," *J. Appl. Phys.*, vol. 114, no. 1, Jul. 2013, Art. no. 014505, doi: 10.1063/1.4812565.

[282] A. Müller et al., "GaN/Si based single SAW resonator temperature sensor operating in the GHz frequency range," *Sens. Actuators A, Phys.*, vol. 209, pp. 115–123, Mar. 2014, doi: 10.1016/j.sna.2014.01.028.

[283] A. Müller et al., "GaN membrane supported SAW pressure sensors with embedded temperature sensing capability," *IEEE Sensors J.*, vol. 17, no. 22, pp. 7383–7393, Nov. 2017, doi: 10.1109/JSEN.2017.2757770.

[284] Y. Shi et al., "A novel self-powered wireless temperature sensor based on thermoelectric generators," *Energy Convers. Manag.*, vol. 80, pp. 110–116, Apr. 2014, doi: 10.1016/j.enconman.2014.01.010.

[285] Y. Zhu et al., "An energy autonomous 400 MHz active wireless SAW temperature sensor powered by vibration energy harvesting," *IEEE Trans. Circuits Syst. I, Reg. Papers*, vol. 62, no. 4, pp. 976–985, Apr. 2015, doi: 10.1109/TCSI.2015.2402937.

[286] C. Li, X. Liu, L. Shu, and Y. Li, "AlN-based surface acoustic wave resonators for temperature sensing applications," *Mater. Exp.*, vol. 5, no. 4, pp. 367–370, Aug. 2015, doi: 10.1166/mex.2015.1247.

[287] R. Tao et al., "Bimorph material/structure designs for high sensitivity flexible surface acoustic wave temperature sensors," *Sci. Rep.*, vol. 8, no. 1, p. 9052, Jun. 2018, doi: 10.1038/s41598-018-27324-1.

[288] C. Fu et al., "Design and implementation of 2.45 GHz passive SAW temperature sensors with BPSK coded RFID configuration," *Sensors*, vol. 17, no. 8, p. 1849, Aug. 2017, doi: 10.3390/s17081849.

[289] G. Bruckner and J. Bardong, "Wireless readout of multiple SAW temperature sensors," *Sensors*, vol. 19, no. 14, p. 3077, Jul. 2019, doi: 10.3390/s19143077.

[290] L. Lamanna, F. Rizzi, V. R. Bhethanabotla, and M. De Vittorio, "GHz AlN-based multiple mode SAW temperature sensor fabricated on PEN substrate," *Sens. Actuators A, Phys.*, vol. 315, Nov. 2020, Art. no. 112268, doi: 10.1016/j.sna.2020.112268.

[291] L. Li et al., "A novel design method for SAW temperature sensor with monotonic and linear frequency-temperature behavior in wide temperature range," *Sens. Actuators A, Phys.*, vol. 307, Jun. 2020, Art. no. 111982, doi: 10.1016/j.sna.2020.111982.

[292] L. Li, B. Peng, J. Zhu, Z. He, Y. Yang, and W. Zhang, "Strain measurements with langasite SAW resonators at high temperature," *IEEE Sensors J.*, vol. 21, no. 4, pp. 4688–4695, Feb. 2021, doi: 10.1109/JSEN.2020.3032477.

[293] X. Yan, Q. Tan, X. Li, T. Xue, and M. Li, "Test and analysis of SAW high temperature strain sensor based on langasite," *IEEE Sensors J.*, vol. 22, no. 13, pp. 12622–12628, Jul. 2022, doi: 10.1109/JSEN.2022.3176689.

[294] J. Streque et al., "Design and characterization of high-Q SAW resonators based on the AlN/sapphire structure intended for high-temperature wireless sensor applications," *IEEE Sensors J.*, vol. 20, no. 13, pp. 6985–6991, Jul. 2020, doi: 10.1109/JSEN.2020.2978179.

[295] X. Gao et al., "Development of wireless and passive SAW temperature sensor with very high accuracy," *Appl. Sci.*, vol. 11, no. 16, p. 7422, Aug. 2021, doi: 10.3390/app11167422.

[296] X. Zhou, Q. Tan, X. Liang, B. Lin, T. Guo, and Y. Gan, "Novel multilayer SAW temperature sensor for ultra-high temperature environments," *Micromachines*, vol. 12, no. 6, p. 643, May 2021, doi: 10.3390/mi12060643.

[297] C. Zhao et al., "Anti-irradiation SAW temperature sensor based on 128° YX $LiNbO_3$ single crystal," *Sens. Actuators A, Phys.*, vol. 333, Jan. 2022, Art. no. 113230, doi: 10.1016/j.sna.2021.113230.

[298] R. Fachberger and A. Erlacher, "Applications of wireless SAW sensing in the steel industry," *Proc. Eng.*, vol. 5, pp. 224–227, Jan. 2010, doi: 10.1016/j.proeng.2010.09.088.

[299] A. Binder and R. Fachberger, "Wireless SAW temperature sensor system for high-speed high-voltage motors," *IEEE Sensors J.*, vol. 11, no. 4, pp. 966–970, Apr. 2011, doi: 10.1109/JSEN.2010.2076803.

[300] Md. N. Alam, R. H. Bhuiyan, R. A. Dougal, and M. Ali, "Design and application of surface wave sensors for nonintrusive power line fault detection," *IEEE Sensors J.*, vol. 13, no. 1, pp. 339–347, Jan. 2013, doi: 10.1109/JSEN.2012.2217317.

[301] J. Furniss, D. Carka, I. Voiculescu, K.-L. Lee, D. Xiang, and F. Li, "Surface acoustic wave (SAW) sensors for cryogenic temperature and strain sensing," in *Proc. 6th IEEE Int. Conf. Wireless Space Extreme Environments (WiSEE)*, Dec. 2018, pp. 206–211, doi: 10.1109/WiSEE.2018.8637326.

[302] B. Hu et al., "Fabrications of L-band $LiNbO_3$-based SAW resonators for aerospace applications," *Micromachines*, vol. 10, no. 6, p. 349, May 2019, doi: 10.3390/mi10060349.

[303] S. Kim, M. R. Adib, and K. Lee, "Development of chipless and wireless underground temperature sensor system based on magnetic antennas and SAW sensor," *Sens. Actuators A, Phys.*, vol. 297, Oct. 2019, Art. no. 111549, doi: 10.1016/j.sna.2019.111549.

[304] I. Tomaz et al., "The development of a smart additively manufactured part with an embedded surface acoustic wave sensor," *Additive Manuf. Lett.*, vol. 1, Dec. 2021, Art. no. 100004, doi: 10.1016/j.addlet.2021.100004.

[305] D. Leff, A. Maskay, and M. P. da Cunha, "Wireless interrogation of high temperature surface acoustic wave dynamic strain sensor," in *Proc. IEEE Int. Ultrason. Symp. (IUS)*, Sep. 2020, pp. 1–4, doi: 10.1109/IUS46767.2020.9251428.

[306] D. C. Jiles, "Theory of the magnetomechanical effect," *J. Phys. D, Appl. Phys.*, vol. 28, no. 8, pp. 1537–1546, Aug. 1995, doi: 10.1088/0022-3727/28/8/001.

[307] E. Hristoforou and A. Ktena, "Magnetostriction and magnetostrictive materials for sensing applications," *J. Magn. Magn. Mater.*, vol. 316, no. 2, pp. 372–378, Sep. 2007, doi: 10.1016/j.jmmm.2007.03.025.

[308] M. Bagheri, A. Zollanvari, and S. Nezhivenko, "Transformer fault condition prognosis using vibration signals over cloud environment," *IEEE Access*, vol. 6, pp. 9862–9874, 2018, doi: 10.1109/ACCESS.2018.2809436.

[309] B. L. S. Lima, F. L. Maximino, J. C. Santos, and A. D. Santos, "Direct method for magnetostriction coefficient measurement based on atomic force microscope, illustrated by the example of Tb–Co film," *J. Magn. Magn. Mater.*, vol. 395, pp. 336–339, Dec. 2015, doi: 10.1016/j.jmmm.2015.07.079.

[310] F. Narita and M. Fox, "A review on piezoelectric, magnetostrictive, and magnetoelectric materials and device technologies for energy harvesting applications," *Adv. Eng. Mater.*, vol. 20, no. 5, May 2018, Art. no. 1700743, doi: 10.1002/adem.201700743.

[311] S. Mohammadi and A. Esfandiari, "Magnetostrictive vibration energy harvesting using strain energy method," *Energy*, vol. 81, pp. 519–525, Mar. 2015, doi: 10.1016/j.energy.2014.12.065.

[312] T. Ueno, "Micro magnetostrictive vibrational power generator for battery-free wireless sensor in machine tool," *Proc. SPIE*, vol. 11379, pp. 94–101, Apr. 2020, doi: 10.1117/12.2558336.

[313] M. R. J. Gibbs, E. W. Hill, and P. J. Wright, "Magnetic materials for MEMS applications," *J. Phys. D, Appl. Phys.*, vol. 37, no. 22, pp. 237–244, Oct. 2004, doi: 10.1088/0022-3727/37/22/R01.

[314] J. D. S. Vincent, M. Rodrigues, Z. Leong, and N. A. Morley, "Design and development of magnetostrictive actuators and sensors for structural health monitoring," *Sensors*, vol. 20, no. 3, p. 711, Jan. 2020, doi: 10.3390/s20030711.

[315] Z. He, W. Li, H. Salehi, H. Zhang, H. Zhou, and P. Jiao, "Integrated structural health monitoring in bridge engineering," *Autom. Construct.*, vol. 136, Apr. 2022, Art. no. 104168, doi: 10.1016/j.autcon.2022.104168.

[316] L. Ren, K. Yu, and Y. Tan, "Applications and advances of magnetoelastic sensors in biomedical engineering: A review," *Materials*, vol. 12, no. 7, p. 1135, Apr. 2019, doi: 10.3390/ma12071135.

[317] R. Gonçalves et al., "Synthesis of highly magnetostrictive nanostructures and their application in a polymer-based magnetoelectric sensing device," *Eur. Polym. J.*, vol. 84, pp. 685–692, Nov. 2016, doi: 10.1016/j.eurpolymj.2016.09.055.

[318] W. Zheng, B. Wang, H. Liu, X. Wang, Y. Li, and C. Zhang, "Bio-inspired magnetostrictive tactile sensor for surface material recognition," *IEEE Trans. Magn.*, vol. 55, no. 7, pp. 1–7, Jul. 2019, doi: 10.1109/TMAG.2019.2898546.

[319] V. R. Monaji and D. Das, "Influence of Zr doping on the structural, magnetic and magnetoelastic properties of cobalt-ferrites," *J. Alloys Compounds*, vol. 634, pp. 99–103, Jun. 2015, doi: 10.1016/j.jallcom.2015.02.084.

[320] B. C. Sekhar, G. S. N. Rao, O. F. Caltun, B. D. Lakshmi, B. P. Rao, and P. S. V. S. Rao, "Magnetic and magnetostrictive properties of Cu substituted co-ferrites," *J. Magn. Magn. Mater.*, vol. 398, pp. 59–63, Jan. 2016, doi: 10.1016/j.jmmm.2015.09.028.

[321] L. Jiang et al., "Giant enhancement in the magnetostrictive effect of FeGa alloys doped with low levels of terbium," *Appl. Phys. Lett.*, vol. 102, no. 22, Jun. 2013, Art. no. 222409, doi: 10.1063/1.4809829.

[322] G. Xi, L. Wang, and T. Zhao, "Magnetic and magnetostrictive properties of RE-doped cu-co ferrite fabricated from spent lithium-ion batteries," *J. Magn. Magn. Mater.*, vol. 424, pp. 130–136, Feb. 2017, doi: 10.1016/j.jmmm.2016.10.031.

[323] B. C. Keswani, S. I. Patil, Y. D. Kolekar, and C. V. Ramana, "Improved magnetostrictive properties of cobalt ferrite ($CoFe_2O_4$) by Mn and Dy co-substitution for magneto-mechanical sensors," *J. Appl. Phys.*, vol. 126, no. 17, Nov. 2019, Art. no. 174503, doi: 10.1063/1.5114815.

[324] V. Pepakayala, S. R. Green, and Y. B. Gianchandani, "Passive wireless strain sensors using microfabricated magnetoelastic beam elements," *J. Microelectromech. Syst.*, vol. 23, no. 6, pp. 1374–1382, Dec. 2014, doi: 10.1109/JMEMS.2014.2313809.

[325] S. D. Bhame and P. A. Joy, "Enhanced strain sensitivity in magnetostrictive spinel ferrite $Co_{1-x}ZnxFe_2O_4$," *J. Magn. Magn. Mater.*, vol. 447, pp. 150–154, Feb. 2018, doi: 10.1016/j.jmmm.2017.09.075.

[326] P. N. Anantharamaiah, H. M. Shashanka, R. Kumar, J. A. Chelvane, and B. Sahoo, "Chemically enabling $CoFe_2O_4$ for magnetostrictive strain sensing applications at lower magnetic fields: Effect of Zn substitution," *Mater. Sci. Eng., B*, vol. 266, Apr. 2021, Art. no. 115080, doi: 10.1016/j.mseb.2021.115080.

[327] M. Ghodsi et al., "Analytical, numerical and experimental investigation of a giant magnetostrictive (GM) force sensor," *Sensor Rev.*, vol. 35, no. 4, pp. 357–365, Sep. 2015, doi: 10.1108/SR-12-2014-0760.

[328] A. Yoffe, Y. Weber, and D. Shilo, "A physically based model for stress sensing using magnetostrictive composites," *J. Mech. Phys. Solids*, vol. 85, pp. 203–218, Dec. 2015, doi: 10.1016/j.jmps.2015.09.013.

[329] A. Al-Hajjeh, E. Lynch, C. T. Law, and R. El-Hajjar, "Characteristics of a magnetostrictive composite stress sensor," *IEEE Magn. Lett.*, vol. 7, pp. 1–4, 2016, doi: 10.1109/LMAG.2016.2540613.

[330] M. R. Karafi and S. J. Ehteshami, "Introduction of a hybrid sensor to measure the torque and axial force using a magnetostrictive hollow rod," *Sens. Actuators A, Phys.*, vol. 276, pp. 91–102, Jun. 2018, doi: 10.1016/j.sna.2018.03.033.

[331] L. Wan, B. Wang, Q. Wang, J. Han, and S. Cao, "The output characteristic of cantilever-like tactile sensor based on the inverse magnetostrictive effect," *AIP Adv.*, vol. 7, no. 5, Jan. 2017, Art. no. 056805, doi: 10.1063/1.4975050.

[332] Y. Li et al., "Design and output characteristics of magnetostrictive tactile sensor for detecting force and stiffness of manipulated objects," *IEEE Trans. Ind. Informat.*, vol. 15, no. 2, pp. 1219–1225, Feb. 2019, doi: 10.1109/TII.2018.2862912.

[333] L. Weng, G. Xie, B. Zhang, W. Huang, B. Wang, and Z. Deng, "Magnetostrictive tactile sensor array for force and stiffness detection," *J. Magn. Magn. Mater.*, vol. 513, Nov. 2020, Art. no. 167068, doi: 10.1016/j.jmmm.2020.167068.

[334] K. Liang et al., "Sensor to monitor localized stresses on steel surfaces using the magnetostrictive delay line technique," *Sensors*, vol. 19, no. 21, p. 4797, Nov. 2019, doi: 10.3390/s19214797.

[335] L. Shu, J. Yang, B. Li, Z. Deng, and M. J. Dapino, "Impact force sensing with magnetostrictive Fe–Ga alloys," *Mech. Syst. Signal Process.*, vol. 139, May 2020, Art. no. 106418, doi: 10.1016/j.ymssp.2019.106418.

[336] L. Ren, K. Wang, X. Wang, and Y. Tan, "A moment and axial force sensor using a self-decoupled, passive and wireless method," *IEEE Sensors J.*, vol. 21, no. 19, pp. 21432–21440, Oct. 2021, doi: 10.1109/JSEN.2021.3103748.

[337] L. Ren, W. Zhang, K. Wang, P. Zhang, S. Wang, and Y. Tan, "Spindle-mounted self-decoupled force/torque sensor for cutting force detection in a precision machine tool," *Measurement*, vol. 204, Nov. 2022, Art. no. 112119, doi: 10.1016/j.measurement.2022.112119.

[338] Y. Tan, J. Zhu, and L. Ren, "A two-dimensional wireless and passive sensor for stress monitoring," *Sensors*, vol. 19, no. 1, p. 135, Jan. 2019, doi: 10.3390/s19010135.

[339] Y. Tan, X. Wang, and L. Ren, "Design and experiment of a cardan-type self-decoupled and self-powered bending moment and torque sensor," *IEEE Trans. Ind. Electron.*, vol. 68, no. 6, pp. 5366–5375, Jun. 2021, doi: 10.1109/TIE.2020.2991931.

[340] V. Apicella, C. S. Clemente, D. Davino, D. Leone, and C. Visone, "Analysis and modeling of a passive force sensor based on villari effect," *Math. Comput. Simul.*, vol. 183, pp. 234–243, May 2021, doi: 10.1016/j.matcom.2020.01.013.

[341] S. Talebian, "Theoretical and experimental study on optimum operational conditions of a magnetostrictive force sensor," *J. Magn. Magn. Mater.*, vol. 562, Nov. 2022, Art. no. 169847, doi: 10.1016/j.jmmm.2022.169847.

[342] R. Shi, C. Wang, C. Yu, M. Xiong, Y. Wang, and Z. Chen, "Output characteristics and experimental study of a highly linear and large-range force sensor based on the Villari effect," *AIP Adv.*, vol. 11, no. 5, May 2021, Art. no. 055317, doi: 10.1063/5.0050384.

[343] S. Mirzamohamadi, M. M. Sheikhi, M. R. Karafi, M. Ghodsi, and S. Ghorbanirezaei, "Novel contactless hybrid static magnetostrictive force-torque (CHSMFT) sensor using galfenol," *J. Magn. Magn. Mater.*, vol. 553, Jul. 2022, Art. no. 168969, doi: 10.1016/j.jmmm.2021.168969.

[344] G. S. N. Rao, O. F. Caltun, K. H. Rao, P. S. S. Rao, and B. P. Rao, "Improved magnetostrictive properties of Co–Mn ferrites for automobile torque sensor applications," *J. Magn. Magn. Mater.*, vol. 341, pp. 60–64, Sep. 2013, doi: 10.1016/j.jmmm.2013.04.039.

[345] G. Raghunath, A. B. Flatau, A. Purekar, and J.-H. Yoo, "Non-contact torque measurement using magnetostrictive galfenol," *Presented at the ASME Conf. Smart Mater., Adapt. Struct. Intell. Syst., Amer. Soc. Mechanical Eng. Digit. Collection*, Feb. 2014, doi: 10.1115/SMASIS2013-3227.

[346] H. Muro, C. Saito, M. Shimada, and Y. Furuya, "Magnetostrictive-ring type torque sensor using two Hall ICs with differential magnetic field detection," in *Proc. IEEE SENSORS*, pp. 412–415, Nov. 2014, doi: 10.1109/ICSENS.2014.6985022.

[347] J. K. Lee, H. M. Seung, C. I. Park, J. K. Lee, D. H. Lim, and Y. Y. Kim, "Magnetostrictive patch sensor system for battery-less real-time measurement of torsional vibrations of rotating shafts," *J. Sound Vibrat.*, vol. 414, pp. 245–258, Feb. 2018, doi: 10.1016/j.jsv.2017.11.023.

[348] Y. Huang, Y. Yang, X. Zhang, and M. Zhao, "A novel torque sensor based on the angle of magnetization vector," *EURASIP J. Wireless Commun. Netw.*, vol. 2018, no. 1, p. 230, Sep. 2018, doi: 10.1186/s13638-018-1247-6.

[349] M. Hein, J. Park, J. A. Cozzo, A. Flatau, and B. J. H. Stadler, "Electrodeposited Fe–Ga alloy films for directly coupled noncontact torque sensing," *IEEE Sensors J.*, vol. 19, no. 16, pp. 6655–6661, Aug. 2019, doi: 10.1109/JSEN.2019.2906062.

[350] S. Beirle and K. Seemann, "Non-contact high-frequency measurements of mechanically loaded ferromagnetic thin films: An alternative approach for torque sensors," *Sens. Actuators A, Phys.*, vol. 301, Jan. 2020, Art. no. 111788, doi: 10.1016/j.sna.2019.111788.

[351] F. Xu, V. K. Dhimole, and C. Cho, "Torque measurement technology by using a magnetostrictive ring and multiple magnets," *Actuators*, vol. 10, no. 6, p. 124, Jun. 2021, doi: 10.3390/act10060124.

[352] X. Niu et al., "Non-contact torque sensor based on magnetostrictive $Fe_{30}Co_{70}$ alloy," *AIP Adv.*, vol. 12, no. 3, Mar. 2022, Art. no. 035112, doi: 10.1063/5.0081248.

[353] A. M. Aragón, M. Hernando-Rydings, A. Hernando, and P. Marín, "Liquid pressure wireless sensor based on magnetostrictive microwires for applications in cardiovascular localized diagnostic," *AIP Adv.*, vol. 5, no. 8, Aug. 2015, Art. no. 087132, doi: 10.1063/1.4928605.

[354] M. Löffler, R. Kremer, A. Sutor, and R. Lerch, "Hysteresis of the resonance frequency of magnetostrictive bending cantilevers," *J. Appl. Phys.*, vol. 117, no. 17, May 2015, Art. no. 17A907, doi: 10.1063/1.4916162.

[355] J. J. Park, K. S. M. Reddy, B. Stadler, and A. Flatau, "Magnetostrictive Fe–Ga/Cu nanowires array with GMR sensor for sensing applied pressure," *IEEE Sensors J.*, vol. 17, no. 7, pp. 2015–2020, Apr. 2017, doi: 10.1109/JSEN.2017.2657789.

[356] H.-C. Chang et al., "Designs of planar sensing inductor on inverse-magnetostrictive type pressure sensor," in *Proc. IEEE SENSORS*, Nov. 2013, pp. 1–4, doi: 10.1109/ICSENS.2013.6688400.

[357] H.-C. Chang, S.-C. Liao, H.-S. Hsieh, J.-H. Wen, C.-H. Lai, and W. Fang, "Magnetostrictive type inductive sensing pressure sensor," *Sens. Actuators A, Phys.*, vol. 238, pp. 25–36, Feb. 2016, doi: 10.1016/j.sna.2015.11.023.

[358] L. Liu, Y. Yang, and B. Yang, "A resonant pressure sensor based on magnetostrictive/piezoelectric magnetoelectric effect," *IOP Conf. Ser., Mater. Sci. Eng.*, vol. 825, no. 1, Apr. 2020, Art. no. 012037, doi: 10.1088/1757-899X/825/1/012037.

[359] C. A. R. Díaz et al., "Liquid level measurement based on FBG-embedded diaphragms with temperature compensation," *IEEE Sensors J.*, vol. 18, no. 1, pp. 193–200, Jan. 2018, doi: 10.1109/JSEN.2017.2768510.

[360] C. A. F. Marques, G.-D. Peng, and D. J. Webb, "Highly sensitive liquid level monitoring system utilizing polymer fiber Bragg gratings," *Opt. Exp.*, vol. 23, no. 5, pp. 6058–6072, 2015, doi: 10.1364/OE.23.006058.

[361] C.-W. Lai, Y.-L. Lo, J.-P. Yur, W.-F. Liu, and C.-H. Chuang, "Application of Fabry–Pérot and fiber Bragg grating pressure sensors to simultaneous measurement of liquid level and specific gravity," *Measurement*, vol. 45, no. 3, pp. 469–473, Apr. 2012, doi: 10.1016/j.measurement.2011.10.026.

[362] D. Sengupta and P. Kishore, "Continuous liquid level monitoring sensor system using fiber Bragg grating," *Opt. Eng.*, vol. 53, no. 1, Jan. 2014, Art. no. 017102, doi: 10.1117/1.OE.53.1.017102.

[363] E. Vorathin et al., "FBG water-level transducer based on PVC-cantilever and rubber-diaphragm structure," *IEEE Sensors J.*, vol. 19, no. 17, pp. 7407–7414, Sep. 2019, doi: 10.1109/JSEN.2019.2916469.

[364] E. Vorathin, Z. M. Hafizi, A. M. Aizzuddin, M. K. A. Zaini, and K. S. Lim, "A novel temperature-insensitive hydrostatic liquid-level sensor using chirped FBG," *IEEE Sensors J.*, vol. 19, no. 1, pp. 157–162, Jan. 2019, doi: 10.1109/JSEN.2018.2875532.

[365] D. Song, "Liquid-level sensor using a fiber Bragg grating and carbon fiber composite diaphragm," *Opt. Eng.*, vol. 50, no. 1, Jan. 2011, Art. no. 014401, doi: 10.1117/1.3525286.

[366] D. Sengupta, M. S. Shankar, P. S. Reddy, R. L. N. Sai Prasad, and K. Srimannarayana, "Sensing of hydrostatic pressure using FBG sensor for liquid level measurement," *Microw. Opt. Technol. Lett.*, vol. 54, no. 7, pp. 1679–1683, Jul. 2012, doi: 10.1002/mop.26890.

[367] Y. Zhao, Y.-F. Gu, R.-Q. Lv, and Y. Yang, "A small probe-type flowmeter based on the differential fiber Bragg grating measurement method," *IEEE Trans. Instrum. Meas.*, vol. 66, no. 3, pp. 502–507, Mar. 2017, doi: 10.1109/TIM.2016.2631779.

[368] Y. Fan, Z. Yang, X. Ma, Q. Xiao, H. Qi, and T. Li, "A MOBA-root-MUSIC-based demodulation method for surface acoustic wave torque sensor," *IEEE Sensors J.*, vol. 22, no. 23, pp. 22770–22777, Dec. 2022, doi: 10.1109/JSEN.2022.3213841.

[369] J. Xiaoxia, C. Huibin, C. Zikai, and L. Songxin, "The research on torque measurement system based on surface acoustic wave sensor," in *Proc. Int. Conf. Inf., Commun. Eng. (ICICE)*, Nov. 2017, pp. 400–403, doi: 10.1109/ICICE.2017.8479286.

[370] X. Ye et al., "Studies of a high-sensitive surface acoustic wave sensor for passive wireless blood pressure measurement," *Sens. Actuators A, Phys.*, vol. 169, no. 1, pp. 74–82, Sep. 2011, doi: 10.1016/j.sna.2011.05.022.

[371] S. Grousset et al., "SAW pressure sensor based on single-crystal quartz layer transferred on silicon," in *Proc. Joint Eur. Freq. Time Forum Int. Freq. Control Symp. (EFTF/IFC)*, Jul. 2013, pp. 980–983, doi: 10.1109/EFTF-IFC.2013.6702082.

[372] Z.-Y. Jia, H.-F. Liu, F.-J. Wang, and C.-Y. Ge, "Research on a novel force sensor based on giant magnetostrictive material and its model," *J. Alloys Compounds*, vol. 509, no. 5, pp. 1760–1767, Feb. 2011, doi: 10.1016/j.jallcom.2010.10.035.

Yazan Hamed (Member, IEEE) received the B.Sc. degree in mechanical engineering from Birzeit University, Birzeit, Palestine, in 2012, and the M.Sc. degree in mechanical and manufacturing engineering from Trinity College Dublin, Dublin, Ireland, in 2019, where he is currently pursuing the Ph.D. degree in mechanical and manufacturing engineering.

From 2020 to 2023, he was a Research and Teaching Assistant with the Department of Engineering, Trinity College Dublin. His research centers around the development of wireless strain sensors and remote process monitoring for digitalized tools and intelligent industrial processes.

Mr. Hamed's awards and honors include the Irish-Palestinian Fellowship Program (IPSP) and the TCD Studentship Award in partnership with the School of Mechanical and Manufacturing Engineering.

Garret O'Donnell is currently an Associate Professor with the Department of Mechanical and Manufacturing Engineering, Trinity College Dublin, Dublin, Ireland, and a Former Graduate with the Dublin Institute of Technology, University of Dublin, Dublin, and the National University of Ireland (NUI Dublin), Dublin. His research interests include advancing the scientific understanding underpinning advanced manufacturing technologies in sectors, such as medical devices, automotive, and aerospace sectors. The core focus of his research work is the characterization of measurable phenomena in materials processing spanning length scales and spanning domains from machining to energy and resource consumption at the factory systems' level.

Natalia Lishchenko is currently a Research Fellow with the Department of Mechanical, Manufacturing and Biomedical Engineering, Trinity College Dublin, Dublin, Ireland, and a Former Graduate with Odesa Polytechnic National University, Odesa, Ukraine, and the Kharkiv Polytechnic Institute, Kharkiv, Ukraine. She has experience working as a metrologist at a leading enterprise in Ukraine and solid knowledge of the production and technological processes of manufacturing parts and modern methods of quality assurance in the manufacturing sector. Her research activities are based on sensing and process monitoring; signal processing; measurement and inspection in manufacturing; and grinding thermophysics.

Irina Munina (Member, IEEE) received the B.Sc. and M.Sc. degrees in radio engineering and the Ph.D. degree in antennas and microwave devices from Saint Petersburg Electrotechnical University "LETI," Saint Petersburg, Russia, in 2009, 2011, and 2016, respectively.

From 2016 to 2022, she was a Research Fellow in projects supported by the Ministry of Education and Science of the Russian Federation, the Russian Science Foundation, and industrial companies. From 2020 to 2022, she was an Associate Professor with the Department of Microelectronics and Radio Engineering, Saint Petersburg Electrotechnical University "LETI." Since 2022, she has been a Research Fellow with the Department of Mechanical, Manufacturing and Biomedical Engineering, Trinity College Dublin, Dublin, Ireland. Her research interests include the design of microwave devices, including antennas and antenna arrays, metamaterials, metasurfaces, beamformers, additive manufacturing for the design of antennas, and antenna arrays.